INFORMATION TO USERS

This manuscript has been reproduced from the microfilm master. UMI films the text directly from the original or copy submitted. Thus, some thesis and dissertation copies are in typewriter face, while others may be from any type of computer printer.

The quality of this reproduction is dependent upon the quality of the copy submitted. Broken or indistinct print, colored or poor quality illustrations and photographs, print bleedthrough, substandard margins, and improper alignment can adversely affect reproduction.

In the unlikely event that the author did not send UMI a complete manuscript and there are missing pages, these will be noted. Also, if unauthorized copyright material had to be removed, a note will indicate the deletion.

Oversize materials (e.g., maps, drawings, charts) are reproduced by sectioning the original, beginning at the upper left-hand corner and continuing from left to right in equal sections with small overlaps. Each original is also photographed in one exposure and is included in reduced form at the back of the book.

Photographs included in the original manuscript have been reproduced xerographically in this copy. Higher quality 6" x 9" black and white photographic prints are available for any photographs or illustrations appearing in this copy for an additional charge. Contact UMI directly to order.

UMI

A Bell & Howell Information Company
300 North Zeeb Road, Ann Arbor MI 48106-1346 USA
313/761-4700 800/521-0600

Université d'Ottawa · University of Ottawa

Petrology and Geochemistry of the Nimish Formation, western Labrador, Newfoundland.

By

Donald Watanabe

A thesis submitted to the School of Graduate Studies and Research, University of Ottawa, in partial fulfillment of the requirements for the degree of Master of Science in Earth Sciences

Ottawa-Carleton Geoscience Centre
University of Ottawa
Ottawa, Ontario, Canada
September 1996

Abstract

The Nimish Formation comprises an accumulation of Early Proterozoic (1879 Ma) volcanic, intrusive, and volcaniclastic rocks which occur in the second cycle supracrustal succession of the Knob Lake Group, New Québec Orogen.

The volcanic and intrusive suites are predominantly composed of basalt and gabbro with minor intermediate and felsic differentiates. The latter suite also includes previously unrecognized sill-like bodies of peridotite and pyroxenite. The basalts and gabbros exhibit a lower greenschist mineral assemblage with clinopyroxene as the only remaining primary phase. Thin lenses of volcaniclastic strata occur in many parts of the study area ranging from mafic tuff and agglomerate, to volcanic and jasper clast-rich conglomerates. The flows, sills, and volcaniclastic rocks are coeval with Lake Superior-type iron formation (Sokoman Formation) and occur in allochthons of a foreland fold and thrust belt that has been transported westwardly over the Archean Superior Craton.

The Nimish volcanic suite ranges from alkali basalt to trachyte in composition and has alkaline to transitional geochemical affinities based on major and trace element abundances. Further, the relatively evolved chemistry of the basalts indicates that they are not the direct products of primary melts. The rare earth element spectra for the mafic lavas show a LREE enrichment trend (La_n/Lu_n = 4-8) typical of alkali basalts, with no Eu anomalies. The gabbros also have alkaline affinities as shown by their high field strength element abundances and clinopyroxene mineral chemistry. The overall similarities in elemental abundances, geochemical affinities, and REE spectra between the basalts and gabbros indicate that the suites are comagmatic.

In contrast, the petrology and primitive geochemistry of the peridotites and pyroxenites reveals that they are cumulates representative of crystallization processes by which the primitive Nimish alkaline magma became differentiated prior to the formation of the basalts and gabbros.

The strong incompatible trace element enrichment patterns of the Nimish basalts, as shown on normalized extended trace element diagrams, demonstrate that the basalts are similar to other alkaline volcanic rocks from oceanic and continental settings. As such, they indicate derivation from a relatively undepleted or enriched mantle source.

Sm-Nd isotopic data obtained for two samples further indicate that the lavas represent partial melts derived from a relatively undepleted source with minor contributions from either a depleted mantle component or continental crust. Other evidence for crustal contamination is implied by the presence of quartz xenocrysts in a sample of syenite and the occurrence of negative Nb anomalies in the normalized extended trace element patterns for basalts and gabbros. However, such a process was not considered to have significantly affected the geochemistry of the volcanic or intrusive suites. Nonetheless, the compositional variations observed in the Nimish Formation reveal the effect of many processes including fractional crystallization, crustal assimilation, variation in mantle source, and post-crystallization phenomena.

The alkaline magmatism of the Nimish Formation therefore represents the localized products of crustal extension on the margin of the Superior Craton during the early part of the second depositional cycle of the Knob Lake Group.

Sommaire

La formation Nimish du Protérozoïque Inférieur (1879 Ma) comporte une accumulation de roches volcaniques, intrusives, et volcaniclastiques se retrouvent dans la succession supracrustale de deuxième cycle du groupe Knob Lake, l'Orogène du Nouveau-Québec.

Les séries volcaniques et intrusives sont composées principalement de basalte et de gabbro, avec de faibles quantités de produits de différentiation intermédiares et felsiques. La série intrusive comprend également des filons-couches de péridotite et de pyroxénite qui n'avaient pas été observés antérieurement. Les basaltes et les gabbros montrent un assemblage minéralogique du faciés schiste vert inférieur, le clinopyroxène étant le seul minéral ayant conservé son état primaire. De minces lentilles de strates volcaniclastiques se retrouvent en des nombreux endroits de la région d'étude, variant de tufs mafiques et d'agglomérats à des conglomérats enrichis en fragments de jaspe et de roches volcaniques. Les coulées de laves, filon-couches, et roches volcaniclastiques son contemporaines aux formations de fer du type Supérieur (formation Sokoman), et se retrouvent à l'intérieur d'allochtones d'une ceinture plissée et chevauchée de l'avant-pays qui fut transportée vers l'ouest par-dessus le craton archéen du Supérieur.

La série volcanique de Nimish a une composition variant de basalte alcalin à trachyte, et une affinité géochimique alcaline à transitionelle tel que démontré par les éléments majeurs et traces. De plus, la chimie relativement évoluée des basaltes démontre qu'ils ne sont pas le produit de magmas primaires. Le patron des terres rares des laves mafiques montre un enrichissement au niveau des terres rares légères (La_n/Lu_n = 4-8) qui est typique des basalts alcalins, avec une absence d'anomalies en Eu. Les gabbros ont également une affinité alacaline tel que démontré par les éléments à haute charge ionique et par la chimie du clinopyroxène. Les similarités générales au niveau de la composition et de l'affinité géochimique des basaltes et des gabbros indique que les deux séries sont comagmatiques.

À l'opposé, la pétrologie et la géochimie primitive des péridotites et des pyroxénites montre qu'ils sont des cumulats issues de processus de cristallisation à partir duquel le magma alcalin primitif de Nimish devient différencié avant la formation de basaltes et des gabbros. L'enrichissement prononcé des éléments traces incompatibles des basaltes de Nimish, tel que démontré à l'aide des diagrammes arachnides, indique que ces roches volcaniques alcalines sont similaires à celles typiquement retrouvées dans les environnements océaniques et continentaux. En tant que tel, ils indiquent une dérivation à partir d'une source mantellique relativement non-appauvrie ou enrichi.

Des valeurs isotopiques de Sm-Nd obtenues à partir de deux échantillons de roches volcaniques démontrent en plus que les laves représentent des produits de fusion partielle dérivés d'une source relativement non-appauvrie, avec une faible contribution d'un constituant du manteau appauvri ou de la croûte continentale. Une contamination par la croûte est également suggérée par la présence de xénocristaux de quartz dans un échantillon de syénite ainsi que par l'existance d'anomalies en Nb dans les diagrammes arachnides des basaltes et des gabbros. Par contre, ce processus ne fut pas considéré comme ayant affecté de façon significative la géochimie des séries volcaniques et intrusives. Néanmoins, les variations observées au niveau de la composition des roches de la formation Nimish démontre l'action de nombreux processus, incluant la cristallisation fractionée, l'assimilation de la croûte continentale, la variation de la source mantellique, et les phénomènes suivant la cristallisation.

Le magmatisme alcalin associé à la formation de Nimish répresente ainsi les produits localisés de l'extension de la croûte à la marge de craton du Supérieur durant les stages précoces du deuxième cycle de déposition du groupe Knob Lake.

Schefferville, le dernier train

Paroles et musique: Michel Rivard
extrait du microsillon "Sauvage" (1983)

Il n'y a plus rien au Roxy
Depuis quelques mois
Y'a de la neige dans la porte
Du vieux cinéma
Dans la rue un chien jappe
Et se prend pour un loup
La nuit tombe sur la ville
Qui m'a donné le jour

A la brasserie ça chante
Plus fort que d'habitude
Pour la fête à Johnny
Qui s'en retourne dans le sud
Mais le sud de Schefferville
C'est pas la Jamaïque
C'est Québec ou Matane
Ou le Nouveau-Brunswick

En novembre passé
Ils ont fermé la mine
J'ai vu pleurer mon père
Sur la table de cuisine

C'était pas tant de perdre
Une job assurée
Que de voir s'évanouir le rêve
De trente années

Quand je suis venu au monde
Ils étaient jeunes mariés
Venus trouver l'amour
Et la prospérité
Dans une ville inventée
Par une grosse compagnie
En plein nord en plein froid
Et en plein paradis.

Acknowledgements

The author owes a large debt of gratitude to many people without whose help this thesis would not have been completed. I particularly wish to thank my supervisor, Dr. Anthony Fowler, for his guidance, constant encouragement, and unfailing patience, throughout the duration of this project. I would like to also acknowledge Dr.'s André Lalonde and Owen Dixon for their continued support of the project as Directors of Graduate Studies for the Department of Geology.

I wish to thank Dr. Tyson Birkett for suggesting the study area and acting as scientific authority for contract work related to the project. Logistic and financial support was provided by the Geological Survey of Canada under the auspices of the Canada-Newfoundland Mineral Development Agreement (1984-1989). I am also grateful to Dr. Charlie Jefferson of the Mineral Deposits Subdivision, Geological Survey of Canada, for kindly providing me access to computing facilities and office space during the completion of the thesis.

I wish to acknowledge Dr.'s Steven Kumerapeli and Karen Stamatelopoulou-Seymour, Concordia University, Montréal, for the support and encouragement that they gave me to pursue graduate work during my time as a student there.

Jonathan Findlay generously provided his advice, knowledge and assistance during the first summer of mapping in the study area. His expertise throughout the course of this project has been invaluable to me. The dedicated field assistance and scientific advice of Dan Richardson is gratefully acknowledged. Additional field assistance was provided by Ross Knight and Michael Regular. The expertise of Ron Hartree, John Loop, Peter Bélanger, Dr. Richard Ernst, and Dr. Ralph Kretz helped me understand the intricacies of analytical geochemical methods as well as the various techniques involved in subsequent data analysis.

The support of Dr.'s Sharon Watanabe, Kathleen Feldkircher, and Roger McNeely during the completion of the thesis is also gratefully acknowledged.

Finally, I wish to thank my fellow colleagues Georges Beaudoin, Murray Jones, David Lentz, Robert Thériault, and Pierre Thériault for providing a stimulating working environment characterized by enlightening discussions as well as mutual support and encouragement.

Table of Contents

Chapter 4 Geochemistry

Chapter 5 Petrogenesis and Geological Evolution

Chapter 6 Conclusions

List of Figures and Maps

List of Tables

List of Plates

List of Abbreviations

CIPW	Cross-Iddings-Pirrson-Washington
CHUR	chondritic uniform reservoir
DCP-ES	direct current plasma emission spectrometry
FA-DCP	fire assay with analysis by direct current plasma emission spectrometry
FA-NA	fire assay with analysis by inductively coupled plasma mass spectrometry
GSC	Geological Survey of Canada
HFSE	high field strength element
HREE	heavy rare earth element
IC and AA	pyrohydrolysis with analysis by ion chromatography (IC) and hydride extraction with analysis by atomic absorption (AA)
ICP-ES	inductively coupled plasma emission spectrometry
ICP-MS	inductively coupled plasma mass spectrometry
INAA	instrumental neutron activation analysis
LFSE	low field strength element
LOI	loss on ignition
LREE	light rare earth element
NiS-FA	nickel-sulphide fire assay
N-MORB	normal-type mid-ocean ridge basalt
OIB	ocean island basalt
Pb-FA	lead fire assay
PGE	platinum group elements (Ir, Os, Pd, Pt, Re, Rh, Ru)
POLY	Ecole Polytechnique, Université de Montréal, Québec
REE	rare earth element
T-MORB	transitional-type mid-ocean ridge basalt
XRAL	X-Ray Assay Laboratories Limited (Toronto, Ontario)
XRF	X-ray fluorescence

Chapter 1

Introduction

1.1 General Statement and Objectives

The Nimish Formation (Wardle, 1982) comprises a sequence of Early Proterozoic volcanic, intrusive, and volcaniclastic rocks which predominantly outcrop in the Dyke Lake-Astray Lake region of western Labrador, Newfoundland (Figure 1.1).

It is part of the New Québec Orogen (also known as the Labrador Trough), a northwest-trending fold and thrust belt comprising two volcano-sedimentary successions intruded by a sequence of mafic and ultramafic rocks and underlain by Archean basement of the Superior Province. Each volcano-sedimentary sequence records a transition from continental sedimentation and local alkaline volcanism to marine sedimentation and tholeiitic basaltic volcanism. The Nimish Formation represents an interval of alkaline magmatic activity during the early stages of the second sequence, contemporaneous with the deposition of Superior-type iron formation of the Sokoman Formation, and records rifting of the Superior continental margin succession.

The broad outlines of the stratigraphic setting and petrology of the Nimish Formation were first described by Retty (1937), Fahrig (1949), Sauvé (1953), and Perrault (1955). Subsequent work by Evans (1978) showed that the geochemistry of the volcanic suite has an alkaline affinity and suggested that it formed in an extensional tectonic regime, possibly on the margin of a crustal rift system. He also indicated that the volcanic and intrusive suites were cogenetic due to their similar trace element geochemistry.

However, little has been published regarding the petrology and geochemistry of the mafic intrusive rocks. Further, there is an overall lack of trace-element, isotopic, and mineral chemistry data necessary to better constrain the magmatic affinities of the Nimish Formation, evaluate the petrogenetic relation between the volcanic and intrusive suites, and characterize the

possible source regions in the upper mantle for these postulated intra-continental suites. In light of the different tectonic models proposed for the generation and evolution of the Labrador Trough, a more detailed understanding of the role and significance of this episode of mafic alkaline magmatism is essential.

This thesis presents the results of a detailed petrological, geochemical, and petrogenetic study of the Nimish Formation. The principal objectives of the study are:

1. to contribute data to an updated geological compilation map of the Dyke Lake-Astray Lake region at a scale of 1:50,000.
2. to document the petrologic characteristics and geochemical variation of the volcanic and intrusive suites.
3. to evaluate the influence of various petrologic processes upon the observed compositional variations of the suites.
4. to determine the petrogenetic history of the volcanic and intrusive suites as well as investigate the genetic relationship between them.
5. to substantiate the alkaline nature of the volcanic and intrusive rocks, to constrain the paleotectonic setting in which the Nimish Formation may have formed, and to estimate the characteristics of the source region of the Nimish magmas in the upper mantle.
6. to integrate the results of this study into the larger tectonic and evolutionary framework of the New Québec Orogen.

1.2 Location and Access

The Nimish Formation in the Dyke Lake-Astray Lake region is centered approximately at 54°28′N, 66°20′W, fifty kilometers southeast of Schefferville, Québec.

The study area occupies parts of 1:50,000 map sheets 23J/8 (Marble Lake), 23J/9 (Cavers Lake), and 23J/10 (Stakit Lake). Almost all of the region is accessible by float plane service from Schefferville and the northern part is readily accessible by two unmaintained

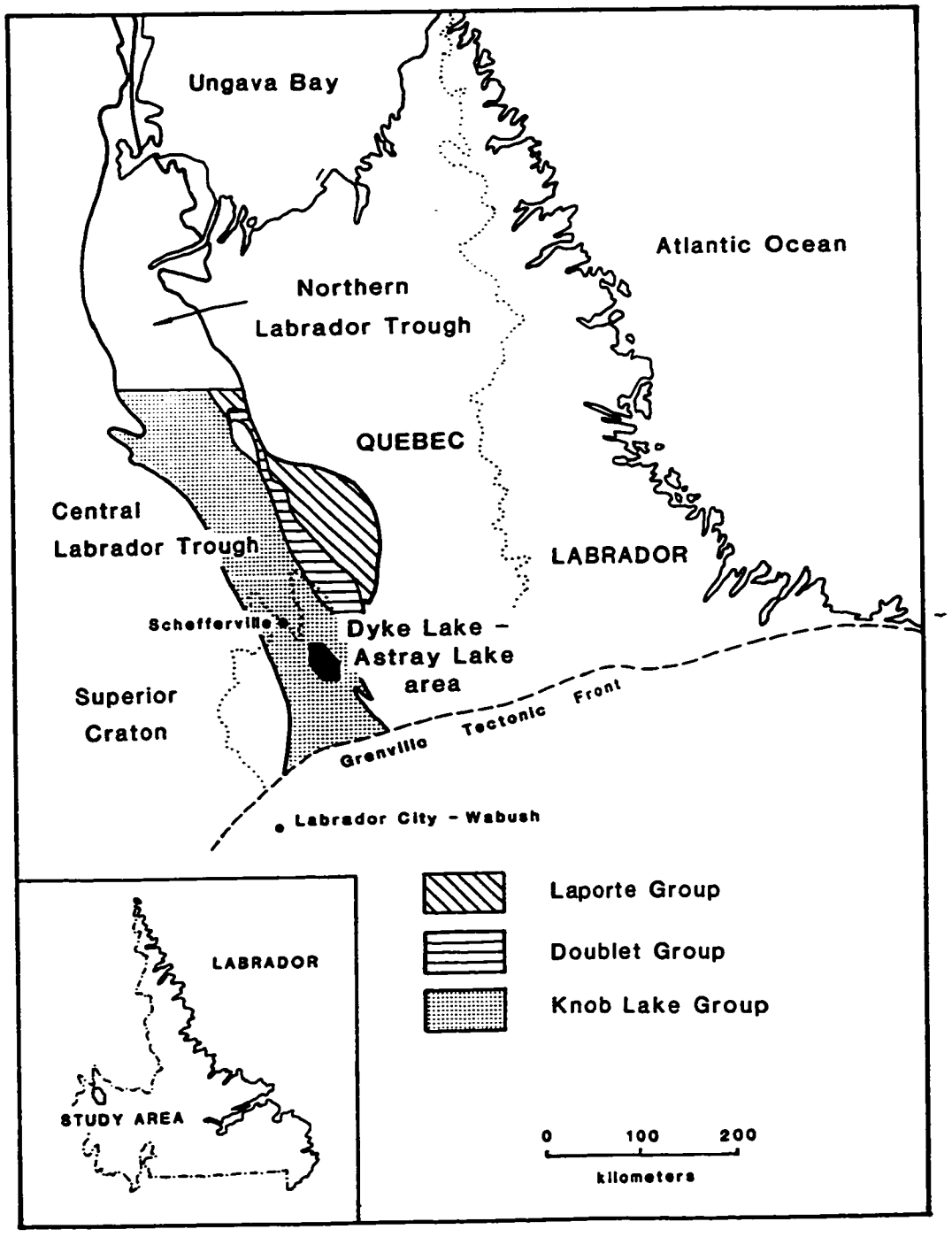

Figure 1.1. Location of the Dyke Lake-Astray Lake study area in the south-central Labrador Trough.

gravel roads from Schefferville to Astray and Dyke Lakes and then by boat along the Astray Lake-Dyke Lake system. The interconnected nature of this lake system greatly facilitates travel within the study area.

1.3 Previous Work

Retty (1937) mapped much of the Dyke Lake-Astray Lake region in search of prospective areas for iron ore and identified volcanic, volcaniclastic, and intrusive rocks of the Nimish Formation. He found these units to be intercalated with sedimentary rocks and hence considered them to be part of the Kaniapiskau "Series," what is now known as Knob Lake Group.

Evans (1978) reported that the first systematic mapping effort of the study area was undertaken at 1:32,000 scale by Fahrig (1949) as part of a larger regional exploration programme by the Iron Ore Company of Canada. Fahrig (1949) defined the Nimish "Volcanics" as a thick accumulation of volcanic and pyroclastic rocks that were intercalated with quartzites, slates, and iron formation and he considered the "Volcanics" and sedimentary units to comprise the Sawyer-Nimish Group. In addition, he concluded that the volcanic rocks were mafic to intermediate in composition and that the pyroclastic units encompassed a number of lithologies including tuffs, agglomerates, breccia, and jasper-rich conglomerates. Further, he found that sills and intrusions of diorite and gabbro commonly intruded the Nimish volcanic rocks and suggested that they probably were emplaced within all the sedimentary units of the Knob Lake Group. Finally, Fahrig (1949) postulated the presence of four major northwest-southeast trending thrust faults running the length of the study area. Other studies by the Iron Ore Company of Canada are listed in Evans (1978).

Sauvé (1953) completed a M.Sc. thesis on the description and origin of the Nimish volcaniclastic rocks. In order to account for their spatial and temporal relationship to the Nimish lavas and Sokoman Formation, he postulated that they were locally derived by erosion

of volcanic islands in what is now Dyke Lake-Astray Lake area. The volcanic islands were paleogeographic highs, and thus the source areas for Nimish volcaniclastic rocks in an otherwise shallow and quiescent sedimentary basin. According to the spatial distribution of the clast sizes of conglomeratic rocks within the study area, Sauvé (1953) inferred that the main volcanic centre was located on the peninsula between Astray and Dyke Lakes in the vicinity of Jasper Mountain. He ascribed the volcanic centres to tectonic activity that caused thick accumulations of volcanic flows and localized uplift of the sea floor above sea level.

Perrault (1955) studied the general geology of the region with emphasis on the Sokoman and Nimish Formations as part of his Ph.D. thesis. Contributions by the geologists of the Geological Survey of Canada to the mapping and understanding of the Dyke Lake-Astray Lake region include those of Frarey (1961), Gross (1968), and Zajac (1974). Frarey (1961) published one of the earliest geological compilation maps of the study area, whereas Gross (1968) and Zajac (1974) studied the stratigraphy, mineralogy, and depositional environment of the Sokoman Formation and its relation to the rocks of the Nimish Formation.

Evans (1978) mapped the Dyke Lake-Astray Lake map area at 1:50,000 scale as part of a larger regional mapping programme of the Labrador portion of the New Quebec Orogen by the Newfoundland Department of Mines and Energy. As such, his was the first detailed work concerning the stratigraphy and geochemistry of the Nimish Formation. Based on stratigraphic, petrologic, and geochemical data, Evans (1978) subdivided the Nimish igneous rocks into lower and upper suites separated by the Sokoman Formation. He proposed the terms Petitsikapau Lake Formation and Astray Lake Formation for the lower and upper suites respectively. Furthermore, he designated the term Nimish Subgroup to include the Petitsikapau Lake and Astray Lake Formations as well as the intrusive rocks associated with both.

The 1:100,000 scale compilation map by Wardle (1982) presents a more general subdivision scheme of the Nimish rocks, hence reducing the Evan's (1978) Subgroup to

formational status. In addition, Wardle (1982) extended the Nimish Formation into the rest of the Schefferville zone beyond Evan's map area.

Exploration for non-ferrous mineral deposits in the Dyke Lake-Astray Lake region has been done almost exclusively by the Labrador Mining and Exploration Company Limited, details of which are included in numerous unpublished company reports. A compilation of all the indications, showings, and prospects in the study area are shown on the 1:100,000 scale mineral occurrence maps of Smith (1987).

1.5 Methods of Study

This study is based on field mapping carried out over a period of seven weeks during the summers of 1986 and 1987. Regional and detailed mapping, with emphasis on the Nimish Formation, was done at 1:32,000 scale and subsequently compiled at a scale of 1:50,000.

In addition, samples of the Nimish Formation collected in the study area during a one week period in the summer of 1985 were provided by Dr. Tyson Birkett of the Geological Survey of Canada, Ottawa, Ontario.

Petrologic investigation of the Nimish Formation comprised examination of approximately 50 thin and polished thin sections, and the determination of the chemistry of 50 mineral grains by electron microprobe. Whole-rock major (weight %) and trace (ppm) element analyses of 293 samples were determined using a variety of techniques at the University of Ottawa, X-Ray Assay Laboratories Limited (Toronto), and the Geological Survey of Canada (Table B1.1). A suite of Nimish Formation volcanic and intrusive rocks were also analyzed for rare earth elements (REE) by instrumental neutron activation analysis (INAA) at Ecole Polytechnique, Université de Montréal, Québec. A number of sulphide-bearing Nimish mafic volcanic and plutonic rocks were analyzed for whole rock gold and platinum group element (PGE) concentrations by INAA or direct current plasma emission spectrometry (DCP-ES) techniques following nickel-sulphide fire-assay (NiS-FA) preconcentration.

Chapter 2

General Geology

2.1 Regional Setting

The linear belt of Lower Proterozoic (Aphebian) sedimentary and volcanic rocks in New Québec and western Labrador, commonly known as the Labrador Trough, has recently been renamed by Wardle *et al.* (1990) the Western Division of the Labrador Segment of the Trans-Hudson Orogen and, alternatively, the New Québec Orogen by Hoffman (1988).

The Labrador Segment of the Trans-Hudson Orogen is divided into Western, Central, and Eastern Divisions (Wardle *et al.*, 1990). It is bounded to the west by the Superior craton and to the east by the North Atlantic craton (Figure 2.1). In contrast, Hoffman (1988) interpreted the Labrador Segment to be comprised of two orogens (New Québec and Torngat) separated by the southern extension of the Rae Province. To avoid confusion, and in keeping with Wardle *et al.* (1990), the terms "Labrador Trough" and "Western Division" will be retained and used synonymously throughout the rest of the thesis.

The Labrador Trough trends southeast for 1,200 km from west of Ungava Bay in the north to within the Grenville parautochthon (Rivers and Chown 1986) to the south. On its southwestern margin this belt unconformably overlies Archean basement of the Superior Craton. It is bounded northeastwardly to the Central Division of the Labrador Segment along a series of major, east-dipping ductile shear zones (Wardle *et al.*, 1990). Regional syntheses of the stratigraphy, structure, and tectonic evolution of the Western Division include those of Frarey and Duffell (1964), Dimroth *et al.* (1970), Dimroth (1978), Baragar and Scoates (1981), Wardle and Bailey (1981), Wardle (1982), LeGallais and Lavoie (1982), Hoffman (1987, 1988), and Wardle *et al.* (1990).

From southwest to northeast, the Western Division is subdivided into four major allochthonous sequences (Wardle *et al.*, 1990): the Schefferville and Howse zones, and the Doublet and Laporte terranes (Figure 2.2).

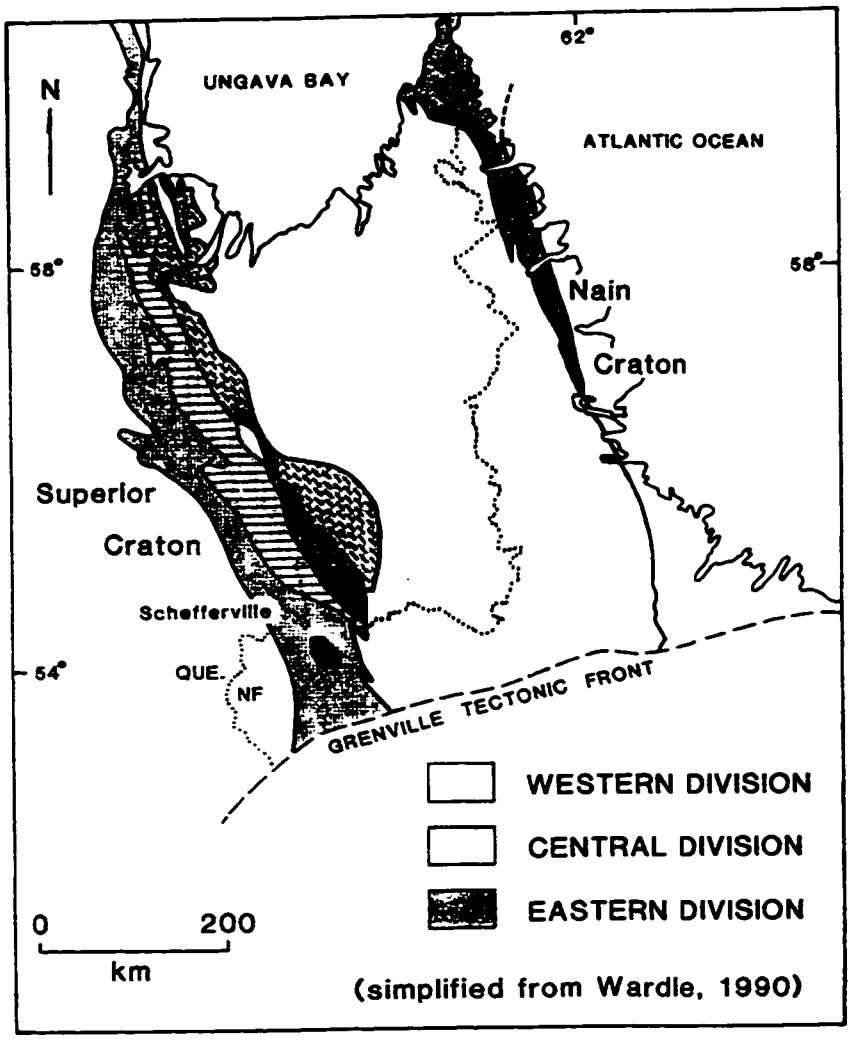

Figure 2.1 The Western, Central, and Eastern Divisions of the Labrador Segment of the Trans-Hudson Orogen (from Wardle *et al.*, 1990).

The Schefferville zone, west of the Ferrum River thrust, comprises rocks of the Knob Lake Group, a predominantly sedimentary succession divided into 2 segments, the Lower and Upper Knob Lake Groups (Wardle and Bailey, 1981). The Lower Knob Lake Group (Seward and Attikamagen Subgroups) is separated from the Upper Knob Lake Group (Ferriman Subgroup and terrigenous clastic sediments of the Tamarack River Formation) by a postulated regional unconformity (Dimroth, 1970). Each sequence began with the deposition of shallow

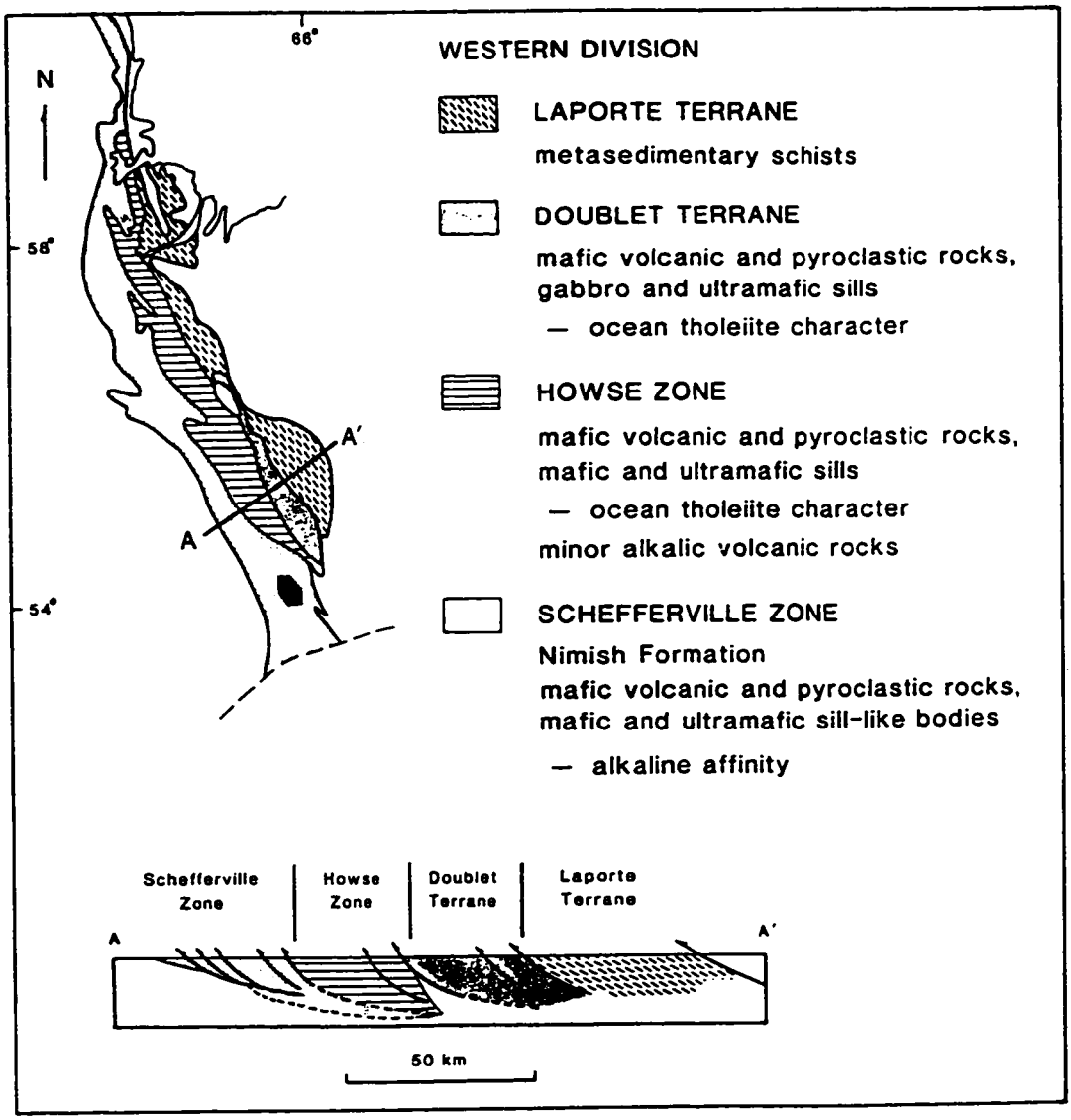

Figure 2.2 The four lithotectonic subdivisions of the Western Division: the Schefferville and Howse Zones, Doublet and Laporte Terranes (from Wardle *et al.*, 1990).

water clastic and chemical sedimentary rocks and culminated in the deposition of deeper water clastic sediments (Table 2.1).

Similarly, east of the Ferrum River thrust, the Howse zone includes rocks of the Knob Lake Group by predominantly comprises the mafic (Wakuach Gabbro) and ultramafic (Retty Peridotite) sills of the Montagnais Group. The Walsh Lake thrust separates the Howse zone

Table 2.1 Simplified table of formations for the Kaniapiskau Supergroup, south-central Labrador Trough (modified after Wardle and Bailey (1981) and Wardle (1982)).

Kaniapiskau Supergroup	
Montagnais Intrusive Suite	
Retty Peridotite	peridotite
Wakuach Gabbro	glomeroporphyritic gabbro, gabbro
Doublet Group	
Willbob Formation	pillow basalt, minor tuff and pillow breccia
Thompson Lake Formation	banded siltstone and black slate
Murdoch Formation	mafic pyroclastic rocks, sedimentary rocks, pillow lava
Knob Lake Group	
Upper Knob Lake Group	
Tamarack River Formation	algal dolomite, arkose, argillite
Ferriman Subgroup	
Menihek Formation	siltstone, shale, mafic lava and tuff
- Sokoman Formation	iron formation
- Nimish Formation	mafic flows, gabbro sills, volcaniclastic rocks
Wishart Formation	orthoquartzite, quartzite, siltstone
Lower Knob Lake Group	
Attikamagen Subgroup	
Fleming Formation	chert breccia, chert
Dolly Formation	grey shale and siltstone
Denault Formation	dolomite, stromatolitic dolomite
Le Fer Formation	shale, siltstone, pillow basalt and tuff
Seward Subgroup	
Sawyer Lake Formation	siltstone and shale
Snelgrove Lake Formation	arkosic sandstone and conglomerate
Discovery Lake Formation	sandstone, granule conglomerate

and the Doublet terrane. The Doublet Group is a thick sequence dominated by mafic pyroclastic and tholeiitic volcanic rocks.

The Laporte terrane is overthrust onto the eastern margin of the Doublet terrane along the Gill Lake thrust. The terrane comprises the Laporte Group, predominantly metasedimentary schists of a probable shale-graywacke protolith (Baragar, 1967) of a presumed turbidite character (Wardle *et al.*, 1990).

Igneous activity in the Labrador Trough is largely mafic in nature and appears to be of two associations. In the Schefferville Zone, volcanic rocks of alkaline affinity were extruded in subaerial to shallow water conditions and are associated with fluvial deposits of the Seward

Subgroup and aranaceous sediments and iron formation of the Ferriman Subgroup. In the Doublet terrane, an occurrence of mafic tuff is found to be interbedded with eastern depositional facies dolomites of the Denault Formation (Wardle and Bailey, 1981; Wardle, 1982).

Wardle and Bailey (1981) interpreted the synsedimentary volcanic rocks of the Seward Subgroup to have been extruded during a period of continental rifting. This was based on palinspastic reconstruction of the Subgroup showing a thick (1500-3000 m) accumulation of sediments along the axial region of the Labrador Trough within what they interpreted as a rift valley. Based upon similar compatible and incompatible elemental abundances as well as similar differentiation trends, Evans (1978) considered the Late Miocene-Early Pliocene Little Aden volcanic suite (Cox *et al.*, 1970), Republic of Yemen, to be a comparable modern compositional analogue to the Nimish Formation. As such, he postulated that the Nimish Formation was extruded in a similar tectonic environment to that of the Little Aden Suite, specifically on the margin of a major crustal rift system.

In the Howse zone, volcanic and pyroclastic rocks of the Le Fer and Menihek Formations as well as the comagmatic Montagnais Group sills, are predominantly of oceanic tholeiite character (Baragar, 1967; Dimroth, 1978; Findlay, 1996). The association of volcanic and pyroclastic rocks with deeper water sediments suggests two periods of shelf collapse concomitant with increased submarine rifting activity and subsidence to the east of the zone (Wardle and Bailey, 1981). However, Findlay (1989, 1996) shows that the volcanic and pyroclastic rocks of the Le Fer Formation in the vicinity of Howse Lake have an alkaline affinity. Volcanic rocks of the Doublet terrane are tholeiitic and represent a renewed and final period of submarine rifting activity marking the close of Labrador Trough development.

2.2 Geology of the Dyke Lake-Astray Lake region

In the Dyke Lake-Astray Lake region, the stratigraphy comprises lithologies of both the upper and lower depositional cycles of the Knob Lake Group. The thinly bedded shales of the

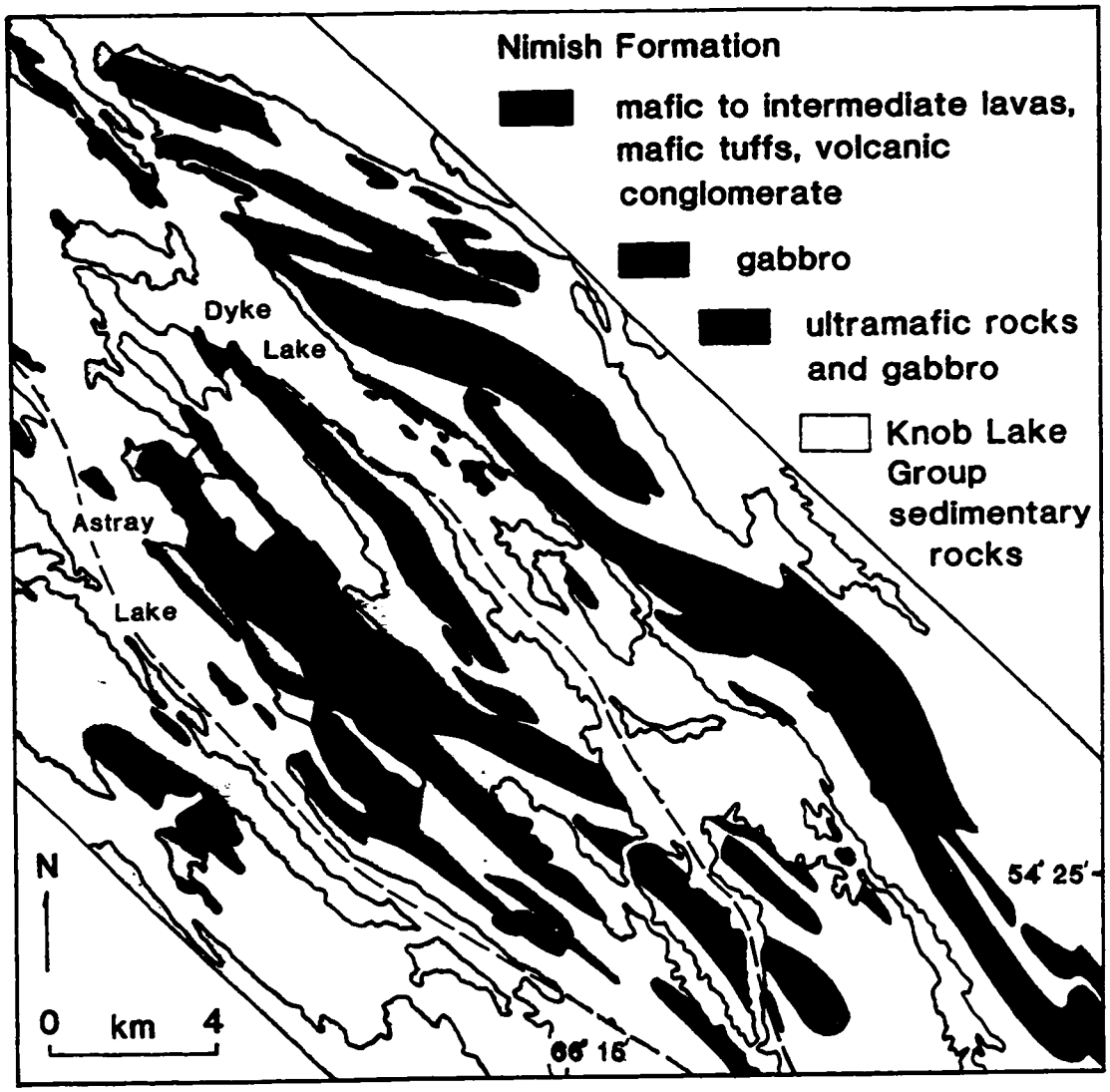

Figure 2.3 Simplified geological map the Dyke Lake-Astray Lake study area showing the general distribution of Nimish Formation rocks.

Le Fer Formation represent the oldest unit exposed in the region whereas the shales and siltstones of the Menihek Formation mark the close of activity in the area. However, the local stratigraphy is unique within the Labrador Trough in that it includes the Nimish Formation; a sequence of basaltic lavas, gabbro sills, and volcaniclastic rocks (Figure 2.3; Map A). Evans (1978) and Zajac (1974) considered the lavas and associated sills to be cogenetic. In addition to the basalts and gabbros which forms the bulk of the sequence, minor intermediate to felsic

differentiates and ultramafic sill-like bodies have been recognized. Thus, the Nimish Formation includes a variety of rock types which, during the course of field studies, showed complicated internal relationships suggesting a complex volcanic stratigraphy.

Based on stratigraphic, petrologic, and geochemical considerations, Evans (1978) subdivided the Nimish into Petitsikapau Lake and Astray Lake Formations; the former being interbedded with the lower Sokoman Formation while the latter occurs above and is interbedded with the upper Sokoman Formation. As such, the position of the Sokoman Formation in the study area serves as a marker by which to subdivide the Nimish as well as forming the basis upon which the Nimish is considered to be time equivalent to the Sokoman (Wardle, 1982).

The Nimish Formation is also interbedded to a lesser extent with the Wishart and Denault Formations. Rivers (1982) and Noel (1992) noted that the Nimish lavas are intimately interbedded with the Denault Formation in the Gabbro Lake-McKay River region, approximately 100 km to the south of the study area. Tuffaceous equivalents of the Nimish within the Attikamagen or Le Fer Formation, as noted by Evans (1978) were not recognized during the course of this study.

According to Evans (1978) the stratigraphy of the Nimish is dominated by massive to amygdaloidal, mafic to intermediate flows except in two locations where abundant porphyritic mafic to intermediate lavas, acid volcanic- and jasper-bearing conglomerates, and pyroclastic rocks are also present. He interpreted the occurrence and restricted nature of these units to indicate proximity to volcanic centres postulated to have been at Jasper Mountain and in the immediate vicinity of Point Lake. The centres are considered to be former, subaerially exposed volcanic islands which produced interbeds of acidic volcanic rocks during the final stages of a volcanic cycle.

Field mapping during the present study (Map A) reveals that the distribution of volcaniclastic rocks, particularly the mafic tuffs and volcanic conglomerate units, is more

widespread than had been previously reported. In light of this new information, the interpretation of two previously existing volcanic centres requires modification.

2.2.1 Le Fer Formation

Following the usage of Wardle (1982), the Le Fer Formation includes the gray shales and siltstones which only occur above the Sawyer Lake Formation of the Seward Subgroup and below the Denault Formation of the Attikamagen Subgroup.

In the Dyke Lake-Astray Lake region, the Le Fer Formation is restricted to the southwestern portion of the study area and its northeastern limit is marked by the Astray Lake Fault. Over most of its area, the Le Fer Formation consists of laminated to thinly bedded, gray to black, fissile shales and siltstones with minor argillitic beds. According to Wardle and Bailey (1981), they are part of the western depositional facies of the formation in the south-central Labrador Trough. The unit comformably overlies the Sawyer Lake Formation and passes gradationally, with lense-like interbedding, into the Denault Formation (Evans, 1978). It was probably deposited in a near shore, low energy environment of shallow to moderate water depths.

2.2.2 Denault Formation

The best exposures of the Denault Formation in the region are seen on the islands and shorelines to the southwest and northeast of the Astray Lake and Dyke Lake Faults, respectively (Map A). Evans (1978) subdivided the Denault Formation into a lower unit consisting of laminated dolomite, silty dolomite, and dolomite breccia; and an upper unit of gray and calcareous siltstones, restricted to the northeast of the Dyke Lake Fault. Subsequent re-interpretation by Wardle (1982) indicates that these siltstones are members of the overlying Dolly Formation.

In general, the Denault Formation comprises interbedded and finely laminated dolarenites, dololutites, and dolomite breccias. Field mapping during the course of this study

revealed a more restricted nature of the unit at the south end of Dyke Lake and previously unrecognized gabbro sills were found to intrude the Denault Formation.

One to ten meter thick lensoid units of coarse dolomite breccia are found in the Astray Lake-Marble Lake Peninsula. Here, large (35 cm) angular dolomitic clasts are set in a finer grained dolomitic matrix. It is thought that the dolomite breccias are the products of debris flow slumping on a steep, easterly dipping slope adjacent to a supratidal-intratidal platform (Wardle and Bailey, 1981).

The thickness of the formation in the map area is unknown but Evans (1978) estimates a thickness of at least 500m in the Astray Lake-Marble Lake Peninsula. The Denault Formation is interpreted to have been formed in a lagoonal environment (Wardle and Bailey, 1981).

2.2.3 Dolly Formation

The Dolly Formation includes gray shales and siltstones which lie between the Denault dolomite and the Fleming Formation. They are best exposed along the eastern shores of Dyke Lake and southern Astray Lake, as well as south of Fawley Lake.

Along the eastern shores of Dyke Lake, the dark gray-black shales form thin (3-30 mm) layers interbedded with similarly thin horizons of fine sandstone. Elsewhere in the same area, the formation comprises alternating thin (2-4 mm) and thicker (10-45 mm) beds of gray siltstone. Northwards, some of the interbeds become noticeably coarser (to fine sand size) and thicker (up to 20 cm). Sulphide mineralization is sparse and limited to small pyrite blebs in the shales in addition to disseminations associated with quartz fracture fillings. Within the south-central Labrador Trough, the Dolly Formation defines an area termed the Petitsikapau Sub-basin where rhythmically bedded gray shales and siltstones of turbidite origin are dominant towards the basin centre (Wardle and Bailey, 1981).

2.2.4 Fleming Formation

In the study area, the Fleming Formation represents the southernmost extension of the unit in the south-central Labrador Trough. It is a distinctive chert breccia unit restricted to the

fault block southwest of the Astray Lake Fault where it immediately overlies the Denault Formation (Evans, 1978).

These exposures have been investigated by Birkett (1991a) as part of a stratigraphic and petrologic study of the main occurrences of the Fleming Formation in the Knob Lake region.

2.2.5 Wishart Formation

In the map area, the Wishart Formation consists of thinly bedded (3-12 cm), fine and medium grained feldspathic quartzites, medium grained orthoquartzites, and interbedded fine grained quartzites and green-gray siltstones. Furthermore, they are interbedded with volcanic rocks and intruded by gabbro sills of the Nimish Formation. In one location, medium grained orthoquartzites with approximately four per cent pyrite mineralization were observed to be in contact with gabbro of the Nimish Formation. The Wishart Formation forms the basal unit of the Upper Knob Lake Group and, as such, marks the beginning of the second depositional cycle in the south-central Labrador Trough. It is thought to have been deposited in a near shore, shallow, shelf environment (Wardle and Bailey, 1981).

2.2.6 Sokoman Formation

The Sokoman Formation is composed of lower, middle, and upper iron formation members in addition to a facies unique to the Dyke Lake-Astray Lake region, referred to as magnetite graywacke (Evans, 1978). It consists of intercalated volcaniclastic sediment and iron formation. The Sokoman is intimately interbedded with the Nimish Formation and is interpreted to subdivide the Nimish into two units, the Astray Lake and the Petitsikapau Lake Formations. Detailed descriptions of the iron formation and its relationship to the Nimish Formation are found in Gross (1968), Zajac (1974), and Evans (1978)

2.2.7 Menihek Formation

The Menihek Formation is sporadically distributed in the Dyke Lake-Astray Lake region. It is composed of gray to black siltstones with minor argillaceous and graywacke

interbeds, interpreted to have been deposited in a quiet, deep water environment (Wardle and Bailey, 1981).

Chapter 3

Petrology

3.1 Introduction

Chapter 3 presents a detailed description of the geology of the Dyke Lake-Astray Lake region including field data of the volcanic and intrusive rocks from regional and detailed traverses in the study area. Petrographic descriptions supplement the field descriptions.

3.2 Volcanic Rocks

The volcanic rocks of the Nimish Formation occur throughout the study area and comprise the dominant unit of the formation. They range in composition from alkali basalt to trachyte but are predominantly basaltic.

3.2.1 Basalt

Aphyric and amygdaloidal basalt flows are the most common lithologies in the study area. Massive flows contain occasional minor quartz veining and/or jointing. Locally, the massive basalts grade into amygdaloidal flows and sparsely porphyritic flows.

Amygdaloidal flows contain one to ten per cent by volume (average 5%), round to oval amygdules ranging in diameter from 0.5 to 1.5 cm (average 1.0 cm). They are variably infilled with chlorite and/or calcite. Sparse, medium grained, subhedral, plagioclase phenocrysts are also found in these flows. Vesicular flows occur only to a minor extent in the study area.

The porphyritic basalts are composed of 3 to 15% volume (commonly 8 to 15%), medium grained, subhedral, plagioclase or pyroxene phenocrysts in an aphanitic groundmass. Pillowed flows occur at various locations throughout the study area and are commonly bun-shaped averaging 0.5 m in width and have, in one locality, shelves indicative of low rates of effusion (Dimroth, 1974).

Sauvé (1953) and Evans (1978) have described occurrences of massive to slightly vesicular flows as well as basaltic pillows that appear to exhibit "concentric veining." Evans

(1978) identified the "vein" constituents as chlorite, hematite, quartz, epidote, calcite, and potash feldspar. These last two minerals were also reported to infill the vesicles. Previous workers (as cited in Evans, 1978) interpreted these structures as being liesegang banding resulting from weathering processes in arid environments. Evans (1978) suggested that the "veining" may have resulted from hydrothermal processes.

These structures were identified at two locations in the study area and, at first glance, strongly resembles pillow basalts (Plate 3.1). The core of the feature is basaltic and is alternately "enveloped" with rims of massive basalt and jasper-rich material.

Very similar features have also been identified in the Persillon Formation, Richmond Gulf area, and interpreted to be columnar joints that exhibit post-crystallization weathering phenomena (Chandler, 1988). Subsequent work by Budkewitsch and Robin (1994) lends support to this interpretation. The structures seen in the Nimish Formation basalts are similarly interpreted. Chandler (1988) ascribes the red concentric bands to subaerial surface oxidation but it appear that in the study area, the red bands are related to the abundance of iron-rich material from the Sokoman Formation with which the Nimish lavas are intimately associated.

3.2.2 Intermediate and Felsic Flows

Intermediate to felsic volcanic rocks in the Nimish Formation are volumetrically minor in extent and are thought to be spatially associated with two volcanic centres in the study area, Jasper Mountain and in the vicinity of Point Lake. According to Evans (1978), the centres are considered to be former, subaerially exposed volcanic islands which produced interbeds of acidic volcanic rocks during the final stages of a volcanic cycles.

The intermediate volcanic rocks are most commonly amygdaloidal and rarely massive whereas the rhyolitic rocks are usually porphyritic. The amygdules comprise 1 to 4 per cent volume of the flows, are 4 mm in diameter (average), and are infilled by chlorite and potassium feldspar. Porphyritic volcanic flows typically consist of 8 to 10% subhedral potassium feldspar phenocrysts in a purple to pink coloured aphanitic groundmass. On Jasper Mountain,

Plate 3.1 Concentrically-banded columnar joints of Nimish Formation basalt.

Plate 3.2 Volcanic conglomerate of the Nimish Formation with well rounded clasts and cobbles of jasper and quartz syenite.

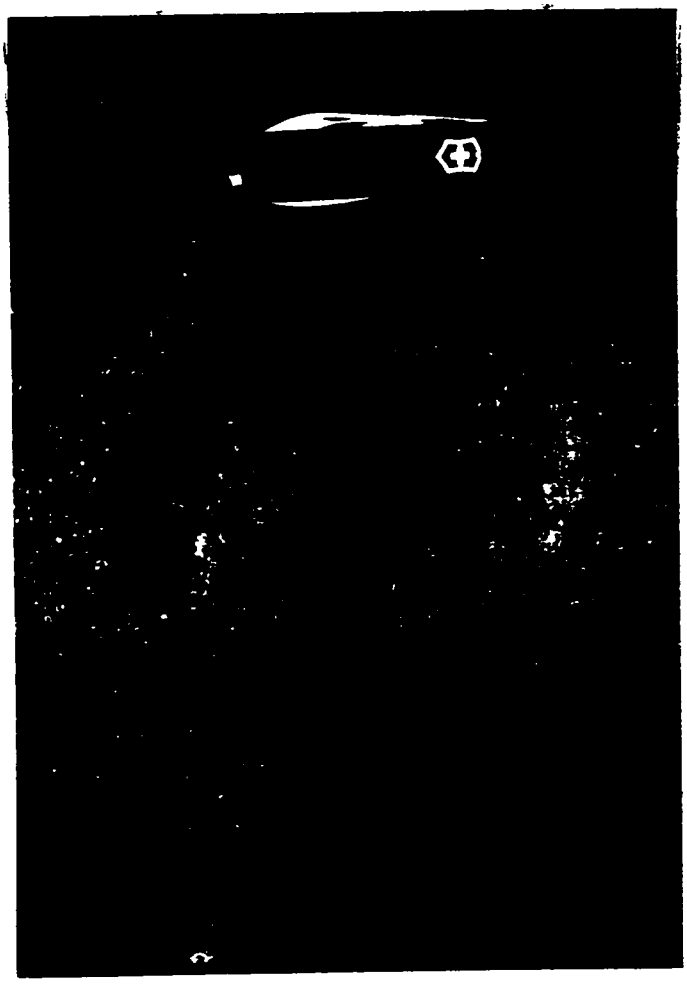

the porphyritic flows contain quartz eyes.

3.3 Intrusive Rocks

3.3.1 Ultramafic Igneous Rocks

Ultramafic sill-like bodies were recognized in the central Dyke Lake area (Figure 2.3). They occur as a series of small discontinuous lenses over a strike length of approximately 5 kilometers and are associated with subophitic and coarse grained, plagioclase porphyritic gabbro. Contacts with surrounding rocks were not exposed except in one location where there appeared to be a possible fault contact between peridotite and medium grained gabbro over a zone of approximately two meters.

Pyroxenites and peridotites were identified in the field with the latter rocks having a distinctive lime green colour on weathered surfaces (Plate 3.3). They are massive, medium grained, and equigranular. Features such as igneous layering were not noted. Both rock types are extensively altered and often are cross-cut by networks of serpentine-talc veins (Plates 3.3 and 3.5).

The peridotites also exhibits a spotty weathering surface that is characterized by resistant dark green clinopyroxene and recessive lime green alteration products after olivine. Olivine (and its alteration products) comprise 50-60% of the rock and clinopyroxene a subordinate amount. Irregularly distributed disseminations (1-2% volume) of pyrite and pyrrhotite were also observed. This is confirmed in thin section (Plate 3.4). Olivine has been completely pseudomorphed by serpentine, chlorite, and talc while clinopyroxene has been variably altered to tremolite and actinolite.

Pyroxenites have a dark brown weathering surface with cross-cutting networks of talc-serpentine veins (Plate 3.5). In addition, they are massive and medium grained. In thin section, clinopyroxene is generally well preserved with olivine pseudomorphed by serpentine, chlorite, and talc (Plate 3.6).

Plate 3.3 Field photograph of peridotite with distinctive weathering surface and lime green colour. Note cross-cutting serpentine-talc veinlets. Hammer is 32 cm long for scale.

Plate 3.4 Photomicrograph of peridotite showing fresh clinopyroxene grains and olivine pseudomorphed by serpentine, chlorite, and talc.


0.35mm

Plate 3.5 Field photograph of pyroxenite with cross-cutting serpentine-talc veinlets. Patches of white lichen obscure the outcrop towards the top of the photo. Hammer is 38 cm long for scale.

Plate 3.6 Photomicrograph of pyroxenite showing fresh clinopyroxene grains.

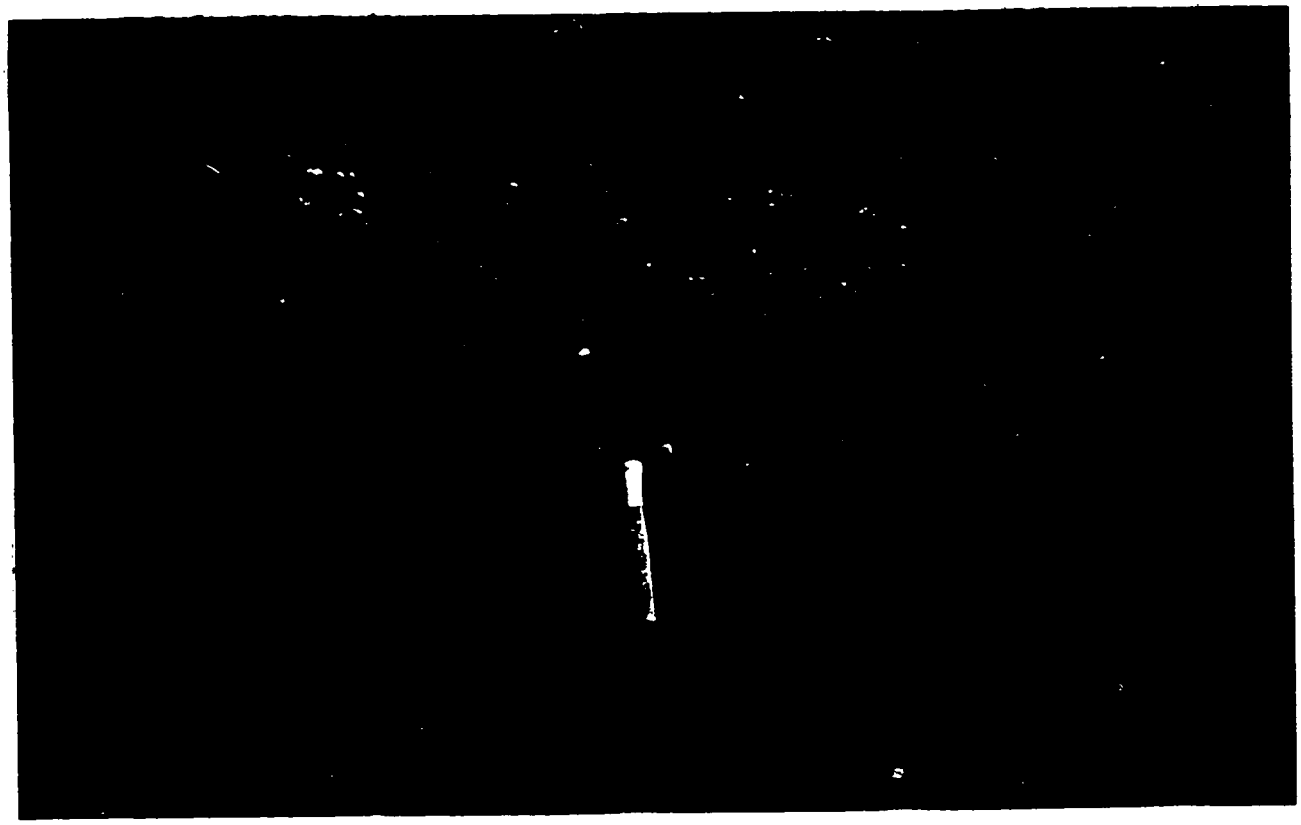


0.35mm

3.3.2 Gabbro

Equigranular, subophitic and ophitic textured gabbros are the dominant intrusive rock types in the study area. They occur almost exclusively as sills within the study area. The gabbros range in composition from melagabbro to leucogabbro but have an essential mineralogy of approximately equal amounts of plagioclase and augite, with accessory magnetite. Porphyritic gabbros are composed of medium-grained plagioclase phenocrysts set in a fine-grained, ophitic groundmass of plagioclase, clinopyroxene, and Fe-Ti oxides. Clinopyroxene shows only moderate alteration to actinolite and tremolite while plagioclase is invariably strongly saussuritized. In two rare occurrences, 1-4 cm large, blocky laths and aggregates of plagioclase are set in a medium-grained, ophitic groundmass.

3.3.3 Branching-textured gabbro

In the northern part of Dyke Lake, a steeply dipping 16 meter section of ophitic gabbro is characterized by branches and plumose arrays of coarse-grained pseudomorphs of what was possibly olivine. For descriptive purposes, the section is referred to as branching-textured gabbro. It is divisible into four zones (Figure 3.1) and described as follows:

The base of zone I is marked by a 10 cm thick chill zone in contact with a shale unit of the Sokoman Formation. This is followed by a medium-grained gabbro, approximately 6 m thick, characterized by randomly oriented, up to 5 cm long, branches of coarse-grained olivine(?) crystals. These impart a black coloured mottling to the rock. Voids interpreted to be miarolitic cavities, 2 to 15 mm in diameter, are sparsely scattered throughout this zone.

A well-defined contact separates zones I and II. Zone II comprises a 1 meter thick zone of gabbro containing plumose arrays of olivine(?) approximately 30 cm in long axis. Their orientation demonstrates that the crystals grew away from the stratigraphic top (Plate 3.7). These arrays form two distinct layers in this zone.

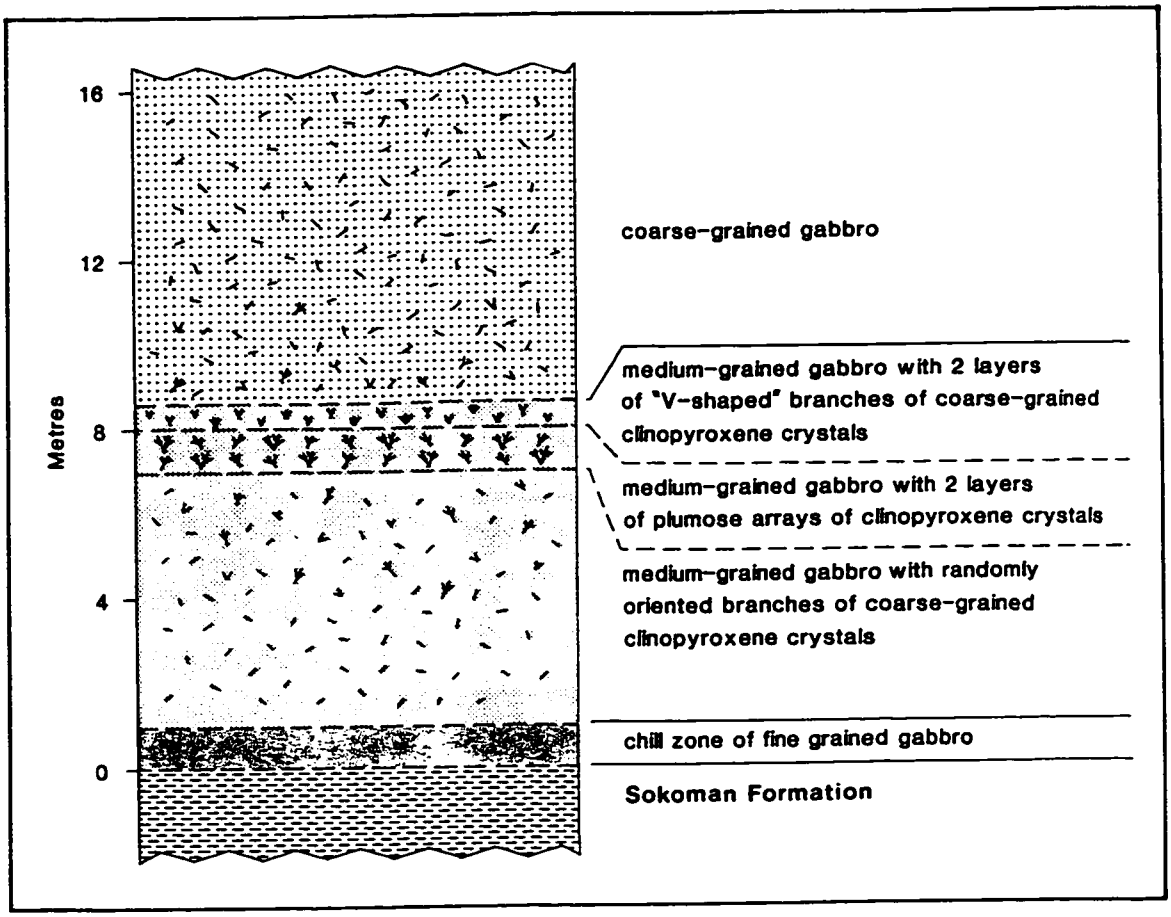

Figure 3.1 Schematic profile of a section of branching-textured gabbro, northern Dyke Lake.

Zone III is a 0.6 m zone of medium-grained gabbro in which two 7-cm thick layers of "V-shaped" branches of coarse-grained olivine(?) crystals are found. These layers are oriented parallel to the lower contact of the zone.

In Zone IV, the individual branches become randomly oriented and gradually pass, over a one meter interval, into a eight meter thick section of very coarse-grained gabbro in which plagioclase laths average six mm in length. In addition, up to five cm long branches of olivine(?) crystals are randomly oriented throughout this section. As in zone I, they impart a brown or black colour to the rock (Plate 3.8). Miarolitic-like cavities of 1 to 1.5 cm diameter are sparsely distributed in this zone but locally can form up to 5-7% of the rock.

Plate 3.7 Branching-textured gabbro:
Zone II: Details of a plumose array of coarse-grained olivine (?).

Plate 3.8 Branching-textured gabbro:
Zone IV: Coarse-grained gabbro with randomly oriented branches.

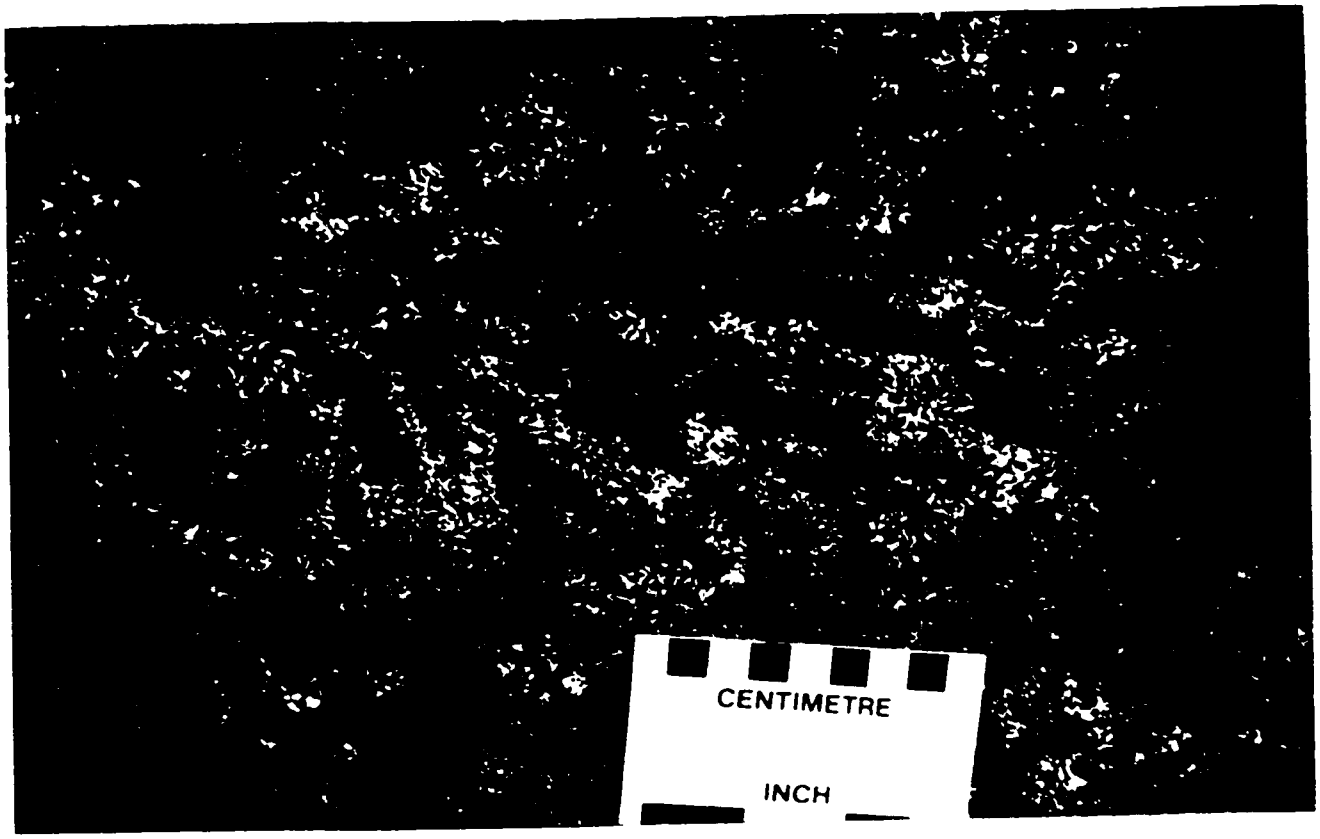
CENTIMETRE
INCH

Branching-textured silicate minerals such as the plumose olivine(?) are an indication of non-equilibrium conditions. They are often initiated by a lack of nucleii in the melt, and a reduction in diffusion rates caused by a sharp drop in temperature (i.e. supercooling) in the melt (Lofgren, 1974). Although in volcanic environments it is clear that disequilibrium textures such as spinifex and spherulites are in large part controlled by the temperature drop associated with eruption, in plutonic environments the cooling rate is necessarily much lower hence other processes are likely involved (Donaldson, 1974). The presence of abundant miarolitic cavities in the gabbro indicates that the elevation of the liquidus temperature associated with the exsolution of a gas phase, may in part be a causative factor in the development of the texture.

3.3.4 Syenite

In the vicinity of Jasper Mountain and Point Lake, well-rounded quartz syenite clasts and cobbles are distinctive features of the volcanic conglomerates found in these areas (Plate 3.2). In addition, jasper clasts derived from the Sokoman Formation are found in the conglomerate unit. Although the syenite intrusive, from which these clasts were eroded, has not been found, the quartz syenites are considered part of the Nimish igneous suite of rocks. This is further investigated by geochemical studies in the following chapter.

The quartz syenites are medium grained, consisting of alkali-feldspar, quartz, sodic plagioclase, secondary chlorite, and accessory apatite, titanite, and zircon.

Chapter 4

Geochemistry

4.1 Introduction

In Chapter 4, whole-rock, major, trace, and selected rare earth element analyses of volcanic and intrusive rocks are presented and interpreted. A primary objective is to test the hypothesis that the Nimish volcanic and intrusive rocks represent suites of cogenetic rocks. Therefore numerous different empirical magmatic-tectonic discrimination schemes have been utilized. The hypothesis is not rejected, however some doubt over the utility of these diagrams for altered Proterozoic suites is expressed. The analyses are interpreted with respect to magmatic affinities (magma series) and possible paleotectonic environments. Electron microprobe analyses of primary and secondary mineral phases in the intrusive rocks are similarly interpreted. Furthermore, the effects of alteration upon the Nimish Formation volcanic and intrusive rocks, as well as the utility of empirical petrotectonic discrimination diagrams for these altered rocks, are discussed.

4.2 Effects of Alteration

Field and petrographic evidence clearly shows that all the volcanic and intrusive rocks of the Nimish Formation have been variably altered with the result that their primary mineralogy is only, at best, partially preserved. In addition, examination of whole rock major and trace element geochemistry indicates that the ranges and abundances of many of the major elements, as well as those of some trace elements, neither represent normal mafic igneous melt compositions nor are they likely to have resulted from primary igneous processes.

The volcanic rocks were extruded in subaerial and submarine environments, the latter possibly having undergone low-grade metamorphism due to submarine hydrothermal activity. Later, the volcanic and intrusive rocks were regionally metamorphosed to the greenschist facies. Other factors possibly involved in obscuring the primary igneous chemistry

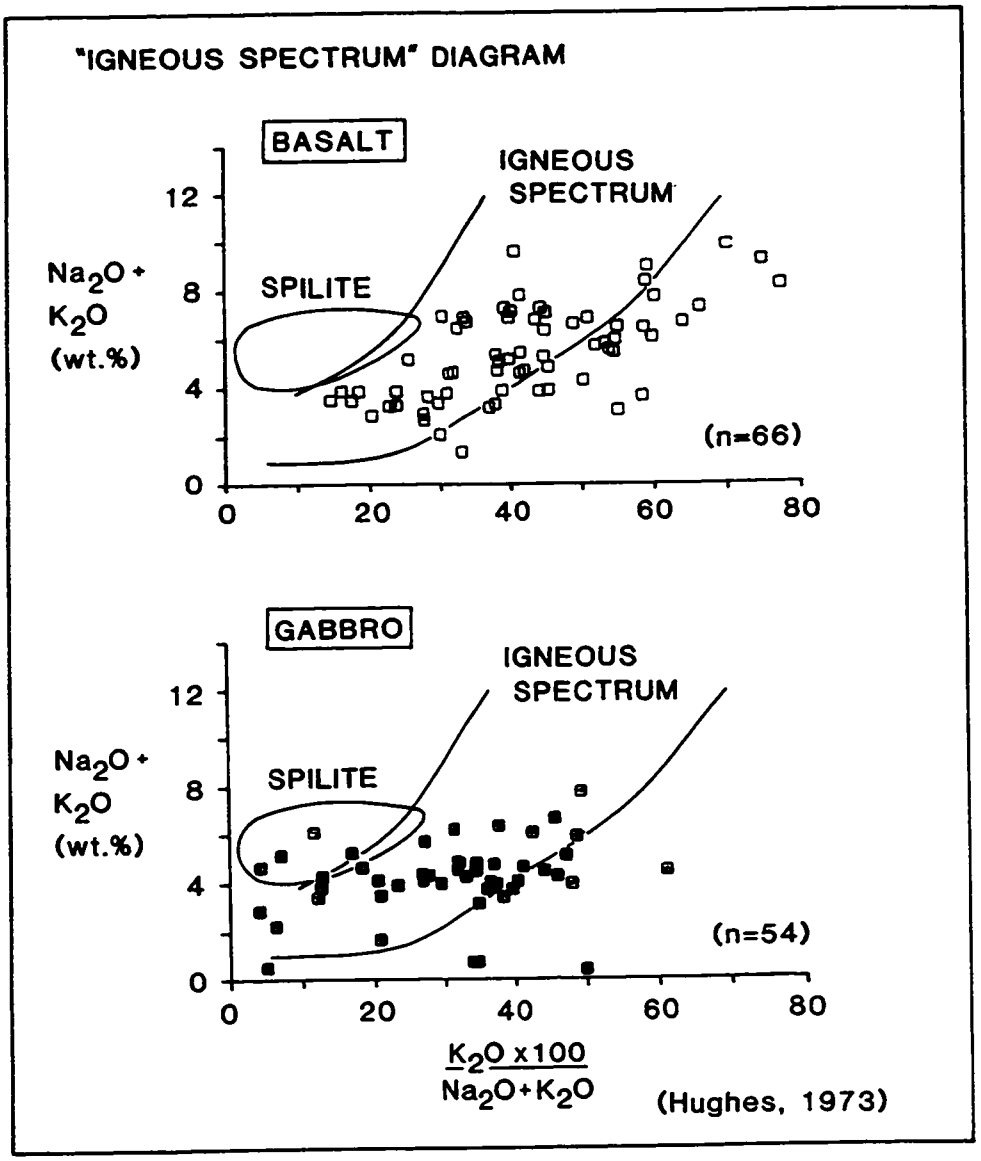

Figure 4.1: "Igneous Spectrum" diagram (Hughes, 1973) for Nimish Formation basalts and gabbros.

of the rocks include retrograde and metasomatic effects. An assessment of the probable effects and extent of these secondary processes on the composition of the rocks is a necessary prerequisite to discussing their geochemistry in detail.

The mobility of the alkali elements Na and K in mafic rocks can be assessed using the igneous spectrum diagram of Hughes (1973) on which fields of normal igneous rocks, spilites,

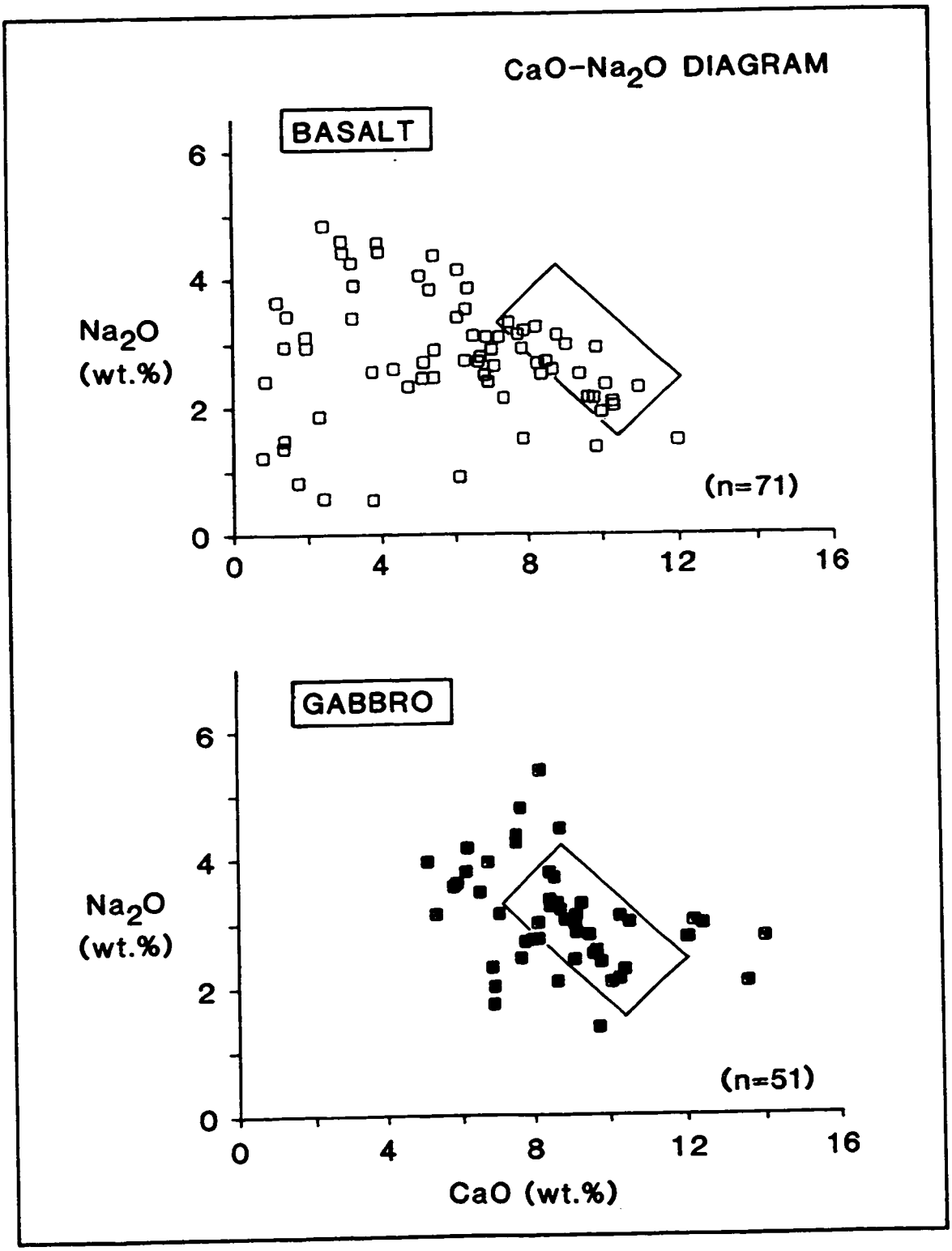

Figure 4.2 Na_2O vs CaO (weight percent, anhydrous) plot for Nimish Formation basalts and gabbros. The box in the diagram outlines the field for normal igneous compositions (Stillman and Williams, 1978).

and keratophyres are defined on a plot of two parameters Na_2O and K_2O (ie. Na_2O+K_2O versus $K_2Ox100/(Na_2O+K_2O)$). On the diagrams shown in Figure 4.1, approximately 5 percent of basalts and 20 percent of gabbros plot outside the "igneous spectrum." Many of the volcanic samples plot below the "spectrum" suggesting substantial Na_2O depletion and addition of K_2O. Similarly, eleven intrusive samples appears to have been affected by this process. Further, five intrusive samples plot in the "spilite field" indicative of Na_2O addition and K_2O depletion. Sample that plot within the "igneous spectrum" may be relatively unaltered. However, it is also possible that they have experienced addition of both K_2O and Na_2O in appropriate proportions so as to have moved their bulk compositions parallel to their field boundaries.

Evans (1978) observed a similar enrichment in K_2O for the Nimish mafic volcanic rocks and ascribed the enrichment to a metasomatic fluid having high ratios of K^+/Na^+ and K^+/Ca^+ which altered the volcanic rocks at temperatures of 200°C to 300°C.

Calcium mobility is tested in Figure 4.2 with reference to a binary plot of Na_2O versus CaO. Approximately 75 and 55 percent of the mafic volcanic and intrusive rocks respectively, plot outside a field defined for the "normal" composition of igneous rocks (Stillman and Williams, 1978). In particular, the mafic volcanic rocks have apparently been depleted in CaO relative to normal igneous rocks. Most intrusive rocks plot in or near the igneous field on the diagram but with appreciable scatter, indicating both the enrichment and depletion of calcium.

The extent of calcium depletion in the volcanic rocks is readily seen where samples have corundum present in their CIPW (weight percent) norm (Gélinas *et al.*, 1982; Lambert, 1988). The depletion of Ca generates an excess of Al_2O_3 with respect to the combined proportions of Na_2O, K_2O, and CaO and results in the appearance of corundum as a norm mineral.

The above discussion suggests that alkali oxides, Na_2O, K_2O, and CaO are less mobile in the gabbroic rocks compared to the lavas in which these oxides have been substantially redistributed.

By inference, the low-field strength trace elements most susceptible to redistribution (i.e. Rb, Ba, and Sr) are also considered to have been affected. Rubidium abundances of the intrusive rocks (ultramafic and mafic) are generally within the normal range for alkali and transitional basalts whereas the volcanic rocks appear to be slightly enriched. Barium and strontium have low abundances in the ultramafic rocks yet shows high values in the gabbros. Similarly, the volcanic rocks are enriched in Ba and Sr. A number of volcanic samples also show a concomitant enrichment in Sr and Ca, indicating that both these elements were controlled by the same chemical processes.

The mobility of iron is important in that the relative amounts of ferrous and ferric iron influence the determination of the normative mineralogy. It is readily apparent that iron is mobile as there is a large variation in the ferric/ferrous ratios in the volcanic and intrusive samples for which these cations were determined.

As there is a considerable range in SiO_2 content in the basalts and gabbros of the Nimish Formation, it is of interest to investigate the mobility of silica. In modern environments, Humphris and Thompson (1978a, 1978b) have shown that silica is depleted during greenschist facies hydrothermal alteration. As such the silica contents of greenschist facies, hydrothermally altered, mafic volcanic rocks can be considered as minimum estimates of original concentration.

There is substantial agreement among most workers that many elements including the low field strength element (LFSE) Th, the high field strength elements (HFSE) P, Ti, Y, Zr, Nb, Hf, Ta, and the rare earth elements (REE) and are essentially immobile during low grade hydrothermal alteration and metamorphism.

4.3 Geochemistry of the Nimish Formation

4.3.1 Volcanic Rocks

Classification

The whole rock SiO_2 content of the Nimish Formation mafic lavas ranges from 41 to 58 weight percent (recalculated to 100% volatile free). Although SiO_2 content is a critical parameter in chemical volcanic rock classification and nomenclature, such a criterion does not appear applicable to the Nimish Formation as it only serves to separate mineralogically and chemically very similar extrusive rocks. The major oxide and trace element abundances of almost all of the samples is typical of basalts; as is the mineralogy where found to be "primary." Thus, in accordance with the Basaltic Volcanism Study Project (1981) which defines basalts as having SiO_2 contents between 38% and 56%, all of the Nimish Formation mafic lavas can be considered basalts.

The abundances of minor and trace elements for the mafic volcanic rocks indicate that they probably represent a single, petrogenetically related suite. Although some elements and oxide exhibit wide compositional ranges, most other have ranges that could have resulted from a relatively simple fractionation process and fall within the average compositional ranges of basalt. For example, Zr contents varies from 102 to 247 ppm, values reasonably with the differentiation range of basalts (Figure 4.3). A similar argument holds for other incompatible and compatible elements such as TiO_2 (1.01% to 3.15%) and Cr (22 ppm to 290 ppm).

The rocks of intermediate and felsic composition comprise only a minor proportion of the extrusive rocks of the Nimish Formation. They form a chemical continuum with the mafic volcanic rocks indicating that, as a whole, the Nimish volcanic rocks describes a suite of progressive differentiation from mafic to felsic rocks.

The range of SiO_2 contents of intermediate and felsic rocks is from 57% to 72%. Magnesium and iron (ferrous and ferric) have an inverse relation in abundance to the increase

in silica content. In addition, incompatible trace elements, both LFSE and HFSE, have generally low abundances in these rocks.

Based on stratigraphic, petrologic, and geochemical data, Evans (1978) subdivided the Nimish igneous rocks into two separate suites, giving each suite formational status. With respect to location, the lower, Petitsikapau Lake Formation, is restricted to the thrust slice east of Dyke Lake whereas the upper, Astray Lake Formation occurs to the west as is found within the thrust block between Astray and Dyke Lakes. The Sokoman Formation is the stratigraphic horizon that separates the two formations (Evans, 1978). The volcanic rocks of each suite were further subdivided according to their SiO_2, TiO_2, P_2O_5, and Zr abundances. As such, he recognized two volcanic cycles, each having followed similar, but slightly different, fractionation schemes.

However, during the course of field mapping it was found that there were no reliable field criteria by which to differentiate the rocks of these two suites. Furthermore, there is pervasive and complex interbedding of the lavas with the Sokoman Formation throughout the study area whereby it was not clear where the Sokoman served to separate the two suites. Moreover, briefly comparing the volcanic geochemistry of these two supposed suites, it does not appear that they are obviously divisible into two separate groups.

Magma Series

Gill (1981) defines magma series as "magmas which are genetically related to each other by some differentiation process(es) or by being separate partial melts of a common source under similar conditions." However, assigning Archean and Proterozoic rocks to a particular magma series is commonly hindered by the variably altered nature of these rocks which renders many of the classifications based on mobile whole rock major elements unreliable. In addition, there are a number of different criteria which have been proposed to distinguish alkaline and subalkaline rock associations (e.g. Miyashiro, 1978).

Nonetheless, there is general agreement as to the division of mafic volcanic rocks into alkaline and subalkaline (or non-alkaline) series. In unaltered rocks, these two major groups can readily be distinguished by their normative mineralogy (Yoder and Tilley, 1962), relative alkali contents (MacDonald and Katsura, 1964; Irvine and Baragar, 1971), and alkali-lime indices (Peacock, 1931). For altered rocks, the high field strength (HFSE) and incompatible elements TiO_2, Zr, Y, Nb, and P_2O_5 may provide a basis for separating these magma series (Pearce and Cann, 1973; Floyd and Winchester, 1975, Winchester and Floyd, 1976). The conclusions obtained can be verified with reference to the primary mineralogy of the rocks, if such minerals can be identified (i.e. clinopyroxene).

In their study of the geochemical characteristics of magma types from different tectonic regimes, Pearce and Cann (1973) noted that there was an increase in the concentration of Nb with respect to either Zr or Y associated with increasing alkalic character of the suite. As such, alkalic ocean island and continental basalts are characterized by a Y/Nb ratio <1 whereas that of ocean-floor alkalic basalt is <2. Except for one sample (#1157), all of the Nimish mafic lavas have Y/Nb ratios <2 characteristic of the alkaline series. Furthermore, 80% of the samples have Y/Nb ratios <1 indicating the basalts have either a continental or ocean island affinity. Winchester and Floyd (1977) inverted the above ratio and suggested that a value of Nb/Y=0.67 satisfactorily divides alkaline and subalkaline magma suites. Using this value, 92% of the mafic volcanic rocks are considered alkaline.

Floyd and Winchester (1975) and Winchester and Floyd (1976) present a series of binary plots that discriminate between alkaline and tholeiitic magma types. In addition to being recognized as immobile elements during alteration and metamorphic processes, they emphasize the use of P, Ti, Y, Zr, and Nb as they are considered to be relatively enriched in alkali basalts compared to tholeiites. As such, the plots can be utilized to distinguish alkaline and subalkaline magma types for altered and metamorphosed rock suites.

The log (Nb/Y) vs. log (Zr/P_2O_5) diagram (Winchester and Floyd, 1977) shows that the mafic lavas of the Nimish Formation are alkaline in nature and shows minor differentiation to trachyandesites and trachytes (Figure 4.4).

Paleotectonic Setting

There are a number of empirical approaches in the geologic literature that allow discrimination between volcanic rocks formed in different tectonic environments. Most compare geochemical trends and abundances of modern rocks in known environments to unknown ancient environments (e.g. Pearce and Cann, 1973; Wood *et al.*, 1979; Meschede, 1986). On the tectonic discrimination plot of Meschede (1986), the geochemistry of the immobile elements Nb, Y, and Zr indicates that the Nimish basalts have "within-plate" affinities of which the majority indicate a continental intraplate setting (Figure 4.6).

There exists but few schemes for the classification and interpretation of paleo-tectonic environment for intermediate and felsic volcanic rocks. Most are designed for mafic volcanic rocks. On the Nb/Y vs. Zr/P_2O_5 plot of Winchester and Floyd (1977), the volcanic rocks have an alkaline affinity and plot as trachyandesites and trachytes (Figure 4.5).

4.3.2 Intrusive Rocks

Ultramafic and mafic intrusive rocks comprise an important part of the igneous activity of the Nimish Formation. Sills of predominantly mafic composition are found throughout the study area whereas discontinuous lenses of ultramafic rocks are restricted to one part of the study area. The ultramafic rocks appear to outcrop as part of a gabbro sill, however due to poor exposure the exact relationship between the two rock types is ambiguous. Nonetheless, the discovery of ultramafic rocks allows for the study of what probably was the most primitive magmatic rocks of the Nimish Formation.

The purpose of this section is two-fold. First, to geochemically assess the ultramafic and mafic intrusive rocks, the latter also being considered in terms of volcanic geochemical

classification and paleotectonic environments. Second, to consider the geochemical relationship between the ultramafic and mafic rocks.

Classification

The ultramafic rocks have SiO_2 contents restricted to between 42% and 46%. There is some overlap with the mafic intrusive rocks in this regard but they can be recognized on the basis of their major, minor, and trace element abundances. For example, MgO content ranges from 21% to 19%, Cr from 5000 ppm to 2500 ppm, and La from 4.8 ppm to 8.5 ppm.

The mafic rocks are predominantly gabbros and have many of the same ranges of major, minor, and trace element abundances as for the mafic volcanic rocks.

The most important observation of the ultramafic and mafic intrusive rock chemistry is that these rocks comprise a chemical continuum in which elemental abundances either show a distinct break (ie. Cr) or gradual increase or decrease (ie. SiO_2). It is most probable that these breaks and chemical discontinuities represent the crystallization sequence of the magmatic phases such as olivine, chromite, and clinopyroxene.

Magma Series

The ultramafic rocks do not conform to the majority of empirical classifications as no diagrams have allowances for such primitive rocks. For example, on the TiO_2 vs. Zr/P_2O_5 diagram of Winchester and Floyd (1976; not shown here), where most of their associated gabbroic rocks plot in the alkaline field, the low TiO_2 abundances of the ultramafic rocks misclassifies them as tholeiites. Nonetheless, their elemental ratios (ie. Y/Nb <1) do indicate that these rocks have alkaline affinities.

The gabbroic rocks are similarly alkaline in nature and generally overlap their volcanic counterparts on empirical diagrams (Figure 4.5). The intermediate and felsic intrusive rocks also have alkaline affinities.

Paleotectonic Environment

Empirical paleotectonic diagrams do not make allowances for ultramafic rocks but the known elemental trends from ultramafic to mafic rocks allows for some estimation of the ultramafic rocks. For the most part, these rocks plot outside boundaries established for the environments of mafic volcanic rocks. Yet, on other diagrams (ex. Meschede, 1986), it can be seen that they plot in chemical continuum with the gabbros (Figure 4.7). The ultramafic and gabbroic rocks have "within-plate" affinities and have continental signatures.

4.4 Mineral Chemistry

4.4.1 Clinopyroxene in Ultramafic Sills and Gabbro

Microprobe analyses of clinopyroxenes fropm selected ultramafic and gabbro samples were done in order to further classify the rocks and to complement the whole rock major and trace-element studies. Clinopyroxene occurs in the ultramafic rocks and gabbros as generally 1-4 mm large, subhedral grains. A minor amount of the crystals have either twinning or compositional zoning. Most grains show some evidence of alteration. These were easily avoided during the microprobe analyses.

Analytical results from microprobe analyses of clinopyroxenes are presented in Appendix C and plotted on the pyroxene quadrilateral in Figure 4.8. The ranges of clinopyroxene compositions of both ultramafic and mafic rocks plot at the augite-diopside boundary with the clinopyroxenes ultramafic rocks being slightly more Mg-rich. In addition, they plot above the Skaergaard trend suggesting that they are non-orogenic in nature.

4.4.2 Pyroxene as Indicators of Magmatic Affinity

Clinopyroxene compositions have been used to discriminate between magma types, especially in those cases where the whole rocks are altered and the pyroxenes are not. As such, they provide a useful check on conclusions reached on the basis of whole rock geochemistry.

LeBas' (1962) work on groundmass pyroxenes showed that the atomic proportions of the major cations change regularly with differentiation and magma type. He constructed fields in the pyroxene quadrilateral to discriminate non-alkaline, alkalic, and peralkaline magma types. Figure 4.9 shows that the clinopyroxenes from the gabbro are alkalic.

4.5 Geochemical Modelling

The trends in the trace element geochemistry of the Nimish volcanic and intrusive suites can be used to distinguish between partial melting and fractional crystallization processes. Their distribution on element-element plots can be explained following the reasoning of Hanson (1989) and Maaloe (1985). The conclusions reached by this method are compared to the technique outlined by Allègre *et al.* (1977).

The R/I discrimination method (Maaloe, 1985) is an extension of the technique developed by Treuil (1973). The method compares two trace elements with substantially different bulk distribution coefficient (D) values to evaluate their distribution on a scatter plot. The term R is assigned to the compatible trace element, and I is given to the incompatible trace element. On a binary plot, the convention is to place the incompatible trace element I on the ordinate and R along the abscissa. The data will have a characteristic distribution for each of the two processes. Specifically, the incompatible element I displays a large variation by partial melting whereas it is the compatible element R which displays a large variation during fractional crystallization (Figure 4.10). Although Hanson (1989) does not use the terms R and I, he does emphasize that on a plot of an element with a D value less than 1 and an element with a D value greater than 1, partial melting can be distinguished from fractional crystallization.

The geochemistry of the Nimish volcanic and intrusive rocks indicates that the suites evolved from fractional crystallization processes. In both cases, the plot of Cr (compatible or R element) versus La (incompatible or I element) serves to illustrate that partial melting is not the dominant process. Figure 4.10 shows the distribution of Cr versus La for volcanic rocks.

It can be seen that the Cr values vary from 250 ppm for the most primitive basalt to approximately 25 ppm for the most evolved felsic volcanic rocks. La abundances vary from approximately 10 to 110 ppm. Thus, Cr shows a greater variation in abundance than La and the distribution of data points is indicative of fractional crystallization processes. Similarly, for the intrusive suite, the Cr-La plot indicates crystallization processes (Figure 4.11).

Allègre *et al.* (1977) outlines another method to test for fractional crystallization processes. By plotting two trace elements , one of which must have a D value much less than one, if the regression line through the data points has a slope less than one (and where the slope = 1-D) then the data are interpreted to have resulted from fractional crystallization processes. If the slope is greater than one, another process other than fractional crystallization must be considered. Log-log plots of La-Ta and La-Th for volcanic rocks shows that, in both cases, the slope of the best-fit line is less than one and therefore the interpretation of the data does not allow rejection of the fractional crystallization hypothesis.

This technique is extended and applied to the Nimish intrusive suites. Using the same incompatible elements as for the volcanic rocks (La, Ta, and Th), it is interpreted that the intrusive suite is similarly related by fractional crystallization. Note that there is a poor fit to the data in comparison to those of the volcanic rocks. Strictly, the technique is only applicable to liquid composition. The intrusive rocks may also record an in-situ fractionation event which would perturb the trace element distribution and possibly account for the greater variance.

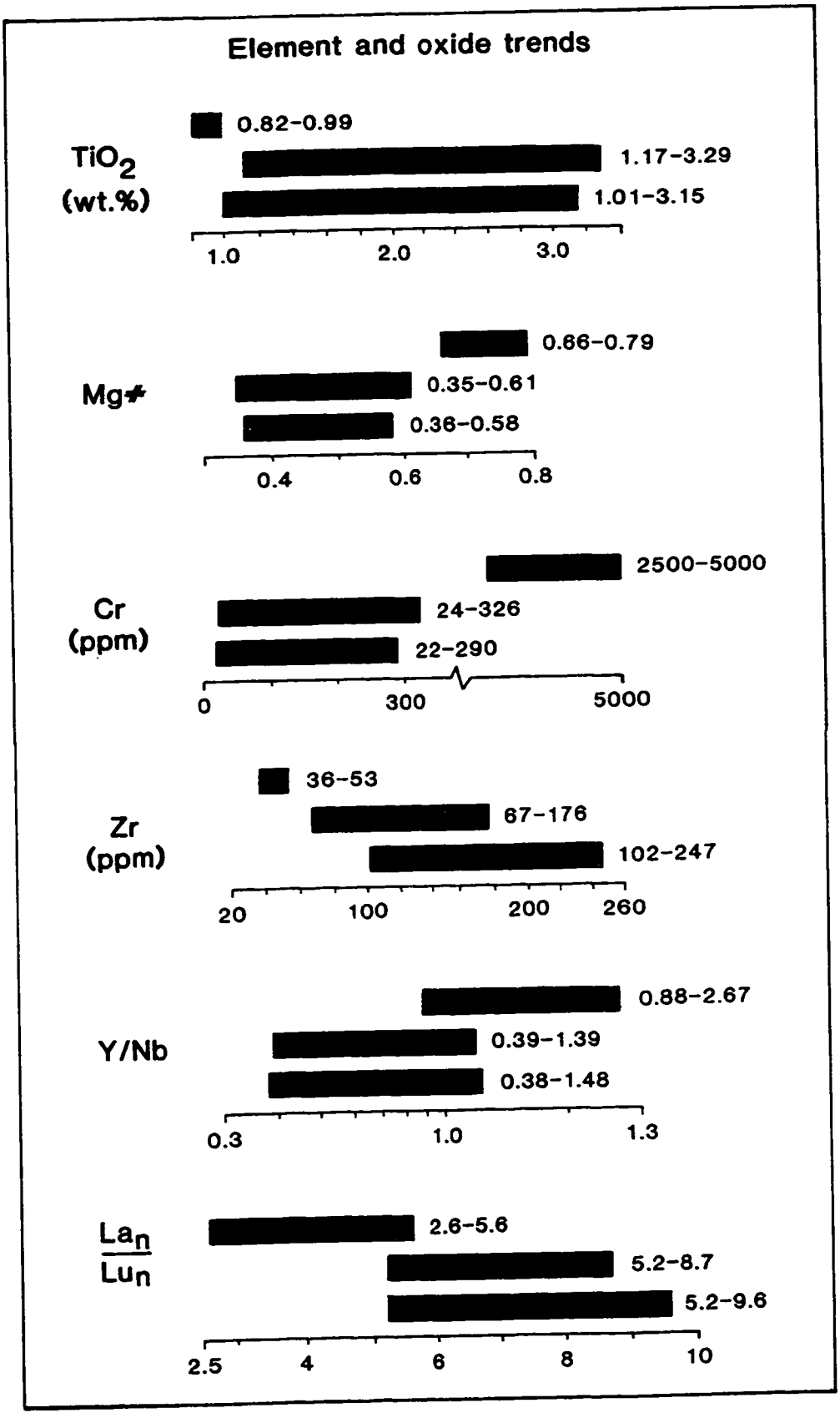

Figure 4.3 Elemental and ratio trends for Nimish Formation basalts (green), gabbros (brown), and ultramafic rocks (purple).

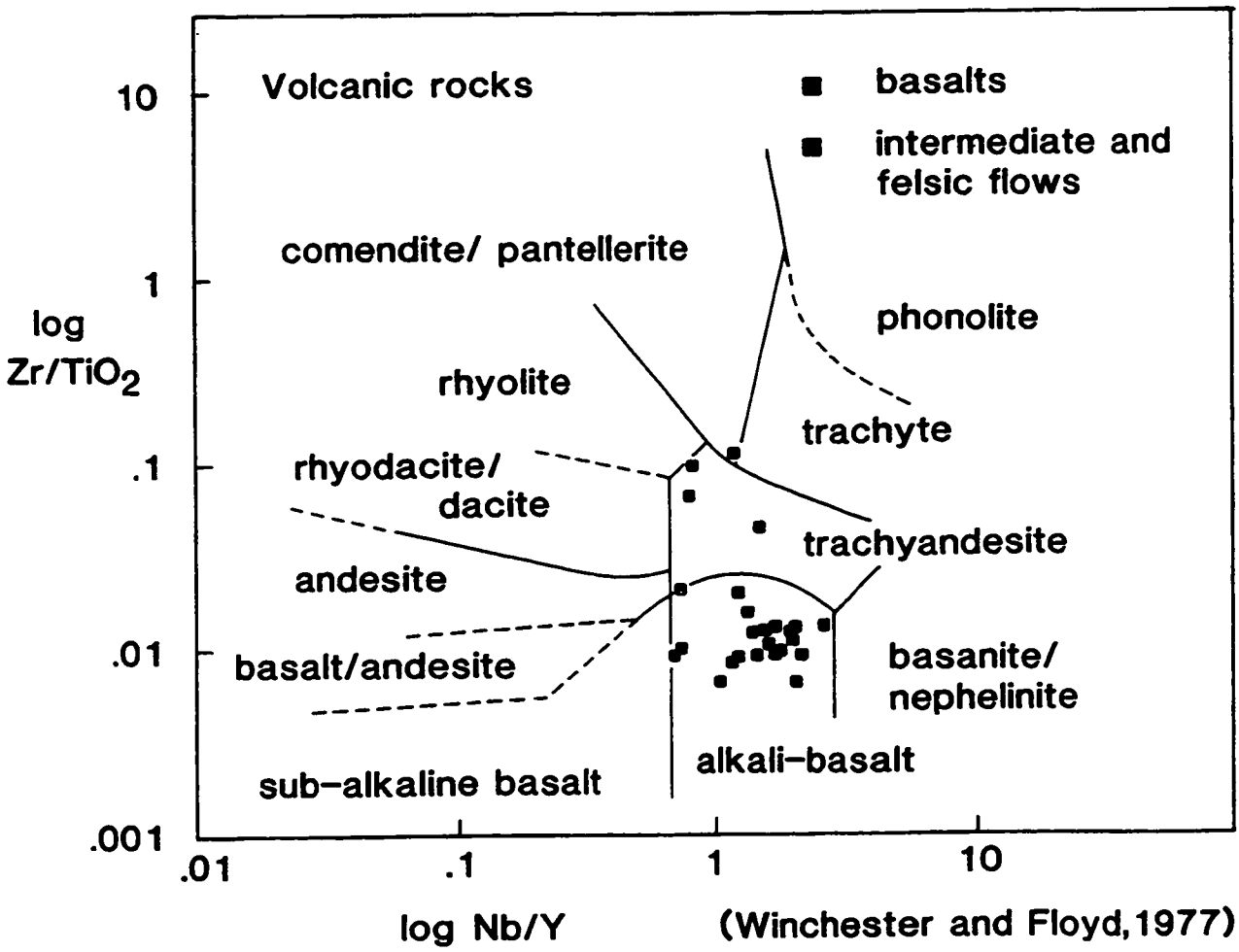

Figure 4.4 Log (Zr/TiO2) vs. Log (Nb/Y) diagram for Nimish Formation volcanic rocks; basalts (green), intermediate and felsic flows (red).

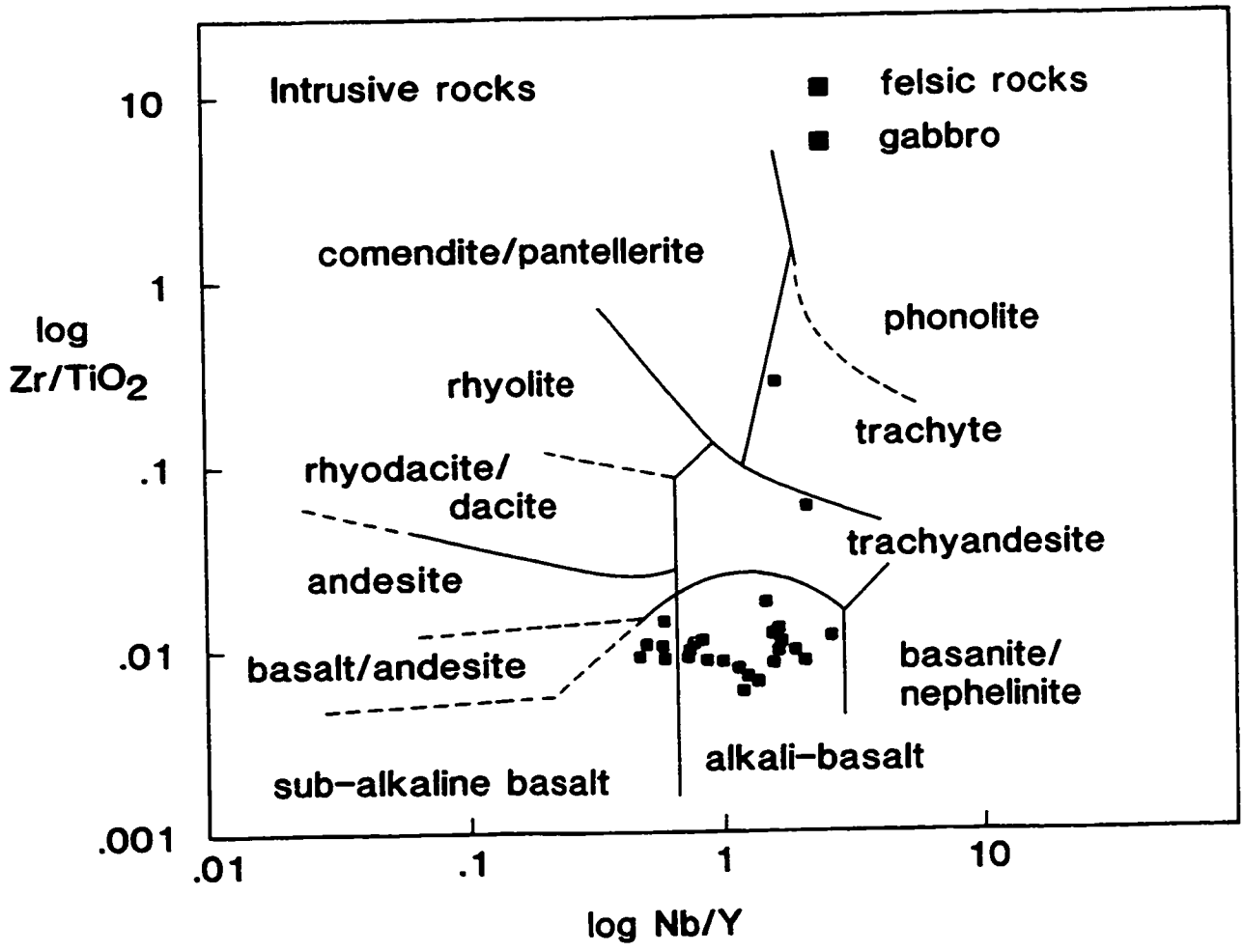

Figure 4.5 Log (Zr/TiO2) vs. Log (Nb/Y) diagram for Nimish Formation intrusive rocks; gabbros (brown), intermediate and felsic differentiates (red).

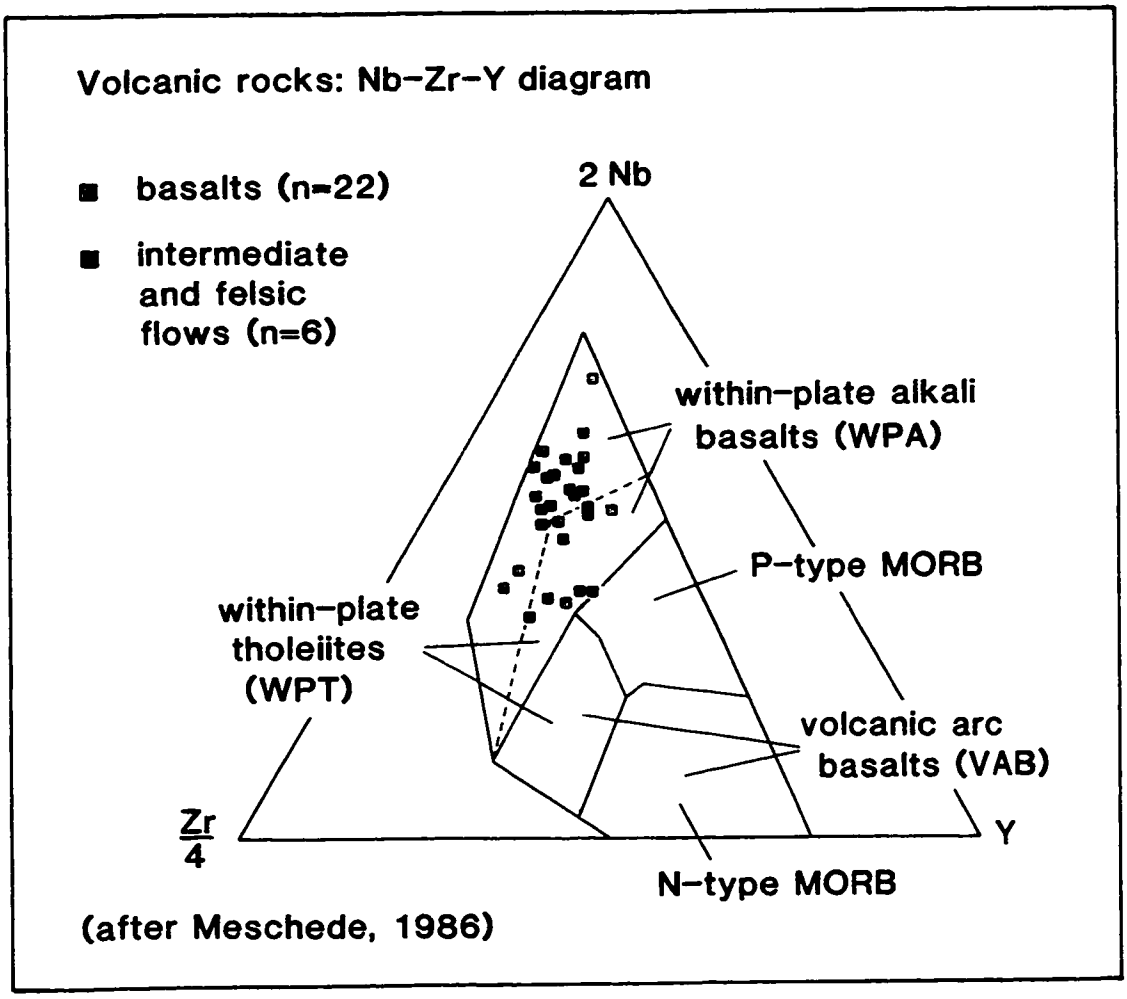

Figure 4.6 Nb-Zr-Y tectonic discrimination diagram for Nimish Formation volcanic rocks; basalts (green), intermediate and felsic flows (red).

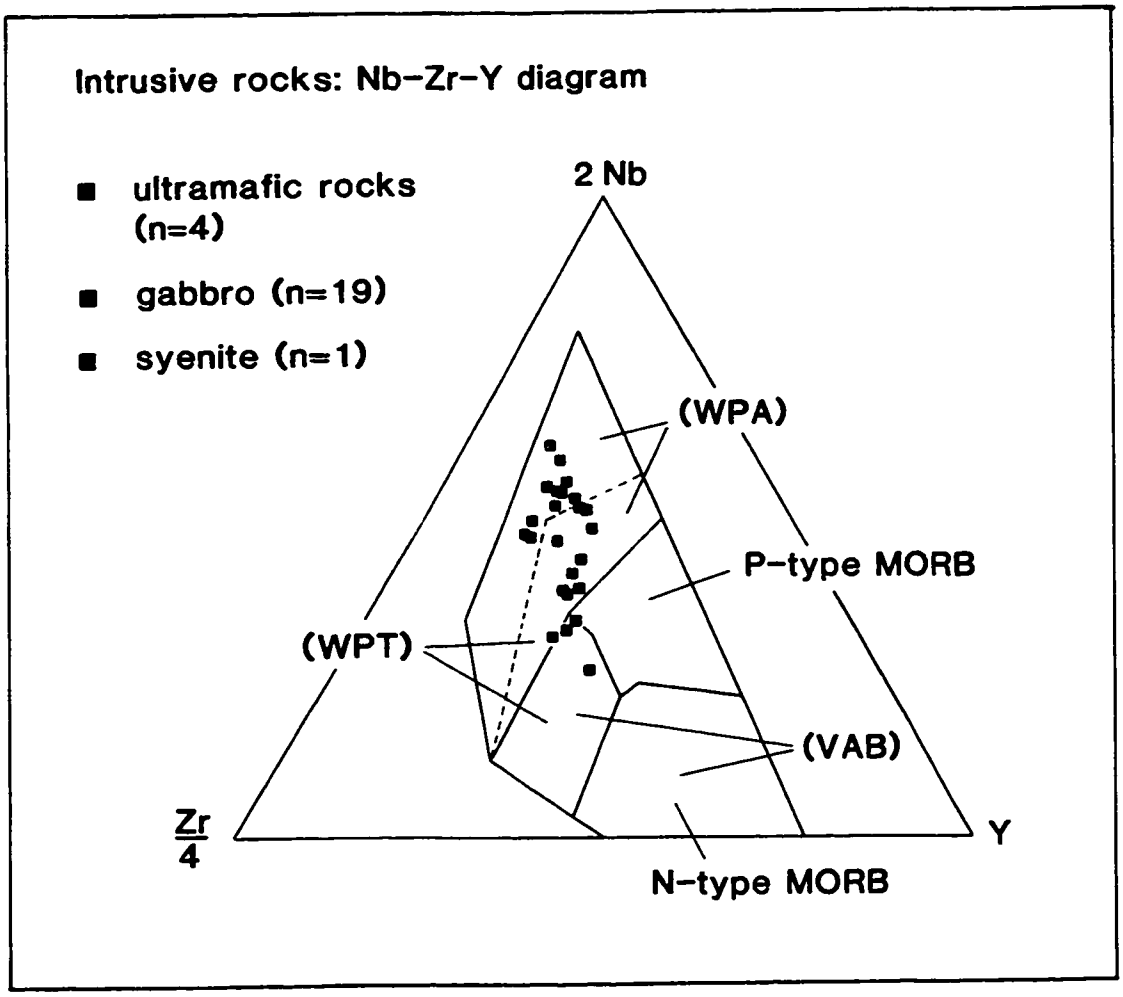

Figure 4.7 Nb-Zr-Y tectonic discrimination diagram for Nimish Formation intrusive rocks; gabbro (brown), syenite (red), and ultramafic rocks (purple).

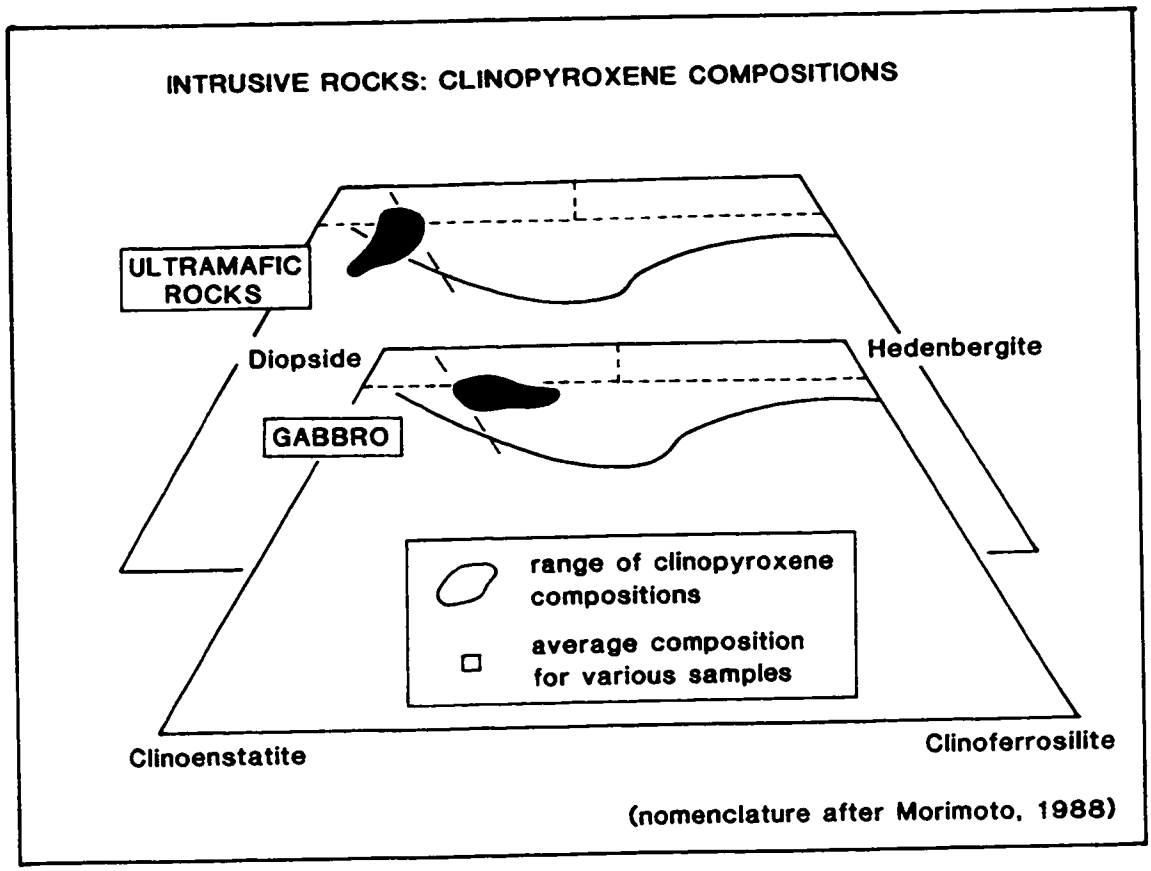

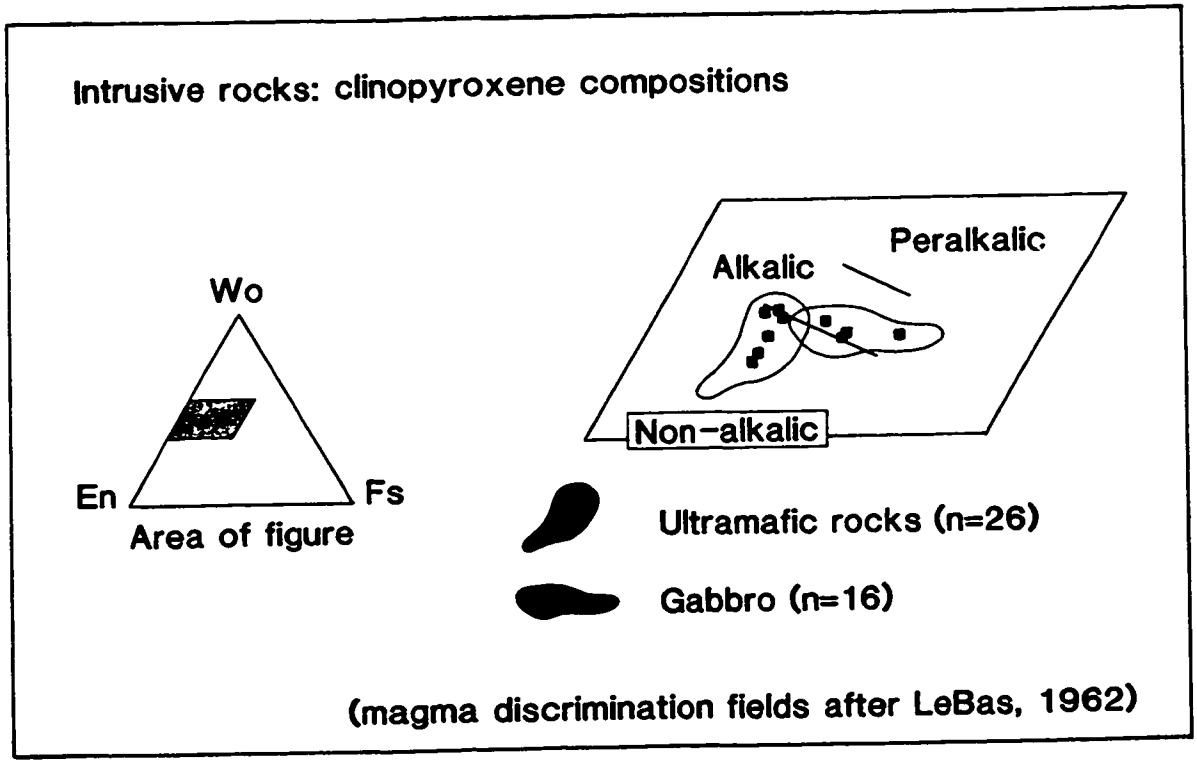

Figure 4.8: Clinopyroxene compositions for ultramafic rocks and gabbro plotted on the pyroxene quadrilateral and **Figure 4.9:** Clinopyroxene compositions plotted in magmatic discrimination fields.

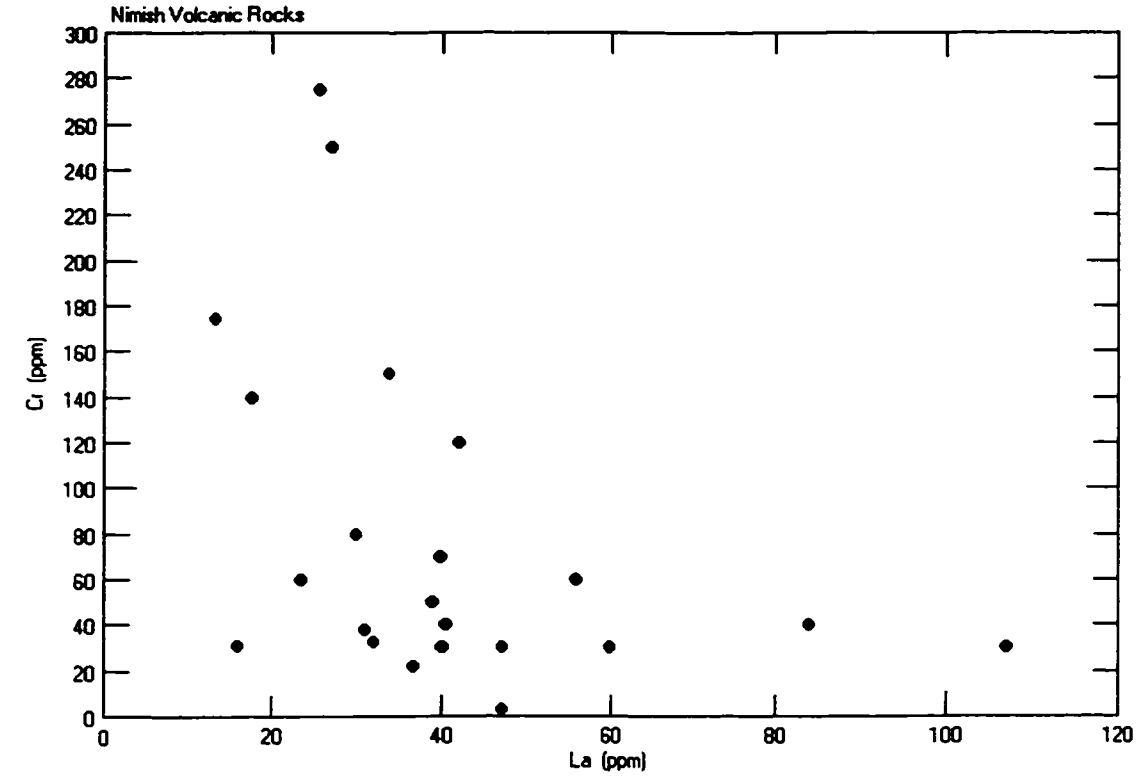

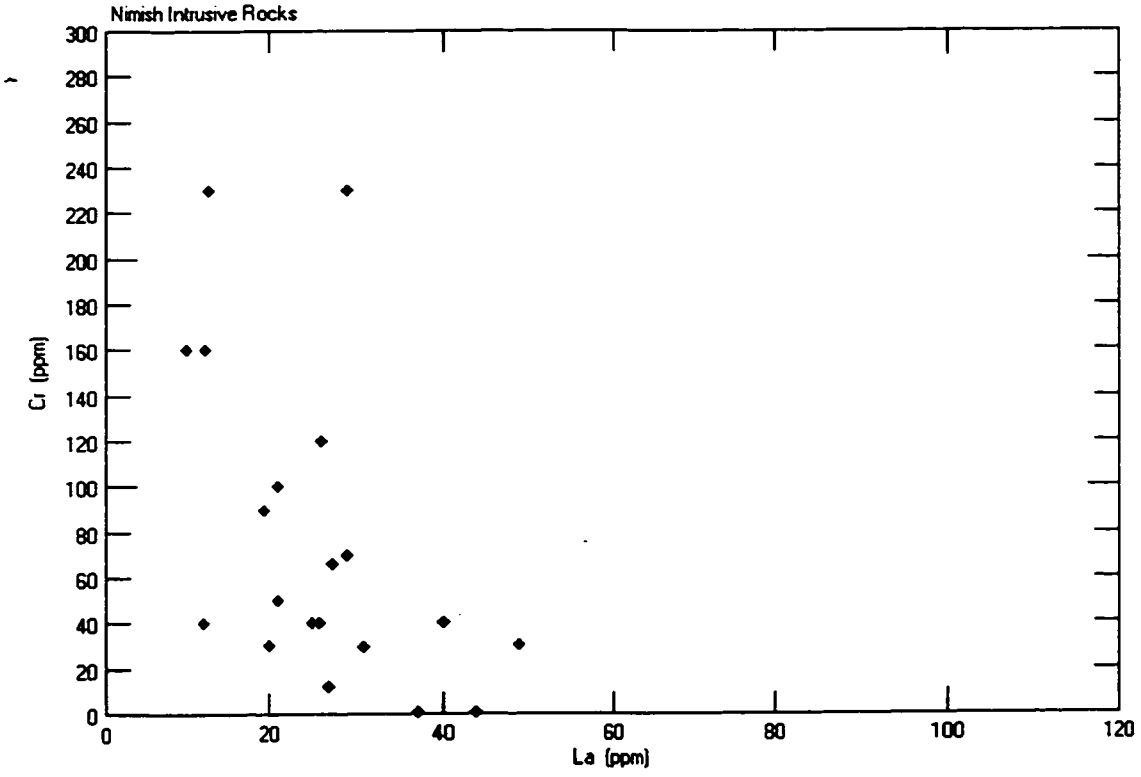

Figure 4.10 Cr-La plot for Nimish Formation volcanic rocks.
Figure 4.11 Cr-La plot for Nimish Formation intrusive rocks.

Chapter 5

Petrogenesis

5.1 Assessment of Crustal Contamination

The rocks of the Schefferville zone have been interpreted by Wardle and Bailey (1981) to represent sedimentation and predominantly volcanic activity upon a rifted continental margin. The geochemistry of the Nimish Formation extrusive and intrusive rocks show that the suite has an alkaline affinity indicative of a rifting environment during this particular time of Schefferville Zone development. The question arises as to whether the alkaline trend is a primary magmatic feature or one inherited through assimilation of continental crust by a basaltic lava. Crustal contamination is evaluated through the inspection of trace element data, the use of extended trace element diagrams and Samarium-Neodymium isotopic systematics.

5.2 Trace Element Geochemistry

The possibility that crustal contamination has affected the Nimish geochemistry is first assessed by an empirical plot of log (Th/Yb) vs. log (Ta/Yb); Pearce (1982). It serves as a discrimination diagram in which a field is outlined for volcanic rocks from within-plate settings. Furthermore, the within-plate setting is subdivided into tholeiitic, transitional, and alkaline fields.

The plot serves as a test for crustal contamination because Th is a component of the diagram. Thorium is enriched in crustal rocks and any appreciable contamination of the magma with crustal material would show such an enrichment on the diagram, i.e. the data points would not plot within the outlined discrimination fields and would have more of a vertical trend (Pearce, 1982). The data for a limited number of Nimish volcanic rocks indicates no significant Th enrichment and plots within the field designated for a within plate setting and appear to span the compositional range from tholeiitic to alkalic.

5.3 Normalized Extended Trace Element Diagrams

Representative volcanic and intrusive rocks of the Nimish Formation were plotted on normalized extended trace element diagrams (Figures 5.1 and 5.2) in order to investigate relative elemental enrichments and/or depletions of the samples of these two suites. Complementary REE profiles are shown in Figures 5.3 and 5.4. The diagrams are a useful tool in assessing crustal contamination processes as well as serving to characterize the magma source for the suites. The elements chosen for the diagrams are immobile high-field strength elements (HFSE) and rare earth element (REE) and are normalized against N-MORB (Pearce, 1982; Sun and McDonough, 1989) for reference. The normalizing values used are listed in Appendix D.

The Nimish volcanic and intrusive rocks show a marked incompatible element enrichment trend on normalized extended trace-element plots. Nb, Zr, and Y depletions relative to adjacent elements are also noted. Such enrichments are very similar to trace-element patterns of alkaline basalts from oceanic (OIB) and continental areas (Norry and Fitton, 1983). As such, the parental magmas to the Nimish were probably derived from an undepleted to enriched mantle source.

5.4 Samarium-Neodymium isotopic systematics

This section presents data from the analysis of two samples representing mafic and felsic members of the Nimish Formation (Table 5.1). A syenite clast, comparable to that analyzed for Sm-Nd isotopes, has been dated by U-Pb zircon methods and yielded a crystallization age of 1877.8 ± 1.3 Ma (Findlay *et al.*, 1995). This age is used for the calculation of initial $^{143}Nd/^{144}Nd$ and ε_{Nd} values. The Sm-Nd isotopic analyses were performed at the geochronology laboratories of the Geological Survey of Canada. Details of the analytical procedures used for the analyses are given by Thériault (1990).

Table 5.1 Sm-Nd isotopic data for Nimish Formation basalt and syenite.

Sample	No.	Description	Sm (ppm)[1]	Nd (ppm)[1]	$^{147}Sm/^{144}Nd$	$^{143}Nd/^{144}Nd$ (2σ)[2]	ε_{Nd} (1879 Ma)[3,4]
86 W10-11	396	Basalt	7.06	36.79	0.1160	0.518807(4)	+3.27
86 B16-5A	708	Syenite	17.74	102.2	0.1049	0.511474(6)	-0.57

[1] Estimated 2σ analytical uncertainty is ± 0.5%

[2] $^{143}Nd/^{144}Nd$ normalized to 0.7219; estimated 2σ analytical uncertainty is ± 0.003%

[3] Parameters for ε_{Nd} calculations are $^{143}Nd/^{144}Nd_0$ (CHUR) = 0.512638 and $^{147}Sm/^{144}Nd_0$ = 0.1967.

[4] 1879 Ma age date obtained from Findlay *et al.*, 1995.

The basalt sample chosen for analysis (#1120) comes from a predominantly aphyric flow intercalated with matrix-supported volcanic conglomerate. This unit overlies thinner bands of iron formation and quartzites of the Sokoman and Wishart Formations respectively. Fractionation indices such as SiO_2, Cr, and Mg# for the sample indicates that it is one of the least evolved members of the Nimish volcanic suite.

The Nimish basalt has a ε_{Nd} value of +3.27 (t=1879 Ma) indicating initial $^{143}Nd/^{144}Nd$ higher than that of CHUR at the time of formation. Further, the positive ε_{Nd} value points to derivation from an isotopic reservoir that was depleted in Nd in comparison to an undepleted CHUR source. This value is comparable to those of basaltic rocks from the northern and central Labrador Trough (Skulski, 1993; Findlay, 1996).

In his study of tholeiites and basalts of the Labrador Trough Basaltic Suite, Findlay (1996) suggested the presence of two compositionally distinct mantle reservoirs during the evolution of the Labrador Trough; a depleted asthenospheric mantle reservoir and a second less depleted source referred to as "undepleted mantle." Modelling calculations by Findlay (1996)

indicated that the Nimish volcanic rocks represent partial melts derived primarily from the undepleted source but with minor contributions from the depleted reservoir.

The Nimish syenite has a ε_{Nd} value of -0.57 (t=1879 Ma). The value had initial $^{143}Nd/^{144}Nd$ lower than that of CHUR at the time of formation. In contrast to the basalt, this value indicates a contribution from a source enriched in Nd relative to CHUR. As such, sialic crust has contributed to the isotopic composition of the syenite.

5.5 Geologic and Paleotectonic History of the Nimish Formation

Alkaline basaltic magmatism is the result of complex, multistage processes, and occurs in a variety of continental and oceanic tectonic settings. They range from alkalic lavas associated with oceanic hot spots (e.g. Hawaii), intraplate rifting (e.g. East African Rift), to those found in island arc environments. In general, alkaline rocks rarely occur in large volumes and, in many cases, they are subordinate to the other volcanic rocks in the region where they are found. Although the magmatism of the Labrador Trough is volumetrically dominated by oceanic tholeiitic volcanism, two events of alkaline magmatism are recorded during the deposition of the Knob Lake Group sedimentary succession. U-Pb dating has established that these two alkaline events were separated by about 300 Ma (Findlay *et al.*, 1995). The older unit is found in the basal Seward Subgroup associated with arkoses and conglomerates interpreted to have been deposited during a rifting event. The trace-element geochemical data of the Nimish Formation indicates that they are a mildly alkaline suite within the continental shelf assemblage of the Knob Lake Group. This is in contrast to the lack of conclusive sedimentological evidence suggestive of extensional conditions during the time of Nimish volcanism.

The geological, geochemical, and isotopic data suggests that the development of the Nimish Formation can be described in four stages.

Stage 1 involves the extrusion of the cycle 1 Chakonipau alkaline volcanic rocks in a rift valley during an initial stage of crustal extension. Stage 2 characterizes the deposition of the shelf sequence of the Knob Lake Group upon the passive margin of the Superior Craton. Stage 3 records the extrusion of Nimish basalts during a second extensional event. Sills of predominantly gabbro composition intrude the shelf assemblage of the Knob Lake Group during this same period. Stage 4 represents the cessation of crustal extension in the Schefferville Zone during the early stages of deeper-water Menihek shale deposition.

Alkakine magmatism of the Chakonipau and Nimish Formations are volumetrically insignificant compared to the ocean tholeiite magmatism of the Montagnais Group (Wakuach Gabbro and Retty Peridotite). The geochemistry of these magmatic suites suggests that the much of the tholeiitic magmatism has T-MORB affinities (Findlay, 1996).

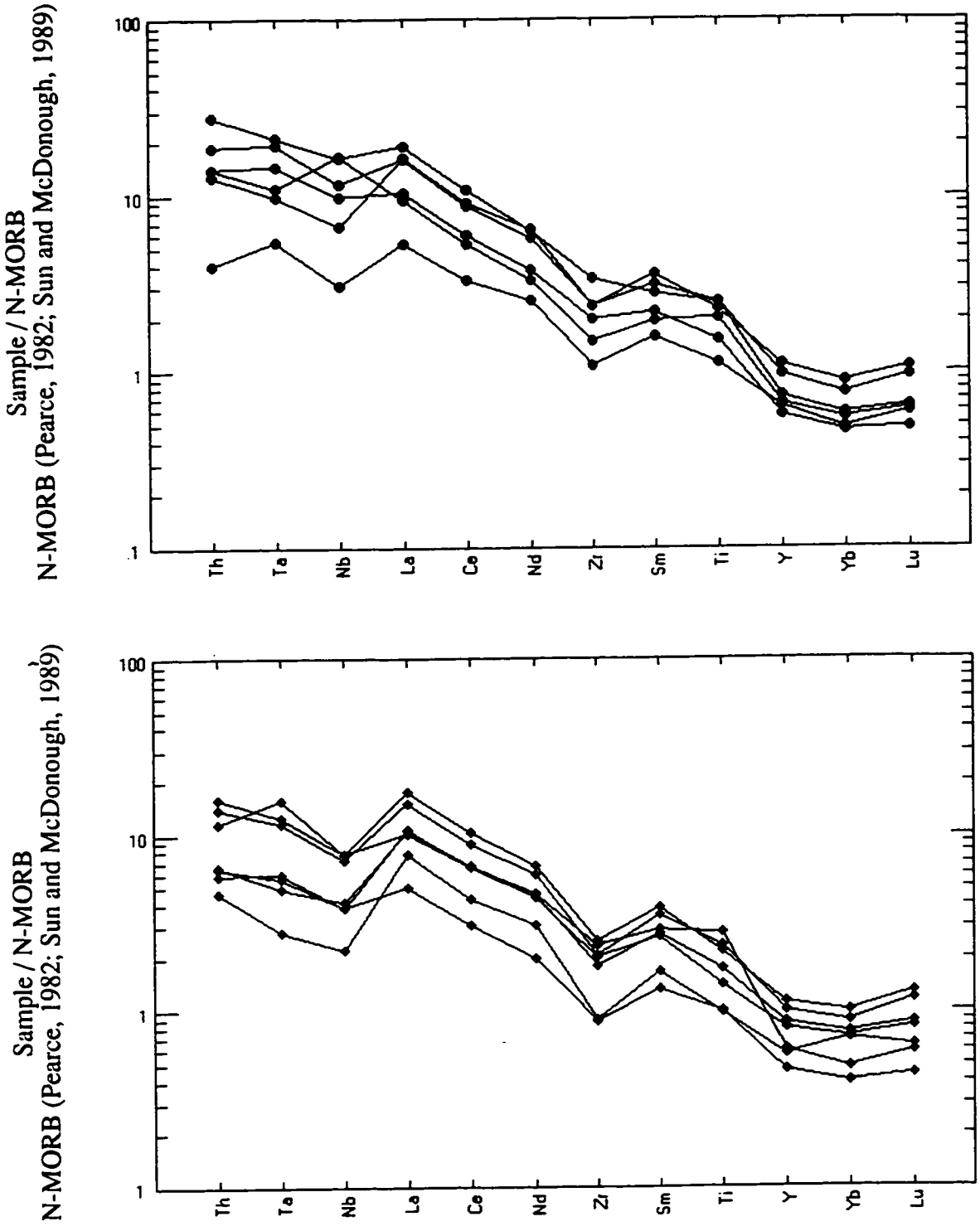

Figure 5.1: Normalized extended trace element diagram for Nimish basalts.
Figure 5.2: Normalized extended trace element diagram for Nimish gabbros.

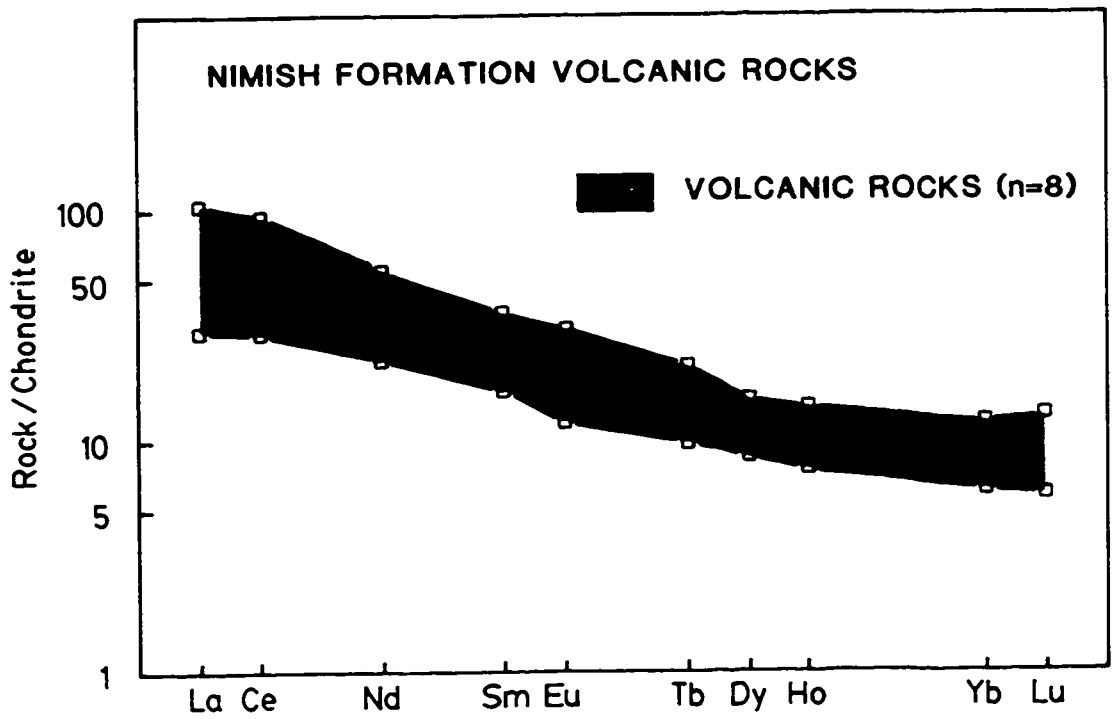

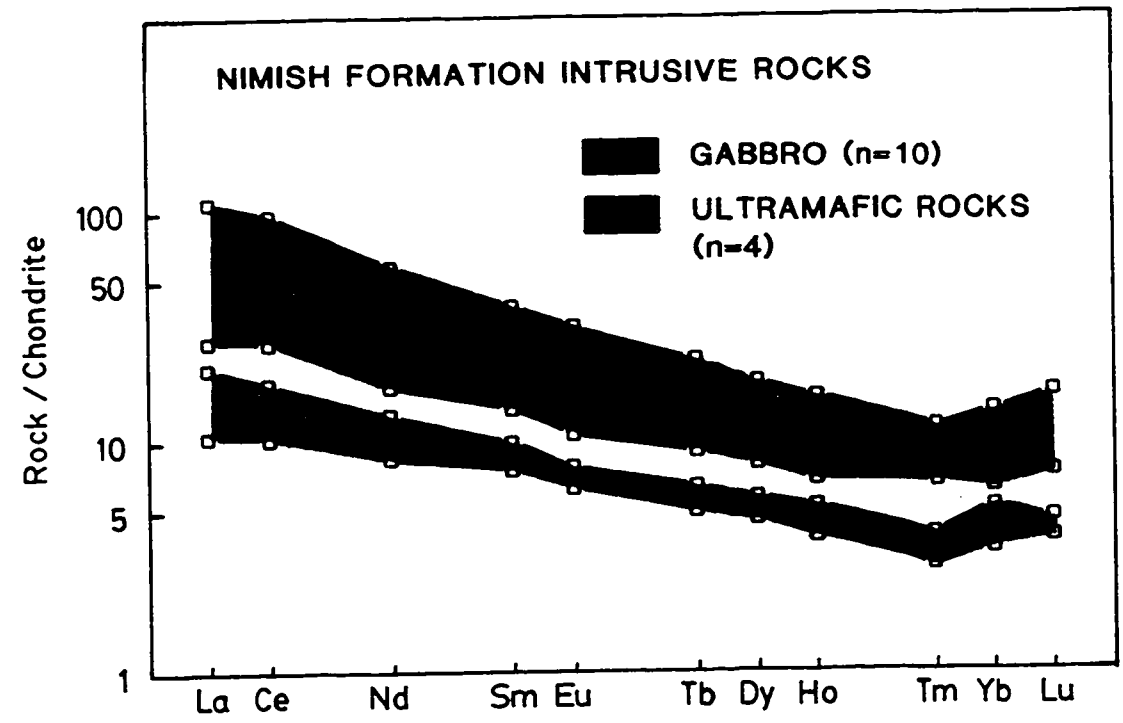

Figure 5.3: REE plot for Nimish Formation basalts.
Figure 5.4: REE plot for Nimish Formation ultramafic rocks and gabbro.

Chapter 6

Conclusions

The results of a field and geochemical study of the Early Proterozoic Nimish Formation, western Labrador, are as follows:

1. The Nimish Formation is an accumulation of volcanic, intrusive, and volcaniclastic rocks unique found in the Schefferville zone of the Western Division, New Québec Orogen.
2. The volcanic rocks range in composition from alkali basalt to trachyte and have a alkaline to transitional affinity.
3. The intrusive rocks are dominated by gabbro sills that show limited differentiation to intermediate and felsic units and, similar to the volcanic rocks, have an alkaline affinity based on HFSE abundances and clinopyroxene mineral chemistry.
4. The volcanic and intrusive suites are considered to be comagmatic considering the similarities in elemental abundances, REE spectra, and geochemical affinities.
5. Peridotites and pyroxenites were recognized in the study area for the first time. These rocks represent the least evolved members of the Nimish suite and suggests that the primitive Nimish alkaline magma became differentiated prior to the formation of the basalts and gabbros.
6. The patterns shown by normalized extended trace element diagrams for Nimish basalts as well as Sm-Nd data for one sample indicate that they represent partial melts derived from a both a depleted and lesser depleted mantle source. The enriched isotopic composition of the Nimish syenite indicates assimilation of continental crust by the parental melt.

References

Allègre, C.J., Treuil, M., Minster, J.-F., Minster, B., and Albarède, F. 1977. Systematic Use of Trace Element in Igneous Process. Part I: Fractional Crystallization in Volcanic Suites. Contributions to Mineralogy and Petrology, 60: 57-75.

Baragar, W.R.A. 1967. Wakuach Lake map-area, Quebec-Labrador (23O). Geological Survey of Canada, Memoir 344, 174p.

Baragar, W.R.A., and Scoates, R.F.J. 1981. The Circum-Superior Belt: A Proterozoic Plate Margin? *In* Precambrian Plate Tectonics. *Edited by* A. Kröner. Developments in Precambrian Geology 4, Elsevier Scientific Publishing Company, Amsterdam, Netherlands, p. 297-330.

Basaltic Volcanism Study Project. 1981. Basaltic Volcanism of the Terrestrial Planets. Pergamon Press, New York, 1286p.

Birkett, T.C. 1991a. Origin of the Lower Proterozoic Fleming chert-breccia, Newfoundland, Labrador-Quebec. Geological Survey of Canada, Paper 91-12, 44p.

Birkett, T.C., Watanabe, D.H., Richardson, D.G., Findlay, J.M., and Fowler, A.D. 1991b. Non-ferrous mineral resource assessment, western Labrador, north of 54 degrees latitude. Geological Survey of Canada, Open File 2370, 95p.

Budkewitsch, P., and Robin, P.-Y. 1994. Modelling the evolution of columnar joints. Journal of Volcanology and Geothermal Research, 59: 219-239.

Chandler, F.W. 1988. The Early Proterozoic Richmond Gulf Graben, East Coast of Hudson Bay, Quebec. Geological Survey of Canada, Bulletin 362, 76p.

Cox, K.G., Gass, I.G., and Mallick, D.I.J. 1970. The Peralkaline Volcanic Suite of Aden and Little Aden, South Arabia. Journal of Petrology 11: 433-461.

Dimroth, E. 1978. Région de la fosse du Labrador entre les latitudes 54°30' et 56°30' - Labrador Trough area between latitudes 54°30' and 56°30'. Ministère des Ressources naturelles, Gouvernement du Québec. Rapport Géologique 193, 396p.

Dimroth, E., Baragar, W.R.A., Bergeron, R., and Jackson, G.D. 1970. The filling of the Circum-Ungava geosyncline. *In* Symposium on Basins and Geosynclines of the Canadian Shield. *Edited by* A.J. Baer. Geological Survey of Canada, Paper 70-40, p. 45-142.

Donaldson, C.H. 1974. Olivine Crystal Types in Harrisitic Rocks of the Rhum Pluton and in Archean Spinifex Rocks. Geological Society of America Bulletin, 85: 1721-1726.

Eckstrand, O.R., Grinenko, L.N., Krouse, H.R., Paktunc, A.D., Schwann, P.L., and Scoates, R.F.J. 1989. Preliminary data on sulphur isotopes and Se/S ratios, and the source of sulphur in magmatic sulphides from the Fox River Sill, Molson Dykes and Thompson nickel deposits, northern Manitoba. *In* Current Research, Part C. Geological Survey of Canada, Paper 89-1C, p. 235-242.

Eckstrand, O.R., and Hulbert, L.J. 1987. Selenium and the source of sulphur in magmatic nickel and platinum deposits. Geological Association of Canada, Program with Abstracts, 12, p.40.

Evans. J.L. 1978. The Geology and Geochemistry of the Dyke-Lake area (parts of 23J/8,9), Labrador. Mineral Development Division, Department of Mines and Energy, Government of Newfoundland and Labrador, Report 78-4, 39p.

Fahrig, W.F. 1949. The Geology of the Astray to Birch Lake area of Labrador. Iron Ore Company of Canada, Internal company report. Mineral Development Division, Department of Mines and Energy, Government of Newfoundland and Labrador, File 23J(2), 30p.

Findlay, J. 1996. Petrology, Geochemistry, and Evolution of the Labrador Trough Basaltic Suite, Labrador and New Québec. Ph.D. thesis. Ottawa-Carleton Geoscience Centre, University of Ottawa, Ottawa, Ontario, 589p.

Findlay, J., Fowler, T.D., and Birkett, T.C. 1989. Geology of the Howse Lake area, western Labrador. Geological Survey of Canada, Open File 2204, 70p.

Findlay, J.M., Parrish, R.R., Birkett, T.C., and Watanabe, D.H. 1995. U-Pb ages from the Nimish Formation and Montagnais glomeroporphyritic gabbro of the central New Québec Orogen, Canada. Canadian Journal of Earth Sciences, 32: 1208-1220.

Floyd, P.A., and Winchester, J.A. 1975. Magma type and tectonic setting discrimination using immobile elements. Earth and Planetary Science Letters, 27: 211-218.

Fowler, A.D., and Jensen, L.S. 1989. Quantitative trace-element modelling of the crystallization history of the Kinojévis and Blake River groups, Abitibi Greenstone Belt, Ontario. Canadian Journal of Earth Sciences, 26: 1356-1367.

Frarey, M.J. 1961. Menihek Lakes, Newfoundland and Quebec. Geological Survey of Canada, Map 1087A (with marginal notes), scale 1:243,440.

Frarey, M.J., and Duffell, S. 1964. Revised Stratigraphic Nomenclature for the Central Part of the Labrador Trough. Geological Survey of Canada, Paper 64-25, 13p.

Gélinas, L., Mellinger, M., and Trudel, P. 1982. Archean mafic metavolcanics from the Rouyn-Noranda district, Abitibi Greenstone Belt, Quebec. 1. Mobility of the major elements. Canadian Journal of Earth Sciences, 19: 2258-2275.

Gill, J.B. 1981. Orogenic andesites and plate tectonics. Springer-Verlag, 390p.

Gordon, G.E., Randle, K., Coles, G.G., Corliss, J.B., Beeson, M.H., and Oxley, S.S. 1968. Instrumental activation analysis of standard rocks with high resolution gamma ray detector. Geochimica et Cosmochimica Acta, 32: 369-396.

Govindaraju, K. 1994. 1994 Compilation of Working Values and Sample Descriptions for 383 Geostandards. Geostandards Newsletter, Volume 18, Special Issue, p. 1-158.

Gross, G.A. 1968. Iron ranges of the Labrador Geosyncline. Volume III. *In* Geology of Iron Deposits in Canada. Geological Survey of Canada, Economic Geology Report 22, 179p.

Hall, G.E.M., and Bonham-Carter, G.F. 1988. Review of methods to determine gold, platinum and palladium in production-oriented geochemical laboratories, with application of a statistical procedure to test for bias. Journal of Geochemical Exploration, 30: 255-286.

Hall, G.E.M., MacLaurin, A.I., and Vaive, J. 1986. The analysis of geological materials for fluorine, chlorine and sulphur using pyrohydrolysis and ion chromatography. Journal of Geochemical Exploration, 26: 177-186.

Hanson, G.N. 1989. An Approach to Trace Element Modelling Using a Simple Igneous System as an Example. *In* Geochemistry and Mineralogy of the Rare Earth Elements. *Edited by* B.R. Lipin and G.A. McKay. Reviews in Mineralogy, Volume 21, p. 79-97.

Hoffman, P.F. 1987. Early Proterozoic Foredeeps, Foredeep Magmatism, and Superior-Type Iron-Formations of the Canadian Shield. *In* Proterozoic Lithospheric Evolution. *Edited by* A. Kröner. American Geophysical Union, Geodynamic Series Volume 17, p. 85-98.

Hoffman. P.F. 1988. United Plates of America. The Birth of a Craton: Early Proterozoic Assembly and Growth of Laurentia. Annual Review of Earth and Planetary Sciences, 16: 543-603.

Hughes, C.J. 1973. Spilites, keratophyres, and the igneous spectrum. Geological Magazine, 109: 513-527.

Humphris, S.E., and Thompson, G. 1978a. Hydrothermal alteration of oceanic basalts by seawater. Geochemica et Cosmochimica Acta, 42: 107-125.

Humphris, S.E., and Thompson, G. 1978b. Trace element mobility during hydrothermal alteration of oceanic basalts. Geochimica et Cosmochimica Acta, 42: 127-136.

Irvine, T.N., and Baragar, W.R.A. 1971. A Guide to the Chemical Classification of the Common Volcanic Rocks. Canadian Journal of Earth Sciences, 8: 523-548.

Kennedy, G., and Fowler, A. 1983. Interference from Uranium in neutron activation analysis of rare-earths in silicate rocks. Journal of Radioanalytical Chemistry, 78: 165-169.

Kretz, R. 1985. Calculation and Illustration of Uncertainty in Geochemical Analyses. Journal of Geological Education, 33: 40-44.

Kretz, R., Hartree, R., Garrett, D., and Cermignani, C. 1985. Petrology of the Grenville swarm of gabbro dikes, Canadian Precambrian Shield. Canadian Journal of Earth Sciences, 22: 53-71.

Lambert, M.B. 1988. Cameron River and Beaulieu River volcanic belts of the Archean Yellowknife Supergroup, District of MacKenzie, Northwest Territories. Geological Survey of Canada, Bulletin 382, 145p.

LeBas, M.J. 1962. The Role of Aluminum in Igneous Clinopyroxenes with Relation to their Parentage. American Journal of Science, 260: 267-288.

Le Gallais, C.J., and Lavoie, S. 1982. Basin Evolution of the Lower Proterozoic Kaniapiskau Supergroup, Central Labrador Miogeocline (Trough), Québec. Bulletin of Canadian Petroleum Geology, 30: 150-166.

Lofgren, G.E. 1974. An experimental study of plagioclase crystal morphology: isothermal crystallization. American Journal of Science, 274: 243-273.

Maaloe, S. 1985. Principles of Igneous Petrology. Springer-Verlag, Berlin, Federal Republic of Germany, 374p.

MacDonald, G.A., and Katsura, T. 1964. Chemical compositions of the Hawaiian Lavas. Journal of Petrology, 5: 82-133.

Meschede, M. 1986. A method of discriminating between different types of mid-ocean ridge basalts and continental tholeiites with the Nb-Zr-Y diagram. Chemical Geology, 56: 207-218.

Miyashiro, A. 1978. Nature of Alkalic Volcanic Rock Series. Contributions to Mineralogy and Petrology, 66: 91-104.

Noel, N. 1992. Geology and geochemistry of the McKay River area volcanic rocks, western Labrador. M.Sc. thesis. Memorial University of Newfoundland, St . John's, Newfoundland, 149p.

Norry, M.J., and Fitton, J.G. 1983. Compositional differences between oceanic and continentla basic lavas and their significance. *In* Continental Basalts and Mantle Xenoliths. *Edited by* C.J. Hawkesworth and M.J. Norry. Shiva Publishing Limited, Nantwich, Cheshire, Great Britain, p. 5-19.

Peacock, M.A. 1931. Classification of Igneous Rock Series. Journal of Geology, 39: 54-67.

Pearce, J.A. 1982. Trace element characteristics of lavas from destructive plate boundaries. *In* Andesites. *Edited by* R.S. Thorpe. John Wiley and Sons, New York, New York, p. 525-548.

Pearce, J.A. 1983. Role of sub-continental lithosphere in magma genesis at active continental margins. *In* Continental Basalts and Mantle Xenoliths. *Edited by* C.J. Hawkesworth and M.J. Norry. Shiva Publishing Limited, Nantwich, Cheshire, Great Britain, p. 230-249.

Pearce, J.A., and Cann, J.R. 1973. Tectonic setting of Basic Volcanic Rocks determined using trace element analysis. Earth and Planetary Science Letters, 19: 290-300.

Perrault, G. 1955. Geology of the western margin of the Labrador Trough. Ph.D. thesis. University of Toronto, Toronto, Ontario, 302p.

Potts, P.J. 1987. A Handbook of Silicate Rock Analysis. Blackie and Son Limited, Glasgow, Scotland, 622p.

Potts, P.J., Hawkesworth, C.J., van Calsteren, P., and Wright, I.P. 1993. Advances in analytical technology and its influence on the development of modern inorganic geochemistry: a historical perspective. *In* Magmatic Processes and Plate Tectonics. *Edited by* H.M. Prichard, T. Alabaster, N.B.W. Harris, and C.R. Neary. Geological Society Special Publication, Number 76, p. 501-520.

Pouchou, J.L., and Pichoir, F. (1986). Basic expression of "PAP" computation for quantitative EPMA. *In* 11th International Congress on X-ray Optics and Microanalysis (ICXOM). *Edited by* J.D. Brown and RH Packwood. p. 249-253.

Pringle, G.J. (1989). EDDI: A FORTRAN Computer Program to Produce Corrected Microprobe Analyses of Minerals Using an Energy Dispersive x-ray Spectrometer. Geological Survey of Canada, Open File 2127, 210p.

Retty, J.A. 1937. The geology and mineral deposits of the Dyke Lake map area and the northern part of the Ossokmanuan Lake map area, Newfoundland Labrador, Annual report for 1937. Labrador Mining and Exploration Co. Ltd., Unpublished report. Mineral Development Division, Department of Mines and Energy, Government of Newfoundland and Labrador, File 23J (81), 48p.

Rivers, T. 1982. Preliminary report on the geology of the Gabbro Lake and McKay River map areas (23H/11 and 23H/12), Labrador. Mineral Development Division, Department of Mines and Energy, Government of Newfoundland and Labrador, Report 82-2, 27p.

Rivers, T., and Chown, E.H. 1986. The Grenville Orogen in eastern Quebec and western Labrador; definition, identification, and tectonometamorphic relationships of autochthonous, parautochthonous, and allochthonous terranes. *In* The Grenville Province. *Edited by* J.M. Moore, A. Davidson, and A.J. Baer. Geological Association of Canada, Special Paper 31, p. 31-50.

Sauvé, P. 1953. Clastic sedimentation during a period of volcanic activity, Astray Lake, Labrador. M.Sc. thesis. Queen's University, Kingston, Ontario, 130p.

Skulski, T., Wares, R.P., and Smith, A.D. 1993. Early Proterozoic (1.88-1.87 Ga) tholeiitic magmatism in the New Québec orogen. Canadian Journal of Earth Science 30: 1505-1520.

Smith, J.L. 1987. Mineral Occurrence Map of the South-Central Labrador Trough. Maps 87-10 and 87-11, scale 1:100,000. Mineral Development Division, Department of Mines, Government of Newfoundland and Labrador.

Stillman, C.J., and Williams, C.T. 1978. Geochemistry and tectonic setting of some Ordovician volcanic rocks in east and southeast Ireland. Earth and Planetary Science Letters, 41:288-310.

Sun, S.S., and McDonough, W.F. 1989. Chemical and isotopic systematics of oceanic basalts: implications for mantle composition and processes. *In* Magmatism in the Ocean Basins. *Edited by* A.D. Saunders and M.J. Norry. Geological Society, Special Publication No. 42, p. 313-345.

Thériault, R.J. 1990. Methods for Rb-Sr and Sm-Nd isotopic analyses at the geochronology laboratory, Geological Survey of Canada. *In* Radiogenic Age and Isotopic Studies: Report 3. Geological Survey of Canada, Paper 89-2, p. 3-6.

Wardle, R.J. 1982. Geology of the South-Central Labrador Trough. Maps 82-5 and 82-6, scale 1:100,000 (with legend and cross-sections). Mineral Development Division, Department of Mines and Energy, Government of Newfoundland and Labrador.

Wardle, R.J., and Bailey, D.G. 1981. Early Proterozoic Sequences in Labrador. *In* Proterozoic Basins of Canada. *Edited by* F.H.A. Campbell. Geological Survey of Canada, Paper 81-10, p. 331-360.

Wardle, R.J., Ryan, B., Nunn, G.A.G., and Mengel, F.C. 1990. Labrador segment of the Trans-Hudson Orogen: crustal development through oblique convergence and collision. *In* The Early Proterozoic Trans-Hudson Orogen of North America. *Edited by* J.F. Lewry and M.R. Stauffer. Geological Association of Canada, Special Paper 37, p. 353-369.

Wilson, A.D. 1960. A modified scheme for the determination of ferrous iron in rocks. Analyst, 85: 823-827.

Winchester, J.A., and Floyd, P.A. 1976. Geochemical magma type discrimination: application to altered and metamorphosed basic igneous rocks. Earth and Planetary Science Letters, 28: 459-469.

Winchester, J.A., and Floyd, P.A. 1977. Geochemical discrimination of different magma series and their differentiation products using immobile elements. Chemical Geology 20: 325-343.

Wood, D.A., Joron, J.-L., and Treuil, M. 1979. A re-appraisal of the use of trace elements to classify and discriminate between magma series erupted in different tectonic settings. Earth and Planetary Science Letters, 45: 326-336.

Yoder, H.S., and Tilley, C.E. 1962. Origin of basaltic magmas: an experimental study of natural and synthetic rock systems. Journal of Petrology, 3: 342-532.

Zajac, I.S. 1974. The Stratigraphy and Mineralogy of the Sokoman Formation in the Knob Lake area, Quebec and Newfoundland. Geological Survey of Canada, Bulletin 220, 159 p.

Appendices

Appendix A: Maps

A1: Geology map of the southern Dyke Lake-Astray Lake region

A geological map covering the southern portion of the Dyke Lake-Astray Lake region is included as Map A in the back pocket of the thesis. A comprehensive geological map covering the entire study area was not completed due to the following considerations: the very large number of sample stations visited over 3 field seasons (1178), the amount of time necessary to intergrate all the new data obtained in this project with the existing geological maps and interpretation (i.e. Evans (1978) and Wardle (1982)), and the time required to compile all previously published maps made during this study (see Birkett, 1991b) at one scale of 1: 50,000. The map will be completed at a future date.

The mapped area is bounded by the latitudes 54°22' and 54°30' and longitudes 66°00' and 66°30'. The outcrop stations marked on the map are from the 1986 field season and the geological interpretation is based upon mapping performed in 1985 and 1986. Geochemical analyses for samples in this part of the study area are found in Table B2.3. A geological legend to accompany the map is presented in Table A1.1.

A2: Sample location map

A 1:50,000 scale map of the study area is included in the back pocket (Map B). It includes the location of approximately 505 of 1178 stations mapped during the course of the field study. The station name is found beside each outcrop or group of outcrops. A number of stations were visited more than once and therefore have a corresponding number of station names. Hand samples were taken at almost all stations and those sites selected for chemical analyses are identified in Table B3.2.

Table A1.1 Legend to accompany Map A: Geology of the southern Dyke Lake-Astray Lake region.

Kaniapiskau Supergroup

Knob Lake Group		
Upper Knob Lake Group		
Ferriman Subgroup		
Unit 8	Menihek Formation	gray to black siltstone with minor argillaceous and graywacke intervals
Unit 7b	Nimish Formation	gabbro sills
Unit 7a		massive, amygdaloidal, porphyritic, and pillowed basalt, felsic volcanic rocks, volcanic conglomerates, mafic tuff, agglomerate.
Unit 6	Sokoman Formation	iron formation
Unit 5	Wishart Formation	feldspathic quartzites, orthoquartzites, intebedded f.gr. quartzites and silstones
Lower Knob Lake Group		
Attikamagen Subgroup		
Unit 4	Fleming Formation	chert breccia, chert
Unit 3	Dolly Formation	gray shales and siltstones
Unit 2	Denault Formation	dolarenites, dololutites, dolomite breccia
Unit 1	Le Fer Formation	shale and siltstone

Note: it is not implied in the legend that Unit 7b is younger than Unit 7a or that the Nimish Formation is younger that the Sokoman Formation; Units 7b, 7a, and 6 are considered to be time equivalent.

Appendix B: Whole rock major (weight %) and trace (ppm) element analyses

A total of 296 samples were analyzed for whole rock major (weight %) and/or trace element (ppm) chemistry. The majority of the analyses comprise volcanic and intrusive rocks of the Nimish Formation. In addition, the compositions of 27 samples of epiclastic and volcaniclastic rocks are included in the data set.

Geochemical data for 48 samples of the Denault, Dolly, Fleming, Wishart, Sokoman, and Menihek Formations are also provided. These samples were analyzed to investigate their economic potential as well as to provide representative analyses of these formations in the study area, for which there was no previously published information. Further, the analyses for the Fleming Formation was used in a larger study (Birkett, 1991a) to investigate the genetic origin of this stratigraphic unit in the Schefferville region of Labrador and Québec.

Table B1.1 summarizes the methods and laboratories used for the analyses of major and trace elements in this study.

Except for a suite of 24 rare earth element analyses of Nimish Formation volcanic and intrusive rocks, all the samples were analyzed at either the commercial laboratory of X-Ray Assay Laboratories Limited (Toronto, Ontario), the X-ray fluorescence laboratory of the Department of Geology (University of Ottawa), or the analytical laboratories of the Geological Survey of Canada, Ottawa, Ontario.

The samples were jointly analyzed at these sites as funding for the geochemical analyses came from both the Geological Survey of Canada (the Canada-Newfoundland Mineral Development Agreement, 1984-1989) and the University of Ottawa. In order to investigate whether there is any compositional bias in the data, relating to the laboratory where the sample was analyzed, estimates of analytical uncertainties for several procedures were calculated. They are presented after the description of the analytical procedure where applicable.

Table B3.2 presents all the analytical data for the study area. It is an updated version of the analyses for the Birch Lake, Dyke Lake, Jasper Mountain, and Marble Lake areas reported in Birkett (1991b).

B1: Preparation of sample powders

Volcanic and intrusive rocks collected for chemical analyses were selected and sampled according to the following methods. For volcanic rocks, the majority of samples were taken from massive aphyric flows. Flows containing amygdules and/or vesicles were also sampled with care taken to obtain specimens from the portions of the outcrop containing the least amount of secondary material if possible. Samples from pillow lavas were taken from only the central portion of a single pillow. When sampling intrusive rocks, specimens were taken from the interiors of sills and only samples #750 (86 CHL-1) and #751 (86 CHL-2) represent analyses of chill margins. In all cases, samples were chosen so as to minimize any veining and obvious secondary alteration.

Whole rock sample powders were prepared at either X-Ray Assay Laboratories Limited (XRAL) or by the author at the University of Ottawa. All samples collected in 1985 were sent directly to XRAL for processing. All subsequent samples collected for geochemistry were first prepared at the University of Ottawa by removing weathered surfaces with a diamond rock saw. Specimens were then sent to XRAL for further processing and analysis. Alternatively, others were kept at the University of Ottawa where the samples were further reduced to approximately 2 cm sized fragments in a steel jaw crusher. The fragments were split to obtain about 100-200 g of material and this amount was pulverized in a tungsten-carbide ring mill using a shatterbox apparatus. To ensure no cross-contamination, the ring mill was cleaned with quartz between samples and then precontaminated with a small amount of the next sample before the full sample was pulverized.

B2: Analytical procedures

B2.1 X-ray Fluorescence (XRF)

X-ray fluorescence spectrometry (XRF) was used at the University of Ottawa, Geological Survey of Canada (GSC), and XRAL to determine the major and trace element chemistry of selected samples from the Nimish Formation as well as those from other

formations found in the study area. The elements analyzed by this technique at each laboratory is listed in Table B1.1.

Table B1.1: Summary of laboratories, analytical methods, number of elements analyzed by each procedure (# elements), and list of elements per procedure.

No.	Laboratory	Method	# elements	Elements
1.	XRAL	XRF	17	wr majors, Cr-Rb-Sr-Y-Zr-Nb-Ba
2.	XRAL	DCP-ES	7	Cr-Co-Ni-Cu-Zn-Pb-Ag
3.	XRAL	INAA	6	Hf-Ta-U-Th-La-Ce
4.	XRAL	ICP-MS	10	Rb-Sr-Y-Zr-Nb-Ba-Hf-Ta-Th-La
5.	XRAL	FA-NA or FA-DCP	1	Au
6.	XRAL	FA-DCP	2	Pt-Pd
7.	XRAL	FA-NA	7	Ir-Os-Pd-Pt-Re-Rh-Ru
8.	U. of Ottawa[1]	XRF	20	wr majors, Rb-Sr-Y-Zr-Nb-Ba-Cr-Co-Ni-Zn
9.	U. of Ottawa[2]	XRF	24	wr majors, Rb-Sr-Y-Zr-Nb-Ba-Cr-Co-Ni-Zn-U-Th-La-Ce
10.	GSC	XRF	16	wr majors, Rb-Sr-Y-Zr-Nb-Ba
11.	GSC	ICP-ES	21	wr majors, Rb-Sr-Y-Zr-Nb-Ba-Co-Ni-Cu-Zn-Pb
12.	GSC	IC and AA	2	S-Se
13.	POLY	INAA	14	La-Ce-Nd-Sm-Eu-Tb-Dy-Ho-Tm-Yb-Lu-U-Ta-Th

wr majors: SiO_2, Al_2O_3, Fe_2O_3(t), MgO, CaO, Na_2O, K_2O, TiO_2, MnO, P_2O_5.
University of Ottawa[1]: analyses performed on a Phillips PW1410/20 AHP X-ray fluorescence spectrometer.
University of Ottawa[2]: analyses performed on a Phillips PW2400 X-ray fluorescence spectrometer.
XRAL: X-Ray Assay Laboratories Limited, Toronto, Ontario.
GSC: Geological Survey of Canada, Ottawa, Ontario.
POLY: Institut de génie énergétique, Ecole Polytechnique, Université de Montréal, Québec.
Method abbreviations: please refer to descriptions of analytical procedures following.
Note: FeO was determined by titration at the University of Ottawa, XRAL, and GSC.

At the X-ray fluorescence laboratory of the Department of Geology, University of Ottawa, fused discs are prepared by mixing a 1.3 g aliquot of sample powder, 3.9 g of lithium tetraborate ($Li_2B_4O_7$), and 0.433 g of lithium carbonate (Li_2CO_3) followed by the melting of

the mixture in a Pt crucible. Analyses were performed on a Philips PW1410/20 AHP X-ray fluorescence spectrometer using a rhodium excitation tube. Two samples were prepared in July 1996 using a lithium tetraborate-lithium metaborate flux and analyzed on a Phillips PW2400 XRF spectrometer. The analyses performed at XRAL and the Geological Survey of Canada similarly involved the preparation of the sample powders as fused discs.

Analytical uncertainty was estimated by replicate measurements on samples of international standards or by duplicate measurements of samples used in the study following the procedures outlined by Kretz (1985). Estimates of analytical uncertainties for the study samples using the above methods are presented in Tables B2.1, B2.2, B2.3, and B2.4.

For samples analyzed on the Philips PW1410/20 AHP instrument at the University of Ottawa, estimates of analytical uncertainties for each element are shown in Table B2.1. Four sets of estimates are provided and are explained as follows. The first set is based on the 10 replicate analyses of the syenite standard SY-2 (Ron Hartree, personal communication). The second presents coefficient of variation (v) values based on 15 analysis of Grenville tholeiitic dykes from Kretz et al. (1985). Coefficient of variation (v) values are also shown for 61 replicate analyses of 4 samples of the gabbro standard MRG-1 and 58 analyses of 3 samples of the diorite standard DR-N as determined in Findlay (1996).

Here, the values represent the higher of the two calculated coefficients of variation determined for MRG-1 and DR-N. Finally, data for 3 replicate determinations of the standard DR-N analyzed with the study samples are provided for comparison purposes only.

The coefficient of variation values used in subsequent error calculations are highlighted in bold type.

Instrumental analytical uncertainty for the Phillips PW2400 XRF spectrometer is estimated from 85 replicate analysis of one disc of the diorite standard DR-N (Table B2.2). The data was provided by Ron Hartree of the Department of Geology, University of Ottawa.

Table B2.1: Mean (x), standard deviation (s), and coefficient of variation (v) for major (weight %) and trace (ppm) elements analyzed on the Department of Geology, University of Ottawa, Philips PW1410/20 AHP X-ray fluorescence spectrometer. Data from four sources. Coefficient of variation values used in error analysis highlighted in bold typeface.

		SY-2 syenite standard (n=10)			Kretz (1985)	Findlay (1996)	DR-N diorite standard (n=3)		
Element	Method	Mean (x)	S.D. (s)	C.V. (v)	C.V. (v)	C.V. (v)	Mean (x)	S.D. (s)	C.V. (v)
SiO_2	XRF	60.18	0.17	0.0028	**0.009**	0.006	53.08	0.05	0.0008
Al_2O_3	XRF	12.23	0.10	0.0080	**0.008**	0.007	17.53	0.08	0.0043
$Fe_2O_3(t)$	XRF	6.25	0.04	0.0058	**0.008**	0.008	9.82	0.11	0.0112
MgO	XRF	2.69	0.05	0.0175	0.010	**0.020**	4.28	0.02	0.0054
CaO	XRF	7.96	0.06	0.0074	**0.008**	0.006	7.04	0.04	0.0051
Na_2O	XRF	4.37	0.07	0.0153	0.020	**0.040**	2.98	0.04	0.0136
K_2O	XRF	4.52	0.04	0.0089	0.012	**0.028**	1.73	0.01	0.0033
TiO_2	XRF	0.14	0.01	0.0357	0.008	**0.034**	0.98	0.01	0.0059
MnO	XRF	0.33	0.00	0.0000	**0.040**	0.240	0.22	0.00	0.0000
P_2O_5	XRF	0.73	0.02	0.0206	0.040	**0.111**	0.16	0.02	0.1414
Rb	XRF	222	3.9	0.018	0.400	1.080	63	3.0	0.0476
Sr	XRF	256	7.2	0.028	0.040	0.015	399	5.9	0.0147
Y	XRF	123	2.5	0.021	0.200	0.137	29	1.7	0.0597
Zr	XRF	269	3.7	0.014	0.100	0.070	125	1.2	0.0092
Nb	XRF	-	-	-	-	0.486	7	1.7	0.2474
Ba	XRF	467	5.2	0.011	0.100	0.055	390	27.4	0.0704
Cr	XRF	10	8.1	0.827	**0.100**	0.046	44	3.6	0.0819
Ni	XRF	2.1	3.2	1.524	-	**0.121**	23	11.0	0.4840
Zn	XRF	239	31.7	0.132	-	0.104	286	118.1	0.4133

Table B2.2: Mean (x), standard deviation (s), and coefficient of variation (v) for major (weight %) and trace (ppm) elements analyzed on the Department of Geology, University of Ottawa, Phillips PW2400 X-ray fluorescence spectrometer.

Element	Method	Unit	Mean (x)	S.D. (s)	C.V. (v)	Element	Method	Unit	Mean (x)	S.D. (s)	C.V. (v)
SiO_2	XRF	wt. %	53.20	0.07	0.001	Y	XRF	ppm	22	1.0	0.045
Al_2O_3	XRF	wt. %	17.66	0.04	0.002	Zr	XRF	ppm	128	1.7	0.013
$Fe_2O_3(t)$	XRF	wt. %	9.74	0.01	0.001	Nb	XRF	ppm	9	0.61	0.071
MgO	XRF	wt. %	4.30	0.01	0.002	Ba	XRF	ppm	389	12.6	0.032
CaO	XRF	wt. %	7.04	0.01	0.002	Cr	XRF	ppm	32	4.9	0.154
Na_2O	XRF	wt. %	3.05	0.04	0.012	Co	XRF	ppm	36	1.6	0.044
K_2O	XRF	wt. %	1.71	0.00	0.002	Ni	XRF	ppm	17	1.1	0.065
TiO_2	XRF	wt. %	1.07	0.00	0.002	Zn	XRF	ppm	148	1.3	0.009
MnO	XRF	wt. %	0.22	0.00	0.005	Pb	XRF	ppm	59	1.4	0.024
P_2O_5	XRF	wt. %	0.23	0.00	0.009	Th	XRF	ppm	7	1.6	0.221
Rb	XRF	ppm	77	1.6	0.021	La	XRF	ppm	20	9.0	0.441
Sr	XRF	ppm	385	2.6	0.007	Ce	XRF	ppm	44	15.1	0.346

Note: The data represents 85 replicate analyses of one disc of DR-N and estimates instrumental uncertainty.

Table B2.3: Mean (x), Standard deviation (s), and coefficient of variation (v) data for replicate analyses of SY-2 and duplicate determinations of samples by XRF, DCP-ES, INAA, and ICP-MS at X-Ray Assay Laboratories Limited.

		SY-2 syenite standard					Duplicate determinations					
Element	Method	n	Mean	S.D. (s)	C.V. (v)	Accepted Rec	n	Mean	S.D. (s)	C.V. (v)	Range	Detection Limit
SiO_2	XRF	6	59.6	0.42	0.0070	60.11 *	5	47.4	0.31	0.0065	42.1-57.1	0.01 wt. %
Al_2O_3	XRF	6	12.2	0.22	0.0178	12.04 *	7	12.0	0.10	0.0080	6.9-15.5	0.01 wt. %
Fe_2O_3(t)	XRF	6	6.27	0.09	0.0149	6.31 *	7	12.05	0.05	0.0044	6.84-15.8	0.01 wt. %
MgO	XRF	6	2.68	0.08	0.0296	2.69 *	6	7.00	0.06	0.0087	4.88-10.00	0.01 wt. %
CaO	XRF	6	7.89	0.12	0.0149	7.96 *	6	7.89	0.09	0.0114	4.51-10.10	0.01 wt. %
Na_2O	XRF	6	4.41	0.05	0.0107	4.31 *	7	3.10	0.03	0.0103	1.56-4.52	0.01 wt. %
K_2O	XRF	6	4.50	0.07	0.0166	4.45 *	5	0.48	0.01	0.0196	0.25-0.64	0.01 wt. %
TiO_2	XRF	5	0.14	0.00	0.0315	0.15 *	6	1.91	0.01	0.0073	0.57-4.30	0.01 wt. %
MnO	XRF	6	0.32	0.01	0.0319	0.32 *	6	0.18	0.00	0.0000	0.10-0.24	0.01 wt. %
P_2O_5	XRF	5	0.44	0.01	0.0205	0.43 *	7	0.32	0.01	0.0169	0.07-0.97	0.01 wt. %
Rb	XRF	5	220	8.62	0.0392	217 *	7	56	20.2	0.3576	10-170	10 ppm
Sr	XRF	6	283	9.95	0.0352	271 *	6	241	7.6	0.0317	50-430	10 ppm
Y	XRF	6	138	4.36	0.0316	128 *	6	30	10.0	0.3333	10-50	10 ppm
Zr	XRF	5	291	11.26	0.0401	280 *	6	356	18.0	0.0507	50-580	10 ppm
Nb	XRF	6	<10	-	-	29	5	93	11.4	**0.1226**	60-160	10 ppm
Ba	XRF	6	460	10.80	0.0235	460 *	6	348	23.3	0.0670	80-1280	10 ppm
Cr	XRF	5	11	1.22	0.1113	9.5	4	450	7.1	0.0157	220-690	10 ppm
Cr	DCP-ES	6	8	6.1	0.8080	9.5	5	211	6.3	0.0297	12-460	2 ppm
Co	DCP-ES	7	12	2.9	0.2499	8.6 *	7	60	3.2	**0.0523**	23-98	1 ppm
Ni	DCP-ES	6	10	2.7	0.2680	9.9	6	67	3.0	0.0445	9-160	1 ppm
Cu	DCP-ES	6	6	5.1	0.8467	5.2	6	65	3.3	**0.0514**	19-130	0.5 ppm
Zn	DCP-ES	8	280	34.6	**0.1237**	248 *	8	127	11.2	0.0801	44-250	0.5 ppm
Pb	DCP-ES	6	79	9.4	**0.1185**	85 *	-	-	-	-	-	2 ppm
Ag	DCP-ES	6	<0.5	-	-	1.1	-	-	-	-	-	0.5 ppm
Ta	INAA	6	<3	-	-	2.01 *	-	-	-	-	-	2 ppm
U	INAA	10	263	25.7	**0.0977**	284 *	-	-	-	-	-	5 ppm
Th	INAA	10	373	64.6	**0.1733**	379 *	-	-	-	-	-	1 ppm
La	INAA	-	-	-	-	75 *	3	78	8.7	**0.1106**	53-106	1 ppm
Ce	INAA	7	227	7.6	**0.0334**	175 *	3	159	5.9	0.0377	146-215	5 ppm
		SY-2 XRAL report					**Duplicate determinations**					
Rb	ICP-MS	-	-	-	-	-	24	56	12.6	**0.2238**	5-161	1 ppm
Sr	ICP-MS	21	277	18.0	0.0651	271 *	22	197	19.3	**0.0978**	31-418	1 ppm
Y	ICP-MS	20	126	14.1	**0.1114**	128 *	23	28	2.6	0.0933	10-74	1 ppm
Zr	ICP-MS	32	280	25.5	0.0911	280	22	187	21.6	**0.1160**	21-607	1 ppm
Nb	ICP-MS	63	29	3.5	0.1191	29	21	29	6.3	0.2153	5-85	1 ppm
Ba	ICP-MS	19	457	32.1	**0.0701**	460 *	22	534	25.4	0.0476	50-1480	1 ppm
Hf	ICP-MS	29	9.31	1.17	**0.1253**	7.7	-	-	-	-	-	1 ppm
Ta	ICP-MS	46	2.18	0.43	**0.1956**	2.01 *	-	-	-	-	-	1 ppm
Th	ICP-MS	58	364	41.2	**0.1130**	379 *	-	-	-	-	-	0.1 ppm
La	ICP-MS	-	-	-	-	-	22	33	1.7	0.0502	3-98	1 ppm

SY-2 syenite standard: all replicate determinations for Nb, Ag, and Ta below detection limit; coefficient of variation (v) values used in error analysis highlighted in bold typeface and underlined; recommended values (Rec) for SY-2 standard by Govindaraju (1994) marked with an asterisk (*) - proposed values are left blank; Range refers to the lower and upper limit concentrations obtained for elements in the duplicate determinations; n is the number of duplicate determinations.

Table B2.4 Mean (x), standard deviation (s), and coefficient of variation (v) for duplicate determinations of study samples by XRF and ICP-ES at the Geological Survey of Canada.

			Duplicate determinations						
Element	Method	Unit	n	Mean (x)	S.D. (s)	C.V. (v)	Range	Detection	Quoted uncertainty
SiO_2	XRF	wt. %	15	48.9	0.3	0.0051	43.7-55.1	0.40	0.40 (abs.) + 1% (rel.)
Al_2O_3	XRF	wt. %	19	14.7	0.1	0.0063	9.6-16.8	0.40	0.40 (abs.) + 1% (rel.)
Fe_2O_3(t)	XRF	wt. %	17	13.5	0.1	0.0042	8.0-18.0	0.10	0.10 (abs.) + 1% (rel.)
MgO	XRF	wt. %	18	5.36	0.04	0.0083	1.18-16.57	0.10	0.10 (abs.) + 1% (rel.)
CaO	XRF	wt. %	18	5.04	0.02	0.0044	0.18-9.51	0.10	0.10 (abs.) + 1% (rel.)
Na_2O	XRF	wt. %	18	1.87	0.00	0.0024	0.60-4.80	0.50	0.50 (abs.) + 1% (rel.)
K_2O	XRF	wt. %	17	2.38	0.03	0.0117	0.18-7.80	0.05	0.05 (abs.) + 1% (rel.)
TiO_2	XRF	wt. %	17	2.00	0.01	0.0074	0.69-3.51	0.02	0.02 (abs.) + 1% (rel.)
MnO	XRF	wt. %	19	0.20	0.00	0.0143	0.06-0.34	0.01	0.01 (abs.) + 2% (rel.)
P_2O_5	XRF	wt. %	18	0.33	0.01	0.0168	0.09-0.62	0.02	0.02 (abs.) + 1% (rel.)
Rb	XRF	ppm	14	83	2.8	0.0337	22-148	10	10 (abs.) + 2% (rel.)
Sr	XRF	ppm	16	204	4.2	0.0205	16-491	10	10 (abs.) + 10% (rel.)
Y	XRF	ppm	9	37	5.2	0.1421	14-107	10	10 (abs.) + 10% (rel.)
Zr	XRF	ppm	27	187	2.7	0.0147	39-474	10	10 (abs.) + 10% (rel.)
Nb	XRF	ppm	13	62	8.5	0.1370	17-322	10	10 (abs.) + 10% (rel.)
Ba	XRF	ppm	17	575	15.1	0.0262	139-1124	10	10 (abs.) + 2% (rel.)
Sr	ICP-ES	ppm	22	190	5.3	0.0278	34-510	-	-
Y	ICP-ES	ppm	22	26	0.8	0.0307	12-68	-	-
Zr	ICP-ES	ppm	22	198	28.7	0.1446	49-590	-	-
Ba	ICP-ES	ppm	22	538	33.9	0.0629	60-1400	-	-
La	ICP-ES	ppm	22	26	1.7	0.0652	3-92	-	-

Range refers to the lower and upper limit concentrations for elements obtained in the duplicate determinations; n indicates the number of duplicate determinations; quoted uncertainty (absolute and relative) was supplied by the GSC; no detection limits of quoted uncertainties obtained for ICP-ES.

The analytical error for samples analyzed at XRAL was estimated using two different methods (Table B2.3). The coefficient of variation (v) was calculated based on the replicate determinations of the SY-2 standard submitted to XRAL as "blind" samples at various times during the course of the study. In addition, these values were obtained based on a number of duplicate analyses of basalts and gabbros.

In general, there is good agreement between the values except where the coefficient of variation is high due to low concentrations of the elements near the detection limit; for example, Cr in SY-2 and Y for duplicate determinations. For comparison purposes, recommended and

proposed concentrations for SY-2 elements (Govindaraju, 1994) are also included in Table B2.3.

The estimate of analytical uncertainties for the samples analyzed at the GSC are based on a number of duplicate analyses of Nimish Formation basalts and gabbros (Table B2.4).

B2.2 FeO titration

The FeO content of a number of Nimish Formation samples was determined by titration at the University of Ottawa, XRAL, and the Geological Survey of Canada.

The procedure at the University of Ottawa employs the modified Wilson (1960) method and involves the dissolution of about 0.2 g of sample powder in cold concentrated HF and a predetermined amount of ammonium metavanadate (NH_4VO_3) solution. The ferrous iron (Fe^{+2}) released from the rock matrix into the solution, oxidizes upon reaction with ammonium metavanadate according to the following reaction (Potts, 1987):

$$V^{V}O_2 + Fe^{+2} + 2H^{+} \rightarrow V^{IV}O^{+2} + H_2O + Fe^{+3} \quad (1)$$

The unreacted V^{+5} is reduced with an known amount of ferrous ammonium sulphate, as in the above equation, and titrated against potassium dichromate in conjunction with an indicator solution. The amount of ferrous iron in the sample can be calculated by the titration result.

The samples submitted to XRAL and the GSC were similarly determined. The Fe_2O_3 content of samples was calculated from the difference in the amount of FeO determined by titration and the Fe_2O_3(t) obtained by XRF.

All FeO determinations were run in duplicate at the University of Ottawa and no estimate of analytical uncertainty in the FeO contents determined at the different laboratories was made. The relative error (coefficient of variation) for FeO is quoted by the laboratory at the University of Ottawa to be 4.6% based on the replicate analysis of the syenite standard SY-3 (John Loop, personal communication, 1996). This error decreases to 3.5% (or 0.035) for replicate analyses of the gabbro standard MRG-1 which has a higher concentration of FeO in the sample.

B2.3 Loss on Ignition (LOI), $H_2O(t)$, and $CO_2(t)$

The volatile content of samples whose whole rock major element (weight %) abundances was determined at the University of Ottawa, XRAL, or the Geological Survey of Canada was estimated by three methods and are described as follows.

At the University of Ottawa, the volatile content of whole rock powders was estimated by weight loss on ignition (LOI). Samples were weighed out in ceramic crucibles, heated to approximately 1050° C in a muffle furnace for one hour, and then re-weighed after removal from the furnace. The per cent weight loss is reported as the LOI.

A similar procedure was also used for the samples analyzed at XRAL where 1.3 g of powder was weighed and roasted at 950° C for one hour. The powder was subsequently fused and analyzed.

For the two samples analyzed on the Philips PW2400 X-ray spectrometer at the University of Ottawa, the volatile content was estimated from the weight difference between the mixture of sample powder, lithium tetraborate, and lithium metaborate and the fused product. The final per cent weight loss is recorded as the LOI after an adjustment is made in consideration of the minor loss of material during the fusion process (Ron Hartree, personal communication, 1996).

At the Geological Survey of Canada, the water and carbon contents of samples are included with the whole rock major and trace element concentrations for each analysis. The total water (H_2O total) content comprises both hydroscopic (H_2O^-) and structural (H_2O^+) water and is determined by combusting the sample powder in a quartz tube and measuring the amount of released water vapour with an infrared detector (the infrared absorption method). The total water content is reported in units of weight percent.

The combustion/infrared absorption method is similarly used to determine the total carbon content of a sample (reported as CO_2 total, weight per cent) and does not distinguish between the different sources of carbon; for example, carbon in carbonate versus graphitic

carbon. The total water ($H_2O(t)$) and carbon ($CO_2(t)$) values are combined and reported as LOI in Table B3.2.

B2.4 Inductively coupled plasma emission spectrometry (ICP-ES)

Inductively coupled plasma emission spectrometry (ICP-ES) was utilized at the Geological Survey of Canada to determine the major and trace element abundances of eight Nimish Formation gabbros.

Two sample digestion procedures were employed and are summarized as follows. For the major elements, 0.5 g of sample is fused with lithium metaborate ($LiBO_2$). The melt is dissolved in 5% HNO_3 and then diluted to a total volume of 250 ml. For the trace elements, 1.0 g of sample was digested in an acid mixture, evaporated to dryness, and dissolved in a HCl solution. Any residue is filtered off and then fused with $LiBO_2$. The cooled melt is dissolved in 10% HCl and finally diluted to a total volume of 100 ml.

Both solutions are then introduced into the instrument where they are atomized and excited in high temperature argon plasma. The optical emission lines are then measured using an optical spectrometer focused on the plasma tail flame (Potts et al., 1993).

The analytical error for five trace elements analyzed at the GSC based on the duplicate determination of study samples is presented in Table B2.4. The data for the major elements are not presented here due to the low number of samples analyzed.

B2.5 Inductively coupled plasma mass spectrometry (ICP-MS)

Inductively coupled plasma mass spectrometry (ICP-MS) involves the dissolution of the whole rock powder by acid attack and the introduction of the final sample solution into an argon plasma excitation source similar to that used in ICP-ES. The difference between the two techniques lies in the extraction of the ions from the argon plasma into a mass spectrometer operating at ultra-high vacuum conditions rather than determining element concentrations with an optical spectrometer.

This technique was used at XRAL to determine the contents of 10 trace elements for a selected number of Nimish Formation volcanic and intrusive rocks. It is especially useful in trace element studies as the mass analyzer offers a very low background signal and high elemental sensitivity resulting in very low detection limits for the elements analyzed (Table B2.3).

Estimates of analytical uncertainties for the trace elements analyzed at XRAL were determined using two methods. The first set of coefficients of variation is based on numerous replicate analyses of the SY-2 syenite standard. This data was supplied by X-Ray Assay Laboratories Limited and comprised part of an internal company report of analytical error. Uncertainties were also calculated using duplicate analyses of Nimish Formation volcanic and intrusive rocks. Where data is available for both methods, there is generally good agreement between the two sets of coefficients of variation.

B2.6 Direct current plasma (DCP) emission spectrometry

The concentrations of 7 trace elements were determined for samples at XRAL using direct current plasma (DCP) emission spectrometry. As in ICP-ES and ICP-MS, the sample is prepared as a solution after decomposition by acids and then passed as an aerosol from a nebulizer into an argon plasma. The difference between this technique and ICP-ES lies primarily in the manner with which the argon plasma is generated.

A direct current plasma (DCP) is created by initiating an electrical discharge within a stream of argon gas between three electrodes. A typical instrumentation set-up would include two anodes and one cathode block. The electrodes are configured such that a continuous plasma discharge is maintained within the argon gas stream. Hence, the sample dissociates in the argon plasma and the resulting atomic and ionic optical emissions lines are measured by a spectrometer. It is of note that this technique has been largely superseded by other methods, particularly ICP-ES and ICP-MS, that have matched or exceeded the ultimate performance of DCP-ES.

The analytical uncertainties for the samples analyzed by DCP-ES was estimated by two methods and are summarized in Table B2.3. Analytical error was calculated based on the replicate analyses the syenite standard SY-2 submitted to XRAL as a "blind" sample. No calculations were made for Ag as all six analyses were reported as below detection limit. In addition, error estimates were also obtained from a number of samples sent in duplicate for analyses. Note that no data is available for lead or silver.

The coefficients of variation obtained by this method are decidedly lower than those by replicate determinations of SY-2. This is due to the near detection limit concentrations of Cr, Co, Ni, and Cu in the syenite standard.

B2.7 Instrumental neutron activation analysis (INAA)

Instrumental neutron activation analysis (INAA) was utilized at XRAL to analyze the trace elements Ta, U, Th, La, and Ce for a large number of study samples. This technique was also employed at the Institut de génie énergétique, Ecole Polytechnique, Université de Montréal, to determine the rare earth and trace element concentrations of a suite of Nimish Formation volcanic and intrusive rocks.

INAA is non-destructive procedure whereby the sample powders are not chemically treated during the course of analysis. As such, it is one of the few routines available to determine elements such as Ta, Th, and Hf which are difficult to incorporate into schemes involving solution chemistry (Potts, 1987).

The general technique of Gordon et al. (1968) involves the irradiation of a small amount of sample powder by a neutron flux in a nuclear reactor. As a result, specific isotopes of the elements of interest become radioactive by neutron capture type reactions. The specimens are removed from the reactor and the gamma-ray spectra from activated samples are then measured using a germanium or lithium-drifted germanium detector. The gamma-ray spectrometry is performed at set intervals after irradiation in order to measure isotopes with different half-lives. Corrections are made for interferences in the analytical spectra (e.g. Kennedy and Fowler,

1983), and concentrations are determined by comparison with the standards analyzed in conjunction with the samples.

For samples analyzed at Ecole Polytechnique, the analytical error for the LREE, Th, and Ta is based upon replicate determinations of USGS rock standards and is estimated to be approximately 5% as cited in Fowler and Jensen (1989). The error for the HREE is assessed to be less than 10% considering the lower abundances of these elements in the standards.

At XRAL, estimates of analytical uncertainties was made for U, Th, and Ce based on a number of "blind" duplicates of the SY-2 standard submitted to the laboratory (Table B2.3). No estimate was available for Ta as all six determinations had concentrations below the detection limit. Uncertainties were also calculated for La and Ce using duplicate analyses of study samples.

B2.8 Fire assay with instrumental neutron activation analysis (FANA) or direct coupled plasma emission spectroscopy (FADCP)

The fire assay procedure is used to determine the precious metal contents of rocks and ores. Two methods were used for samples analyzed at XRAL and are described as follows. Twenty four Nimish Formation volcanic and intrusive rocks and two samples from the Sokoman Formation were analyzed for Au, Pt, and Pd by lead fire assay with analysis by instrument neutron activation analysis (FA-NA) or direct current plasma emission spectrometry (FA-DCP).

The classical lead fire assay (Pb-FA) method involves a fusion during which precious metals are extracted from a sample and collected in a Pb button. At XRAL, 20 g of sample powder is used in the process, an amount about two-thirds that of an assay-ton (1 assay-ton = 29.17g).

A mixture containing sample, litharge (PbO), Ag, and other flux constituents is fused in a furnace at ~1100°C. Here, the litharge is reduced to Pb which falls to the bottom of the crucible carrying Au, Pt, and Pd with it. Once the Pb has solidified, and the associated slag removed from it, the button is subjected to another fusion at ~950°C in a bone ash crucible (also

known as a "cupel"). Most of the Pb is absorbed by the cupel or volatilized to leave a Ag "prill" which contains Au, Pt, Pd, and some remaining Pb (Hall and Bonham-Carter, 1988). At this point, various analytical methods can be used; either analyzing the prill as a solid phase (INAA) or in a solution obtained thereafter (DCP-ES).

For the samples processed by lead fire assay, Pt and Pd were determined exclusively by DCP-ES while Au was analyzed by INAA or DCP-ES. The results are shown in Table B2.5 along with Co, Ni, and Cr. Gold was determined for a large number of study samples and complete results are presented in Table B3.1. The vast majority of analyses show that Au concentrations are below the 1 ppb detection limit set by FA-NA or FA-DCP.

In order to collect Au and the full spectrum of PGE elements (Os, Ir, Ru, Rh, Pt, Pd, and Re), a nickel sulphide fire assay (NiS-FA) method is preferred.

The procedure involves fusing sample powder (25 g at XRAL) and a flux containing Ni, S, and other ingredients. The nickel sulphide button created is crushed to a fine powder and dissolved in hot hydrochloric acid (HCl). The residue is filtered off for analysis directly by INAA or dissolved by acid attack and subsequent determination by DCP-ES or some similar technique. For the Nimish Formation samples, the analyses were performed by INAA and are shown in Table B2.6. Nickel and chromium analyses are included for comparison purposes.

No estimates of analytical uncertainty were made for the methods described above.

B2.9 Pyrohydrolysis-ion chromatography (IC) and Hydride extraction-atomic absorption (AA) techniques.

Eight samples of Nimish Formation volcanic and intrusive rocks were analyzed in order to determine their Se/S ratios (Eckstrand and Hulbert, 1987) and to investigate whether contamination processes may have affected the geochemistry of the two suites.

Sulphur was analyzed at the Geological Survey of Canada using a pyrohydrolysis and ion chromatography (IC) technique developed by Hall et al. (1986) and Hall and Vaive (1989). The method allows for the determination of sulfur at low concentration levels and demonstrates

Table B2.5 Summary of gold, platinum, and palladium analyses for study samples by lead fire assay (Pb-FA) with analysis by INAA (FA-NA) or DCP-ES (FA-DCP) at XRAL.

Sample	Number	Au	Co	Ni	Cr	Pt	Pd
Detection		1 ppb	1 ppm	1 ppm	2 ppm	10 ppb	2 ppb
Basalt							
86 B27-1B	798	<1	58	22	35	<10	<2
87 R1-2	1104	<1	36	19	4	<10	<2
87 B8-4C	1164	<1	24	12	<2	<10	<2
87 B8-6	1166	<1	29	17	6	<10	<2
Pillow Basalt							
87 R1-1	1103	<1	32	24	6	<10	<2
87 R1-3	1105	2	51	35	16	10	<2
87 R1-4	1106	<1	46	29	22	<10	<2
87 R1-5	1107	<1	55	44	22	<10	<2
Porphyritic Basalt							
87 B8-1	1159	<1	43	13	18	<10	<2
87 B8-2A	1160	<1	26	19	16	<10	<2
Peridotite							
87 W10-14B	1018	<1	83	740	2500	<10	4
87 W11-3A	1021	<1	68	630	2800	20	22
Pyroxenite							
87 W10-4	1007	<1	81	1000	5000	10	8
87 W11-6	1025	<1	71	650	3300	10	20
Gabbro							
86 B13-6	679	<1	280	2300	1400	40	150
87 W10-1	1004	<1	34	10	1	<10	<2
87 W10-8	1011	<1	42	9	1	<10	<2
87 B5-1A	1130	<1	45	62	32	<10	<2
87 B5-1B	1131	<1	27	3	1	<10	<2
87 B6-1	1149	<1	38	68	150	<10	<2
87 B7-3A	1154	<1	39	79	280	<10	<2
87 B7-3B	1155	<1	53	92	240	<10	<2
87 B9-1	1167	<1	78	380	930	<10	2
Sokoman Formation							
86 B13-1	674	4	47	140	500	10	13
87 B8-2B	1161	<1	22	18	62	<10	<2

Co, Ni, and Cr data analyzed by DCP-ES at XRAL and are included for comparison purposes.

Table B2.6 Summary of gold and platinum group elements (Os, Ir, Ru, Rh, Pt, Pd, Re) for study samples by nickel-sulphide fire assay (NiS-FA) with analysis by INAA (FA-NA) at XRAL.

Sample	No.	Au	Ni	Cr	Os	Ir	Ru	Rh	Pt	Pd	Re
Detection		1 ppb	-	-	3 ppb	0.1 ppb	5 ppb	1 ppb	5 ppb	5 ppb	5 ppb
Basalt											
86 W4-13	333	1	183	275	<3	0.1	10	<1	17	6	<5
86 W20-1	480	<1	22	38	<3	<0.1	8	<1	15	9	<5
86 W17-3	453	<1	92	175	<3	0.1	10	<1	25	9	<5
Pillow basalt											
86 W18-5	466	1	58	42	<3	<0.1	18	<1	26	9	<5
86 W18-6	467	1	45	33	<3	<0.1	12	<1	15	14	<5
Rhyolite											
86 B7-4	602	<1	0	0	<3	<0.1	<5	<1	<5	7	<5
86 B7-5	604	<1	0	0	<3	<0.1	<5	<1	<5	<5	<5
Gabbro											
86 W4-4	324	<1	86	326	<3	<0.1	<5	<1	<5	7	<5

Ni and Cr data analyzed by XRF (Phillips PW1410/20 AHP X-ray spectrometer) at the University of Ottawa; detection limits were not obtained for this instrument; data included for comparison purposes.

Table B2.7 Summary of sulphur (total) and selenium for Nimish Formation samples analyzed by pyrohydrolysis-ion chromatography (IC) and hydride extraction-atomic absorption (AA) techniques at the Geological Survey of Canada.

Sample	Number	S (total)	Se	Se/S x10^6	Ni	Cr
Detection		50 ppm	0.01 ppm	-	-	-
Basalt						
86 W4-13	333	114	0.40	3509	183	275
86 W17-3	453	78	0.21	2692	92	175
86 W20-1	480	345	1.06	3072	22	38
Pillow basalt						
86 W18-5	466	370	0.55	1486	58	42
86 W18-6	467	2470	0.99	401	45	33
Rhyolite						
86 B7-4	602	82	0.11	1341	0	0
86 B7-5	604	25	0.09	3600	0	0
Gabbro						
86 W4-4	324	1342	0.19	142	86	326

Ni and Cr data from XRF analysis at the University of Ottawa (Phillips PW1410/20 AHP X-ray spectrometer) and are included for comparison purposes; Se/S ratio = Se/S x10^6 (Eckstrand and Hulbert, 1987)

very good accuracy and precision. The detection limit is 50 ppm for sulphur and the process has a +/- 5% relative standard deviation for concentrations greater than 100 ppm (Hall et al., 1986).

Pyrohydrolysis is the decomposition of a sample at high temperature by a stream of water vapour or moist gas (Hall et al., 1986). As such, the sulphur is extracted from the sample in a gaseous form (SO_2 and SO_3), collected in a receiver solution, and then analyzed by an ion chromatograph.

Selenium was determined by a hydride extraction technique (cited in Eckstrand et al., 1989) followed by analysis with atomic absorption (AA) spectrometry. The quoted detection limit for Se is 0.01 ppm. The results for the study samples are presented in Table B2.7.

B3: Compilation of geochemical analysis for the study area

A total of 296 samples were analyzed for whole rock major (weight %) and/or trace (ppm) element chemistry. The complete data set is presented in Table B3.2 except for the PGE and S-Se analyses previously shown in Tables B2.6 and B2.7 respectively. As previously noted, the analyses are an updated version of those reported in Birkett (1991b).

The data are presented in the following order and manner: 1. Denault, Dolly, Fleming, Wishart, Sokoman, and Menihek Formations; 2. Nimish Formation: epiclastic and volcaniclastic rocks; 3. Nimish Formation: volcanic rocks; 4. Nimish Formation: intrusive rocks.

The study area is subdivided into three regions or zones: Dyke Lake-Astray Lake, Marble Lake, and Birch Lake. The analyses for each formation or suite of rocks (i.e. Nimish Formation), are grouped according to the above zones and ordered by their geochemical number. Samples with only trace element analyses are displayed last in their respective zones regardless of year of analysis or geochemical number.

A lithologic acronym is included with each sample for descriptive purposes and these are summarized in Table B3.1. The acronym assigned to each analysis was derived from the field description of the outcrop(s) visited at the time of investigation.

Elements that have values below the detection limit for the method employed are marked as such and no adjustments were made to them. Also, those elements not analyzed in a given sample are left blank.

All samples analyzed at the GSC by XRF and ICP-ES, for whole rock major and/or trace elements, were done in duplicate. Hence, the data presented in Table B3.2 for these analyses represent the average values for the duplicate determinations.

Table B3.1 Summary of acronyms for lithologic units in the study area

Sedimentary rocks: Denault, Dolly, Fleming, Wishart, Sokoman, and Menihek Formations

1.	CHBR	chert breccia
2.	CHIR	cherty iron formation
3.	CHRT	chert
4.	DLBR	dolomite breccia
5.	DLNT	dolomite
6.	IRFM	iron formation
7.	QRTZ	quartzite
8.	SCIF	silica-carbonate iron formation
9.	SHLE	shale
10.	SLSN	siltstone
11.	SNDS	sandstone

Epiclastic and volcaniclastic rocks: Nimish Formation

12.	AGLM	agglomerate
13.	MAAG	mafic agglomerate
14.	TUFF	tuff
15.	VCBR	volcanic breccia
16.	VCCG	volcanic conglomerate

Volcanic rocks: Nimish Formation

17.	AMBS	amygdaloidal basalt
18.	AMIV	amygdaloidal intermed. volcanic rock
19.	BSLT	basalt
20.	IMVC	intermediate volcanic rock
21.	PLBS	pillow basalt
22.	PPBS	porphyritic basalt
23.	PPIV	porphyritic intermediate volcanic rock
24.	RYLT	rhyolite
25.	SIVC	silica-rich volcanic rock
26.	VCBS	vesicular basalt

Intrusive rocks: Nimish Formation

27.	DIBS	diabase
28.	DIRT	diorite
29.	DYKE	dyke
30.	GBBR	gabbro
31.	PPGB	porphyritic gabbro
32.	PRDT	peridotite
33.	PXNT	pyroxenite
34.	SYNT	syenite
35.	ULTR	ultramafic rock

Miscellaneous

36.	QTVN	quartz vein

Table B3.2: Whole rock major (weight %) and trace (ppm) element geochemisty

Formation	Denault Formation							
Location	DL-AL	DL-AL	DL-AL	DL-AL	Marble	Marble	Marble	Marble
Year	1985	1985	1985	1986	1985	1985	1985	1985
Sample	23-6A	23-6B	23-6D	B20-13	29-4B	29-6	29-7	29-8
Lithology	SHLE	DLNT	QRTZ	DLNT	DLNT	DLBR	DLBR	DLBR
Geochem #	79	80	82	765	247	250	251	252
SiO2	49.1	15.0	83.2	46.2	38.8	85.2	87.0	97.2
Al2O3	14.0	2.05	3.07	0.76	0.06	0.08	0.18	0.33
Fe2O3(t)	8.17	8.23	1.44	4.83	0.47	0.14	0.14	0.09
Fe2O3								
FeO								
MgO	5.01	13.7	1.37	2.99	13.3	2.87	2.70	0.27
CaO	6.22	24.9	3.22	22.8	19.2	4.40	4.17	0.47
Na2O	2.35	0.04	0.48	0.01	0.01	0.01	0.01	0.01
K2O	3.43	0.52	1.45	0.04	0.05	0.05	0.08	0.14
TiO2	1.51	0.09	0.22	0.11	0.01	0.02	0.02	0.02
MnO	0.34	0.44	0.05	0.45	0.05	0.02	0.02	0.01
P2O5	0.28	0.03	0.28	0.36	0.03	0.03	0.05	0.03
LOI	9.47	34.6	4.23	20.4	28.3	6.93	6.00	1.00
Total	100.1	99.7	99.1	99.0	100.3	99.7	100.4	99.6
Rb	90	10	40	20	5	5	10	20
Sr	150	280	60	270	5	5	5	5
Y	20	10	30	40	10	10	5	5
Zr	150	20	50	5	5	5	5	5
Nb	50	5	10	10	5	5	10	10
Ba	710	90	340	40	5	70	50	80
Hf								
Ta								
Cr	470	1	46	20	5	20	20	40
Co	63	8	10	4				
Ni	100	15	11	7				
Cu	150	5.0	2.0	1.5				
Zn	54.0	14.0	7.5	120				
Pb	1	2	10	22				
U	2.5	2.5	2.5					
Th	2	2	3					
Au	<1	<1	1	1	1	5	2	3
Ag	<0.5	<0.5	<0.5					
La	30	10	15		0.5	0.5	1	0.5
Ce	58	18	19		2.5	2.5	2.5	2.5
Nd								
Sm								
Eu								
Tb								
Dy								
Ho								
Tm								
Yb								
Lu								

Table B3.2: Whole rock major (weight %) and trace (ppm) element geochemisty

Formation	Denault Fm.	Dolly Formation					
Location	Birch	DL-AL	DL-AL	DL-AL	Birch	Birch	Birch
Year	1985	1985	1985	1985	1985	1985	1985
Sample	19-4	22-13	24-5	22-13B	19-3C	21-3E	21-3F
Lithology	DLNT	CHRT	QRTZ	SHLE	SLSN	SHLE	SHLE
Geochem #	210	68	103	70	209	186	187
SiO2		89.70	95.9		76.7	56.0	39.3
Al2O3		1.17	0.21		11.1	10.6	16.6
Fe2O3(t)		2.15	0.12		0.51	18.4	23.0
Fe2O3							3.3
FeO							17.7
MgO		1.06	0.57		1.11	2.96	5.57
CaO		1.51	0.93		0.29	1.14	2.73
Na2O		0.01	0.01		0.76	0.8	2.2
K2O		0.18	0.10		6.14	1.90	2.04
TiO2		0.05	0.02		0.40	1.70	3.74
MnO		0.03	0.01		0.01	0.13	0.22
P2O5		0.02	0.02		0.06	0.18	0.56
LOI		2.39	1.47		1.62	3.76	6.6
Total		98.30	99.4		98.8	99.5	100.6
Rb		5	5		100	60	66
Sr		5	5		10	57	128
Y		5	10		5	18	26
Zr		10	5		60	256	232
Nb		10	5		20	47	48
Ba		120	50		340	458	706
Hf							
Ta							
Cr	1	30	20	84	90	32	50
Co	0.5			7		40	97
Ni	4			130		31	75
Cu	30.0			47		42.0	160
Zn	18.0			200		52.0	130
Pb	2			12		10	1
U	2.5			9		9	2.5
Th	1			11		6	4
Au	3	<1	<1	6	1	<1	1
Ag	<0.5			<0.5		<0.5	<0.5
La		4	0.5			45	44
Ce		6	2.5			82	94
Nd							
Sm							
Eu							
Tb							
Dy							
Ho							
Tm							
Yb							
Lu							

Table B3.2: Whole rock major (weight %) and trace (ppm) element geochemisty

Formation	Fleming Formation							
Location	Marble	Marble	Marble	Marble	Marble	Marble	Marble	Marble
Year	1985	1985	1985	1985	1985	1985	1985	1985
Sample	27-1	27-2	27-3	28-2	28-3A	28-3B	28-4	28-9
Lithology	SNDS	CHBR	CHBR	CHRT	CHBR	CHBR	CHBR	CHRT
Geochem #	225	226	227	229	230	231	232	237
SiO2	96.4	96.4	96.2	95.2	48.0	89.9	96.2	95.2
Al2O3	0.71	1.44	1.59	2.01	15.4	5.52	0.82	2.09
Fe2O3(t)	0.75	0.10	0.08	0.68	12.4	0.73	0.27	0.65
Fe2O3					2.0			
FeO					9.4			
MgO	0.01	0.005	0.005	0.05	7.60	0.13	0.02	0.06
CaO	0.12	0.02	0.01	0.04	7.91	0.28	0.05	0.06
Na2O	0.01	0.01	0.01	0.01	2.6	0.01	0.01	0.01
K2O	0.19	0.42	0.46	0.46	1.98	1.49	0.21	0.52
TiO2	0.05	0.06	0.09	0.10	1.40	0.19	0.05	0.14
MnO	0.01	0.02	0.01	0.01	0.19	0.01	0.01	0.01
P2O5	0.10	0.02	0.02	0.04	0.16	0.17	0.04	0.06
LOI	1.31	0.70	1.08	0.85	3.7	1.23	0.93	0.77
Total	99.7	99.2	99.6	99.5	100.3	99.7	98.6	99.6
Rb	10	20	20	30	33	40	20	20
Sr	10	5	5	5	372	5	5	5
Y	5	5	10	5	17	30	5	5
Zr	20	40	5	10	83	60	5	20
Nb	10	10	10	30	12	10	20	10
Ba	100	90	70	80	408	180	40	90
Hf								
Ta								
Cr	30	40	30	30	14	40	30	30
Co								
Ni								
Cu								
Zn								
Pb								
U								
Th								
Au	<1	<1	1	<1	<1	1	<1	<1
Ag								
La	4	12	5	12	11	35	5	10
Ce	7	23	9	17	31	43	6	14
Nd								
Sm								
Eu								
Tb								
Dy								
Ho								
Tm								
Yb								
Lu								

Table B3.2: Whole rock major (weight %) and trace (ppm) element geochemisty

Formation	Fleming Formation (continued)				Wishart Formation		
Location	Marble	Marble	Marble	Marble	DL-AL	DL-AL	DL-AL
Year	1985	1985	1985	1985	1985	1985	1986
Sample	28-10	29-4A	29-5A	29-5B	D1-10	D2-9	B20-11
Lithology	CHRT	CHRT	CHBR	CHBR	SLSN	SNDS	QRTZ
Geochem #	238	246	248	249	16	25	763
SiO2	94.1	95.4	89.0	72.9	46.90	82.70	63.2
Al2O3	3.08	0.29	0.10	0.22	16.20	7.86	18.4
Fe2O3(t)	0.65	0.15	0.29	0.22	9.56	1.59	5.11
Fe2O3							
FeO							
MgO	0.04	0.80	2.03	5.62	2.86	0.57	1.92
CaO	0.02	1.38	3.35	8.55	6.58	0.35	0.21
Na2O	0.01	0.01	0.01	0.01	3.48	3.13	1.52
K2O	0.78	0.11	0.06	0.09	4.56	1.36	5.77
TiO2	0.17	0.03	0.03	0.02	1.23	0.13	0.73
MnO	0.01	0.02	0.04	0.03	0.21	0.10	0.03
P2O5	0.03	0.02	0.06	0.11	0.22	0.04	0.11
LOI	0.85	2.16	4.70	12.50	6.54	1.47	3.16
Total	99.7	100.4	99.7	100.2	98.50	99.40	100.3
Rb	20	10	5	10	110	50	290
Sr	5	5	5	5	200	90	110
Y	5	5	5	10	10	10	30
Zr	30	5	5	5	50	210	150
Nb	10	10	10	10	20	20	20
Ba	60	60	70	30	910	310	650
Hf					2		
Ta					1		
Cr	30	30	20	20	30.0	14	130
Co					54	9	24
Ni					100	9	35
Cu					53	3	21.0
Zn					72	14	43.0
Pb					2	8	4
U					2.5	2.5	
Th					0.5	7	
Au	<1	1	1	<1	<1	1	<1
Ag					<0.5	<0.5	
La	17	1	0.5	2	17	17	
Ce	24	2.5	2.5	2.5	38	30	
Nd							
Sm							
Eu							
Tb							
Dy							
Ho							
Tm							
Yb							
Lu							

Table B3.2: Whole rock major (weight %) and trace (ppm) element geochemisty

Formation	Wishart Fm.	Sokoman Formation					
Location	DL-AL	DL-AL	DL-AL	DL-AL	DL-AL	DL-AL	DL-AL
Year	1985	1985	1986	1986	1986	1986	1986
Sample	23-5	D3-11	F6-4	B7-3A*	B13-1	B14-5B	B16-5B
Lithology	SNDS	CHIR	IRFM	IRFM	IRFM	IRFM	IRFM
Geochem #	78	43	553	614	674	687	709
SiO2		49.70	60.0	74.9	49.4	45.7	51.1
Al2O3		1.03	0.17	0.12	13.2	0.87	14.5
Fe2O3(t)		38.70	38.5	22.7	13.2	32.2	17.2
Fe2O3							
FeO							
MgO		2.17	1.51	0.80	9.28	2.95	0.60
CaO		0.29	0.20	0.26	7.35	0.65	0.12
Na2O		0.01	0.01	0.01	2.40	0.01	7.19
K2O		0.09	0.05	0.05	1.28	0.03	0.45
TiO2		0.10	0.04	0.04	0.68	0.06	3.21
MnO		1.97	0.02	0.42	0.32	1.98	0.12
P2O5		0.09	0.02	0.03	0.06	0.05	0.33
LOI		6.00	0.07	0.93	2.47	15.5	0.77
Total		100.20	100.5	100.3	99.8	100.0	98.5
Rb		5	5	20	32	5	10
Sr		5	5	5	145	5	180
Y		5	5	5	5	5	40
Zr		5	5	5	24	50	180
Nb		40	40	10	27	10	70
Ba		160	140	130	371	170	240
Hf							
Ta							
Cr	14	1	50	40	500	50	40
Co	12	20	3	6	47	10	73
Ni	20	2	0.5	0.5	140	5	33
Cu	18.0	0.50	0.25	2.5	17.0	2.5	64.0
Zn	37.0	19	5.5	4.5	130	10.0	75.0
Pb	20	1	1	1	1	1	2
U	2.5	2.5					
Th	7	0.5					
Au	9	<1	<1	<1	4	<1	<1
Ag	<0.5	<0.5			<0.5		
La		9					
Ce		24					
Nd							
Sm							
Eu							
Tb							
Dy							
Ho							
Tm							
Yb							
Lu							

Table B3.2: Whole rock major (weight %) and trace (ppm) element geochemisty

Formation	Sokoman Formation (continued)					Menihek Formation	
Location	DL-AL	DL-AL	DL-AL	DL-AL	Birch	DL-AL	DL-AL
Year	1985	1985	1985	1985	1985	1985	1985
Sample	D3-5A	D4-7	22-3	22-5a(i)	21-2A	D2-1B	D3-3
Lithology	CHIR	SCIF	CHIR	IRFM	IRFM	SNDS	SHLE
Geochem #	31	50	53	57	179	18	29
SiO2						50.70	67.20
Al2O3						16.80	13.40
Fe2O3(t)						2.86	5.07
Fe2O3							
FeO							
MgO						1.65	2.27
CaO						8.09	1.50
Na2O						1.67	2.83
K2O						6.57	2.66
TiO2						0.58	0.64
MnO						0.50	0.13
P2O5						0.13	0.17
LOI						8.93	3.70
Total						98.80	99.70
Rb						190	120
Sr						380	160
Y						30	20
Zr						410	190
Nb						30	20
Ba						1540	670
Hf						11	
Ta						2	
Cr	1	1	1	54	30	10	100
Co	3	4	4	16	5	19	21
Ni	0.5	0.5	1	28	5	22	53
Cu	3.50	0.25	7.5	16	16.0	29	42
Zn	9	8	9.5	34	14.0	38	130
Pb	1	1	1	12	4	18	16
U	2.5	2.5	2.5	2.5	2.5	2.5	2.5
Th	0.5	0.5	0.5	9	7	19	13
Au	1	<1	<1	<1	<1	<1	<1
Ag	<0.5	<0.5	<0.5	<0.5	<0.5	<0.5	<0.5
La						80	46
Ce						114	72
Nd							
Sm							
Eu							
Tb							
Dy							
Ho							
Tm							
Yb							
Lu							

Table B3.2: Whole rock major (weight %) and trace (ppm) element geochemisty

Formation	Menihek Fm (cont.)		Nimish Formation: Epiclastic and volcaniclastic rocks				
Location	DL-AL	DL-AL	DL-AL	DL-AL	DL-AL	DL-AL	DL-AL
Year	1985	1986	1985	1985	1985	1985	1985
Sample	28-8	B27-2B	D1-1C	D3-4	D3-6D	D4-1	22-4B
Lithology	SLSN	SHLE	AGLM	VCCG	VCCG	VCCG	VCCG
Geochem #	236	800	3	30	38	44	55
SiO2	94.7	16.4	62.00	39.10	47.70	59.30	62.10
Al2O3	1.71	2.11	7.22	13.30	16.10	11.10	14.70
Fe2O3(t)	0.85	5.03	20.90	19.10	19.00	13.30	9.39
Fe2O3							
FeO							
MgO	0.04	1.01	2.10	9.85	2.09	2.08	1.17
CaO	0.44	40.4	1.41	5.70	0.19	2.97	0.14
Na2O	0.005	0.005	0.12	0.005	1.21	1.56	1.36
K2O	0.40	0.06	2.13	1.98	8.69	2.80	7.47
TiO2	0.08	0.18	0.75	1.36	2.21	1.72	1.07
MnO	0.01	1.08	0.07	0.26	0.13	0.17	0.03
P2O5	0.33	0.05	0.08	0.20	0.08	0.41	0.08
LOI	1.16	33.3	2.31	9.31	1.70	3.31	1.77
Total	99.7	99.7	99.20	100.30	99.40	98.90	99.50
Rb	10	10	130	30	240	50	160
Sr	5	160	60	80	180	120	30
Y	10	10	5	5	50	30	60
Zr	5	50	20	60	240	240	620
Nb	20	20	20	40	50	40	90
Ba	100	30	340	220	1610	770	890
Hf			1			7	14
Ta			1			2	2
Cr	30	5	470	200	26	19	6
Co		6	28	82	67	50	18
Ni		9	69	140	40	26	8
Cu		5.0	17	87	24	48	20
Zn		18.0	53	120	110	170	110
Pb		6	1.0	1	1	26	8
U			2.5	2.5	2.5	2.5	2.5
Th			1	1	6	5	13
Au	3	<1	<1	<1	<1	2	<1
Ag			<0.5	<0.5	<0.5	<0.5	<0.5
La	9		13	17	48	50	129
Ce	11		24	32	92	94	219
Nd							
Sm							
Eu							
Tb							
Dy							
Ho							
Tm							
Yb							
Lu							

Table B3.2: Whole rock major (weight %) and trace (ppm) element geochemisty

Formation	Nimish Formation: Epiclastic and volcaniclastic rocks (cont.)							
Location	DL-AL	DL-AL	DL-AL	DL-AL	DL-AL	DL-AL	DL-AL	DL-AL
Year	1985	1985	1985	1985	1985	1985	1986	1986
Sample	22-7	23-14B	7-3.	J1-009	4-3.	4-6.	W3-8A	W5-2A
Lithology	VCCG	MAAG	MAAG	TUFF	VCBR	TUFF	VCCG	VCCG
Geochem #	61	95	127	150	156	158	315	343
SiO2	63.90	37.8	41.4	39.6	54.6	46.9	74.0	43.7
Al2O3	14.80	12.1	15.0	13.4	13.7	9.6	13.1	11.7
Fe2O3(t)	7.92	15.4	22.4	16.8	13.8	8.0	0.95	19.5
Fe2O3			2.6	3.1	2.5	1.3		
FeO			17.8	12.3	10.2	6.0		
MgO	0.95	4.04	8.26	13.51	4.86	5.14	0.09	6.68
CaO	0.31	12.5	2.11	6.89	1.97	13.18	0.20	9.91
Na2O	2.84	3.33	0.7	0.8	0.8	0.9	2.52	1.62
K2O	6.25	0.23	2.46	0.18	4.82	1.52	7.52	0.37
TiO2	0.82	2.18	1.52	2.43	2.15	1.24	0.50	2.42
MnO	0.05	0.35	0.15	0.24	0.11	0.34	0.03	0.22
P2O5	0.17	0.23	0.20	0.19	0.61	0.18	0.08	0.06
LOI	1.70	10.9	7.9	7.8	4.4	13.5	0.70	3.16
Total	100.00	99.1	100.1	100.5	100.7	99.8	99.9	99.4
Rb	170	20	56	6	66	72	170	30
Sr	40	90	14	236	102	130	20	40
Y	80	10	15	20	29	16	50	5
Zr	770	130	110	126	218	78	440	20
Nb	110	60	11	26	23	17	70	20
Ba	860	160	222	172	969	142	1060	110
Hf			3					
Ta			1					
Cr	4	6	170				30	50
Co	16	67	45				6	99
Ni	9	39	160				4	86
Cu	2.5	89.0	46.0				2.0	270
Zn	100	120	110				53.0	89.0
Pb	10	1	1				24	1
U	2.5	2.5	2.5					
Th	16	3	1					
Au	<1	<1	<1				1	<1
Ag	<0.5	<0.5	<0.5					
La	149	30	20	18	33	10		
Ce	245	55	42					
Nd								
Sm								
Eu								
Tb								
Dy								
Ho								
Tm								
Yb								
Lu								

Table B3.2: Whole rock major (weight %) and trace (ppm) element geochemisty

Formation	Nimish Formation: Epiclastic and volcaniclastic rocks (cont.)							
Location	DL-AL	DL-AL	DL-AL	DL-AL	DL-AL	DL-AL	DL-AL	DL-AL
Year	1986	1986	1986	1986	1986	1985	1985	1985
Sample	W5-3	W5-4	W9-4	W31-5A	B12-3	D3-8	D3-10	23-6C
Lithology	VCCG	VCCG	VCCL	VCCG	VCCG	VCCG	VCCG	TUFF
Geochem #	345	346	376	520	669	40	42	81
SiO2	59.3	48.1	46.4	37.5	41.2			
Al2O3	12.6	14.7	14.9	13.9	14.2			
Fe2O3(t)	13.2	14.6	22.8	22.3	16.6			
Fe2O3								
FeO								
MgO	1.47	3.11	4.30	7.09	8.53			
CaO	2.39	7.55	0.44	3.54	4.82			
Na2O	2.00	2.28	0.16	0.55	0.20			
K2O	4.08	2.34	4.61	4.63	3.86			
TiO2	1.37	2.54	2.28	1.97	1.92			
MnO	0.17	0.21	0.17	0.29	0.24			
P2O5	0.32	0.59	0.03	0.34	0.34			
LOI	2.23	2.54	4.16	7.47	7.00			
Total	99.5	98.8	100.3	99.7	99.0			
Rb	60	70	5	120	100			
Sr	170	470	10	180	40			
Y	40	10	5	10	20			
Zr	600	200	190	140	130			
Nb	70	40	70	50	40			
Ba	1870	920	490	540	400			
Hf								
Ta								
Cr	50	50	60	40	70	32	240	2600
Co	22	58	67	59	63	38	50	42
Ni	10	23	66	27	66	19	50	750
Cu	9.5	36.0	7.0	5.5	38.0	11	15	120
Zn	110	150	200	81.0	92.0	61	140	65.0
Pb	2	1	1	1	1	2	1	2
U						2.5	2.5	2.5
Th						17	6	1
Au	<1	1	<1	1	<1	8	<1	17
Ag						<0.5	<0.5	<0.5
La								
Ce								
Nd								
Sm								
Eu								
Tb								
Dy								
Ho								
Tm								
Yb								
Lu								

Table B3.2: Whole rock major (weight %) and trace (ppm) element geochemisty

Formation	Nimish Fm: Epiclastic/volcaniclastic rocks (cont.)					Nimish Fm: volcanic rx.	
Location	Marble	Birch	Birch	Birch	Birch	DL-AL	DL-AL
Year	1985	1985	1985	1985	1985	1985	1985
Sample	29-2B	21-3C	21-3D	B2-6A	B2-6B	D1-1B	D1-7
Lithology	MAAG	AGLM	TUFF	VCCG	TUFF	AMBS	BSLT
Geochem #	244	184	185	200	201	2	13
SiO2	56.2	40.6	67.7	56.3	45.6	47.60	49.30
Al2O3	9.90	15.2	5.97	10.9	13.0	16.60	15.80
Fe2O3(t)	21.7	21.8	10.5	16.2	11.4	12.00	11.10
Fe2O3		4.5					
FeO		15.6					
MgO	2.95	6.48	2.37	2.28	10.4	6.58	5.84
CaO	0.36	4.17	5.45	10.7	10.1	6.49	6.21
Na2O	1.10	1.6	0.02	0.005	1.90	2.95	2.33
K2O	4.29	0.58	0.76	0.17	0.34	1.96	3.13
TiO2	0.97	3.48	0.97	0.60	0.64	1.56	1.57
MnO	0.20	0.20	0.13	0.10	0.22	0.19	0.18
P2O5	0.14	0.44	0.12	0.05	0.10	0.25	0.28
LOI	2.31	7.6	5.39	2.47	5.54	3.00	3.00
Total	100.2	100.5	99.5	100.1	99.6	99.30	98.90
Rb	120	20	10	5	5	70	100
Sr	30	117	100	1630	510	560	330
Y	5	16	10	10	20	20	20
Zr	30	202	130	5	5	80	80
Nb	30	40	40	10	10	40	20
Ba	390	377	290	190	300	440	720
Hf							
Ta							
Cr	170	32	26	730	1700	52	18
Co	48	87	35	42	73	62	63
Ni	120	58	23	230	320	84	75
Cu	7.5	110	36.0	67.0	76.0	20	49
Zn	60.0	100	48.0	31.0	100	110	91
Pb	1	1	10	2	1	1	1
U	2.5	2.5	2.5	2.5	2.5	2.5	2.5
Th	0.5	5	3	0.5	1	1	1
Au	1	1	<1	1	2	<1	<1
Ag	<0.5	<0.5	<0.5	<0.5	<0.5	<0.5	<0.5
La	10	44	31	8	8	19	23
Ce	19	80	50	20	18	38	42
Nd							
Sm							
Eu							
Tb							
Dy							
Ho							
Tm							
Yb							
Lu							

Table B3.2: Whole rock major (weight %) and trace (ppm) element geochemisty

Formation	Nimish Formation: volcanic rocks (continued)							
Location	DL-AL	DL-AL	DL-AL	DL-AL	DL-AL	DL-AL	DL-AL	DL-AL
Year	1985	1985	1985	1985	1985	1985	1985	1985
Sample	D3-2	D3-6B	22-5B	22-8	22-9	23-9	23-11	23-14C
Lithology	BSLT	BSLT	PPIV	AMBS	AMBS	BSLT	BSLT	BSLT
Geochem #	28	37	58	62	63	88	90	96
SiO2	45.70	41.80	50.50	48.50	43.80	49.0	49.4	47.2
Al2O3	13.50	19.10	16.40	16.00	12.10	16.5	13.6	14.0
Fe2O3(t)	13.80	21.00	18.00	12.40	12.80	10.9	13.4	15.0
Fe2O3								
FeO								
MgO	7.21	2.75	2.15	5.43	11.90	5.19	3.00	5.05
CaO	10.80	0.17	0.14	7.49	9.16	8.06	4.74	9.40
Na2O	0.01	0.005	0.14	2.80	1.27	2.57	2.27	2.57
K2O	2.05	9.03	8.27	2.27	1.55	1.86	3.38	0.88
TiO2	1.77	2.80	0.76	1.60	1.50	1.29	3.03	2.49
MnO	0.22	0.17	0.10	0.20	0.26	0.19	0.16	0.31
P2O5	0.33	0.12	0.12	0.26	0.16	0.29	0.98	0.25
LOI	3.70	3.08	3.39	2.77	4.77	3.54	5.00	2.85
Total	99.30	100.30	100.20	99.90	99.50	99.6	99.2	100.1
Rb	50	560	150	130	70	50	100	24
Sr	800	70	30	340	160	550	320	384
Y	10	10	70	10	10	30	30	24
Zr	90	150	610	90	90	70	330	145
Nb	20	40	70	30	40	20	100	41
Ba	400	1640	1220	580	510	650	1050	626
Hf								
Ta								
Cr	24	22	1	32	520	58	1	14
Co	52	77	13	70	76	58	65	75
Ni	71	46	3	61	250	64	11	50
Cu	50	9.50	1	46	89	53.0	32.0	140
Zn	110	72	120	97	94	92.0	97.0	130
Pb	4	1	1	1	1	1	4	4
U	2.5	2.5	2.5	2.5	2.5	2.5	2.5	2.5
Th	1	3	8	1	1	1	6	3
Au	4	<1	2	<1	1	<1	<1	<1
Ag	<0.5	<0.5	<0.5	<0.5	<0.5	<0.5	<0.5	<0.5
La	29	29	73	22	14	27	85	26
Ce	56	66	122	48	31	57	144	61
Nd								
Sm								
Eu								
Tb								
Dy								
Ho								
Tm								
Yb								
Lu								

Table B3.2: Whole rock major (weight %) and trace (ppm) element geochemisty

Formation	Nimish Formation: volcanic rocks (continued)							
Location	DL-AL	DL-AL	DL-AL	DL-AL	DL-AL	DL-AL	DL-AL	DL-AL
Year	1985	1986	1986	1986	1986	1986	1986	1986
Sample	4-7.	W3-4B	W3-6	W4-13	W5-1	W5-2B	W6-6	W7-3
Lithology	PPBS	BSLT	AMBS	BSLT	BSLT	BSLT	BSLT	BSLT
Geochem #	159	311	313	333	342	344	356	359
SiO2	49.2	53.0	48.2	43.46	44.3	44.9	45.8	45.7
Al2O3	16.6	15.8	15.4	15.25	15.4	15.4	16.9	15.8
Fe2O3(t)	15.4	15.3	18.5	14.30	12.9	16.2	14.1	14.3
Fe2O3	1.8			2.06				
FeO	12.2			11.01				
MgO	2.14	1.63	3.03	9.15	8.88	5.78	4.73	4.46
CaO	1.69	1.31	1.87	9.40	9.00	5.99	7.75	4.72
Na2O	0.8	1.43	2.78	2.05	1.99	3.65	3.08	3.79
K2O	8.24	7.12	3.40	1.69	0.75	1.23	0.59	3.03
TiO2	2.88	2.35	2.62	1.85	1.56	2.40	2.42	2.41
MnO	0.10	0.17	0.08	0.20	0.21	0.41	0.19	0.40
P2O5	1.11	0.84	0.42	0.17	0.19	0.29	0.30	0.33
LOI	3.75	3.08	2.70	3.53	4.00	2.85	2.70	3.85
Total	100.5	100.3	99.2	100.13	99.3	99.2	98.8	99.0
Rb	111	93	140	86	40	32	14	120
Sr	62	91	260	473	220	172	483	240
Y	36	51	10	17	20	26	27	20
Zr	352	302	260	148	90	102	139	110
Nb	44	37	70	35	10	27	33	60
Ba	1388	970	950	650	420	489	1032	980
Hf		9				4	5	
Ta		0.5		2.63		0.5	0.5	1.95
Cr		40	60	275	290	80	30	60
Co		44	54		62	97	66	160
Ni		18	28	183	140	59	32	100
Cu		43.0	44.0		53.0	110.0	30.0	100.0
Zn		100	97.0	317	99.0	160.0	93.0	150
Pb		8	1		1	4	8	1
U				0.59				0.55
Th		6.0		2.79			3.4	2.81
Au		<1	<1	1	3	1	<1	<1
Ag								
La	60	84		25.6			40	23.4
Ce				60				53
Nd				27.5				24.2
Sm				5.7				5.1
Eu				2.00				1.76
Tb				0.77				0.81
Dy				3.3				3.7
Ho				0.67				0.70
Tm								
Yb				1.58				1.87
Lu				0.22				0.28

Table B3.2: Whole rock major (weight %) and trace (ppm) element geochemisty

Formation	Nimish Formation: volcanic rocks (continued)							
Location	DL-AL	DL-AL	DL-AL	DL-AL	DL-AL	DL-AL	DL-AL	DL-AL
Year	1986	1986	1986	1986	1986	1986	1986	1986
Sample	W7-7	W7-8A	W7-8B	W8-3	W8-5	W9-3A	W10-11	W13-5
Lithology	BSLT	BSLT	AMBS	PPBS	AMBS	IMVC	BSLT	PPIV
Geochem #	363	364	365	368	370	374	396	422
SiO2	48.4	47.5	49.7	49.5	51.7	47.1	44.0	51.06
Al2O3	15.5	16.6	15.3	17.5	15.2	18.3	15.2	14.94
Fe2O3(t)	14.5	14.7	15.0	11.5	13.2	9.65	13.8	13.94
Fe2O3								2.09
FeO								10.67
MgO	4.10	3.71	3.32	3.87	3.36	2.65	8.02	2.91
CaO	3.72	2.99	2.20	5.09	1.29	4.39	8.86	5.27
Na2O	4.20	4.03	1.78	3.68	1.30	2.16	2.36	2.40
K2O	2.15	2.71	6.05	2.86	6.77	6.38	0.69	4.74
TiO2	2.33	2.46	2.26	2.11	2.25	2.48	2.17	2.25
MnO	0.20	0.22	0.20	0.18	0.11	0.21	0.22	0.24
P2O5	0.73	0.78	0.82	0.65	0.79	0.27	0.34	1.01
LOI	3.77	3.31	3.08	3.00	3.31	4.93	3.85	1.28
Total	99.8	99.3	100.0	100.2	99.6	98.8	99.7	99.27
Rb	90	43	150	100	130	190	14	102
Sr	440	290	210	350	100	100	498	530
Y	10	35	20	30	40	30	23	40
Zr	290	247	290	280	310	140	132	226
Nb	70	47	80	50	50	60	41	30
Ba	830	1100	1560	990	1810	1900	654	1503
Hf		7					4	
Ta		0.5					0.5	
Cr	30	30	20	50	20	50	120	
Co	42	49	37	45	42	130	62	
Ni	7	7	8	22	6	60	110	
Cu	11.0	15.0	7.5	16.0	15.0	92.0	55.0	
Zn	160	160	140	120	84.0	120	100	
Pb	4	1	1	1	1	2	2	
U								
Th		4.2					3.6	
Au	<1	<1	<1	<1	2	<1	<1	
Ag								
La		60					42	
Ce								
Nd								
Sm								
Eu								
Tb								
Dy								
Ho								
Tm								
Yb								
Lu								

Table B3.2: Whole rock major (weight %) and trace (ppm) element geochemisty

Formation	Nimish Formation: volcanic rocks (continued)							
Location	DL-AL	DL-AL	DL-AL	DL-AL	DL-AL	DL-AL	DL-AL	DL-AL
Year	1986	1986	1986	1986	1986	1986	1986	1986
Sample	W14-4C	W17-3	W18-4	W18-5	W18-6	W20-1	W21-6	W30-7
Lithology	AMBS	BSLT	PLBS	PLBS	PLBS	BLST	PPBS	PLBS
Geochem #	433	453	465	466	467	480	491	510
SiO2	50.8	48.98	47.69	46.37	45.83	43.00	47.2	45.9
Al2O3	17.7	15.86	17.24	15.55	14.78	15.17	15.1	16.7
Fe2O3(t)	13.1	11.29	20.00	16.51	17.31	16.63	15.1	15.5
Fe2O3		1.52	5.75	2.23	5.26	3.47		
FeO		8.80	12.83	12.85	10.84	11.84		
MgO	2.47	7.45	2.71	6.97	6.74	6.95	3.51	3.27
CaO	1.15	8.53	0.57	3.57	7.08	5.11	5.77	3.00
Na2O	3.52	3.03	0.42	2.44	2.07	2.73	3.96	3.63
K2O	5.08	1.42	6.97	2.84	2.08	1.68	2.63	2.97
TiO2	2.33	1.38	2.45	2.13	2.20	3.36	2.70	2.53
MnO	0.16	0.16	0.15	0.13	0.24	0.50	0.26	0.27
P2O5	0.74	0.10	0.40	0.19	0.25	0.67	0.58	0.41
LOI	2.31	2.33	2.46	4.68	2.85	5.36	2.23	4.47
Total	99.7	99.82	99.80	100.16	100.54	100.09	99.3	98.9
Rb	140	35	153	107	41	41	90	60
Sr	150	396	75	182	270	169	270	310
Y	50	19	46	28	30	19	30	10
Zr	510	81	131	113	165	139	220	190
Nb	40	11	34	28	42	39	40	60
Ba	1560	596	478	556	1100	865	1070	1360
Hf		3						
Ta		0.97						
Cr	40	175	33	42	33	38	60	40
Co	44						64	60
Ni	16	92	35	58	45	22	35	26
Cu	11.0						42.0	22.0
Zn	120	217	115	122	144	98	160	120
Pb	10						4	1
U		0.19						
Th		0.80						
Au	<1	<1		1	1	<1	4	<1
Ag								
La		13.2			32	31		
Ce		33						
Nd		18.4						
Sm		4.2						
Eu		1.31						
Tb		0.66						
Dy		3.6						
Ho		0.79						
Tm								
Yb		1.64						
Lu		0.27						

Table B3.2: Whole rock major (weight %) and trace (ppm) element geochemisty

Formation	Nimish Formation: volcanic rocks (continued)							
Location	DL-AL	DL-AL	DL-AL	DL-AL	DL-AL	DL-AL	DL-AL	DL-AL
Year	1986	1986	1986	1986	1986	1986	1986	1986
Sample	W31-2B	W31-5B	R3-5	R3-10A	F2-1	F2-2	F2-4	F2-6
Lithology	VCBS	PLBS	BSLT	AMBS	BSLT	AMBS	PPBS	AMBS
Geochem #	514	521	527	532	536	537	539	541
SiO2	34.5	43.1	43.7	47.1	50.0	52.6	51.1	52.0
Al2O3	13.6	16.2	14.5	15.3	19.3	16.5	15.6	16.5
Fe2O3(t)	26.1	20.6	13.3	13.3	11.3	11.5	12.6	13.7
Fe2O3	3.40							
FeO	20.42							
MgO	9.21	4.69	9.17	5.89	2.60	2.79	3.00	1.51
CaO	4.69	0.81	9.12	7.23	1.83	2.78	5.81	1.32
Na2O	0.01	2.25	2.04	2.94	2.94	4.43	3.28	2.84
K2O	0.60	4.01	1.60	1.34	4.43	3.12	3.12	6.64
TiO2	1.36	2.56	1.95	1.72	2.99	2.45	2.11	2.20
MnO	0.32	0.51	0.20	0.15	0.14	0.11	0.23	0.99
P2O5	0.21	0.52	0.27	0.27	0.48	0.99	0.63	0.68
LOI	9.85	4.16	3.70	4.00	3.16	2.47	1.85	1.54
Total	100.0	99.6	99.8	99.5	99.4	99.9	99.6	99.2
Rb	30	80	65	30	112	90	70	180
Sr	30	80	442	430	193	220	550	140
Y	10	10	17	30	22	50	30	30
Zr	80	180	141	110	250	350	240	290
Nb	30	70	34	30	58	70	40	40
Ba	90	1540	761	1310	730	890	1080	950
Hf			4		7			
Ta			2		3.79			
Cr	380	50	250	50	30	30	40	60
Co	53	61	68	61	68	42	51	34
Ni	120	26	190	67	27	10	13	26
Cu	66.0	3.0	110	44.0	110	38.0	14.0	2.5
Zn	85.0	99.0	100	110	90.0	140	140	80.0
Pb	1	1	6	1	1	1	2	4
U					1.18			
Th			2.5		5.56			
Au	2	1	1	<1	0.1	<1	<1	<1
Ag								
La			27		47.1			
Ce					108			
Nd					46.1			
Sm					7.3			
Eu					2.45			
Tb					0.93			
Dy					4.9			
Ho					0.91			
Tm								
Yb					1.98			
Lu					0.29			

Table B3.2: Whole rock major (weight %) and trace (ppm) element geochemisty

Formation	Nimish Formation: volcanic rocks (continued)							
Location	DL-AL	DL-AL	DL-AL	DL-AL	DL-AL	DL-AL	DL-AL	DL-AL
Year	1986	1986	1986	1986	1986	1986	1986	1986
Sample	F6-3	B4-2	B7-9	*B7-1	*B7-2	B9-3F	B9-8	B12-5A
Lithology	AMBS	BSLT	BSLT	AMBS	BSLT	PLBS	PLBS	PPBS
Geochem #	552	589	609	612	613	632	639	671
SiO2	48.3	47.8	46.8	46.6	45.6	46.6	47.8	48.1
Al2O3	14.8	14.5	14.1	15.1	15.4	16.5	14.0	14.9
Fe2O3(t)	15.8	14.4	17.6	11.1	14.6	1o.1	15.0	13.7
Fe2O3								
FeO								
MgO	2.29	4.10	5.34	7.77	5.39	4.25	4.35	6.43
CaO	2.34	7.56	4.01	6.21	7.92	3.05	5.92	9.59
Na2O	0.57	3.05	2.41	2.57	2.57	3.23	2.59	1.84
K2O	9.76	2.16	0.94	2.76	1.82	3.33	3.11	0.70
TiO2	2.64	2.54	2.67	1.43	3.02	2.83	2.74	1.44
MnO	0.14	0.25	0.20	0.21	0.23	0.23	0.23	0.21
P2O5	0.45	0.60	0.39	0.18	0.46	0.45	0.67	0.25
LOI	2.00	1.93	5.54	4.93	2.62	2.93	3.00	3.00
Total	99.4	99.1	100.1	99.0	99.8	99.7	99.6	100.3
Rb	270	34	50	100	56	100	64	20
Sr	80	459	80	270	456	340	463	350
Y	20	31	20	5	29	30	33	20
Zr	80	146	90	50	174	270	173	100
Nb	30	21	40	20	42	90	24	30
Ba	2110	894	370	550	755	1060	892	310
Hf		5			5		5	
Ta		0.5			3.50		1.77	
Cr	60	50	60	130	70	30	40	130
Co	80	58	66	76	68	59	59	59
Ni	37	25	33	140	64	20	18	83
Cu	180	24.0	46.0	150	100	83.0	20.0	93.0
Zn	92.0	120	120	120	120	100	140	120
Pb	6	1	1	1	8	10	12	16
U					0.65		0.31	
Th		2.4			3.68		2.55	
Au	1	1	<1	<1	2	<1	<1	<1
Ag								
La		39			39.8		40.4	
Ce					87.4		91.2	
Nd					42.2		46.6	
Sm					8.2		9.4	
Eu					2.47		2.99	
Tb					1.13		1.3	
Dy					5.1		6.0	
Ho					1.16		1.26	
Tm								
Yb					2.6		3.00	
Lu					0.43		0.48	

Table B3.2: Whole rock major (weight %) and trace (ppm) element geochemisty

Formation	Nimish Formation: volcanic rocks (continued)							
Location	DL-AL	DL-AL	DL-AL	DL-AL	DL-AL	DL-AL	DL-AL	DL-AL
Year	1986	1986	1986	1986	1986	1987	1987	1987
Sample	B15-1	B15-3A	B15-3B	B18-9A	B27-1B	R1-2	R1-3	R1-5
Lithology	AMBS	AMIV	PPBS	IMVC	BSLT	BSLT	PLBS	PLBS
Geochem #	696	698	699	733	798	1104	1105	1107
SiO2	45.4	54.25	47.2	49.5	47.7	45.7	47.3	51.1
Al2O3	19.0	19.22	15.5	17.3	16.5	15.2	16.4	13.0
Fe2O3(t)	12.5	10.58	13.7	14.4	15.7	17.1	13.9	17.0
Fe2O3		1.83						
FeO		7.88						
MgO	3.38	2.90	6.42	3.15	4.05	4.01	4.46	5.30
CaO	3.53	1.40	8.26	0.78	2.77	6.51	3.68	5.75
Na2O	0.51	3.35	2.47	1.18	4.22	2.25	4.31	0.86
K2O	7.30	4.80	1.11	6.47	2.73	1.43	2.18	0.42
TiO2	2.45	1.63	1.49	2.96	2.45	2.80	2.56	1.81
MnO	0.11	0.05	0.21	0.14	0.18	0.29	0.19	0.22
P2O5	0.45	0.23	0.27	0.48	0.41	0.74	0.42	0.32
LOI	5.23	2.73	3.00	3.23	2.70	3.54	3.70	3.85
Total	100.1	98.62	99.8	99.8	99.6	99.8	99.4	99.8
Rb	180	122	30	113	55	62	66	25
Sr	170	94	320	163	284	735	455	1090
Y	10	13	10	27	29	32	20	25
Zr	150	85	120	240	169	249	162	86
Nb	40	15	10	46	64	58	53	40
Ba	1880	882	530	872	1210	690	1480	254
Hf				7				
Ta				0.5				
Cr	40	31	120	30	12	4	16	22
Co	69		62	82	58	36	51	55
Ni	75	58	76	59	22	19	35	44
Cu	55.0		65.0	49.0	19.0	26.0	31.0	52.0
Zn	68.0	257	120	120	110	180	130	130
Pb	6		12	2	1	1	1	1
U								
Th				6.5				
Au	<1		1	<1	<1	<1	2	<1
Ag					0.5	0.5	<0.5	<0.5
La		16		60				
Ce								
Nd								
Sm								
Eu								
Tb								
Dy								
Ho								
Tm								
Yb								
Lu								

Table B3.2: Whole rock major (weight %) and trace (ppm) element geochemisty

Formation	Nimish Formation: volcanic rocks (continued)							
Location	DL-AL	DL-AL	DL-AL	DL-AL	DL-AL	DL-AL	DL-AL	DL-AL
Year	1987	1987	1987	1985	1985	1985	1985	1985
Sample	B8-2A	B8-4C	B8-6	D1-1F	D1-5	D4-3	22-2	22-4A
Lithology	PPBS	BSLT	BSLT	VCCG	RYLT	IMVC	RYLT	BSLT
Geochem #	1160	1164	1166	6	11	46	52	54
SiO2	48.9	47.3	48.3	62.20	68.30	56.60	89.20	60.40
Al2O3	15.0	16.1	14.3	9.18	7.31	16.90	0.38	15.80
Fe2O3(t)	13.4	14.5	14.8	16.80	14.10	12.30	8.87	8.91
Fe2O3								
FeO								
MgO	3.28	3.60	3.40	3.39	1.91	1.59	0.39	1.11
CaO	4.81	4.10	6.40	0.99	1.41	0.69	0.26	0.01
Na2O	2.51	2.50	2.35	0.27	0.01	3.33	0.005	1.73
K2O	3.55	4.38	2.81	3.57	2.78	5.28	0.09	8.39
TiO2	2.25	2.30	2.53	0.89	1.15	0.89	0.08	0.89
MnO	0.19	0.17	0.23	0.11	0.05	0.15	0.02	0.04
P2O5	0.59	0.98	0.65	0.06	0.38	0.19	0.02	0.08
LOI	4.70	3.70	3.39	2.47	1.85	2.08	0.54	1.77
Total	99.5	99.9	99.4	100.10	99.30	100.10	99.90	99.40
Rb	77	100	113	110	180	100	10	160
Sr	311	514	483	80	20	130	5	20
Y	32	45	42	10	20	40	5	100
Zr	225	302	225	60	100	260	5	670
Nb	48	67	38	30	40	50	5	110
Ba	1720	1620	976	690	270	1350	110	960
Hf								
Ta								
Cr	16	1	6	470	44	1	1	1
Co	26	24	29	36	26	22	2	19
Ni	19	12	17	53	39	9	2	5
Cu	34.0	11.0	25.0	28	4.50	2	0.5	2.5
Zn	150	170	190	100	46	140	3.5	82
Pb	4	1	1	1	1	2	1	6
U				2.5	2.5	2.5	2.5	2.5
Th				1	2	6	0.5	15
Au	<1	<1	<1	<1	<1	<1	<1	<1
Ag	<0.5	0.5	<0.5	<0.5	<0.5	<0.5	<0.5	<0.5
La				16	37	61	0.5	110
Ce				27	61	106	2.5	172
Nd								
Sm								
Eu								
Tb								
Dy								
Ho								
Tm								
Yb								
Lu								

Table B3.2: Whole rock major (weight %) and trace (ppm) element geochemisty

Formation	Nimish Formation: volcanic rocks (continued)							
Location	DL-AL	DL-AL	DL-AL	DL-AL	DL-AL	DL-AL	DL-AL	DL-AL
Year	1985	1985	1985	1985	1986	1986	1986	1986
Sample	22-5A	22-5C	4-14.	W2-1	W6-4B	W8-1	W11-3A	W13-9
Lithology	IMVC	SIVC	RYLT	AMBS	IMVC	PPBS	PLBS	BSLT
Geochem #	56	59	168	300	352	366	401	427
SiO2	54.20	61.20	56.4	53.6	57.40	57.7	60.1	58.9
Al2O3	16.60	16.10	18.6	12.9	18.13	17.5	17.8	15.1
Fe2O3(t)	9.54	9.09	8.80	16.4	7.26	9.34	8.34	8.45
Fe2O3			1.5		1.04			
FeO			6.6		5.59			
MgO	1.17	1.15	1.05	2.78	0.85	0.79	1.54	0.75
CaO	3.70	0.19	0.58	2.50	0.24	0.67	0.54	1.89
Na2O	4.60	1.72	3.52	1.39	0.00	1.93	2.69	4.24
K2O	2.86	8.18	7.60	4.51	13.32	9.48	4.75	5.56
TiO2	2.02	0.94	0.90	1.95	0.81	0.88	1.45	1.07
MnO	0.16	0.04	0.08	0.14	0.04	0.12	0.03	0.18
P2O5	0.60	0.08	0.18	0.71	0.19	0.06	0.30	0.30
LOI	3.16	1.62	2.10	2.93	1.23	1.54	2.70	1.93
Total	98.80	100.60	99.1	100.1	99.14	100.3	100.4	98.7
Rb	80	160	115	90	187	250	250	90
Sr	320	30	81	30	18	60	100	184
Y	30	70	45	40	69	30	10	56
Zr	300	690	285	370	478	260	100	449
Nb	40	110	48	50	56	60	20	44
Ba	890	950	1200	1470	1174	1390	780	1548
Hf	6		5.9		15			13
Ta	1		2.2		0.5		0.52	0.5
Cr	10	1	14	80		20	140	30
Co	39	15	14	32		12	63	14
Ni	15	4	42	8	5	6	71	4
Cu	33	2	32	5.0		4.0	550	6.5
Zn	230	120	125	100	120	110	92.0	140
Pb	10	6	14	1		1	2	8
U	2.5	2.5	0				0.26	
Th	4	9	1		8.9		0.87	6.7
Au	9	<1	<1	3		<1	12	<1
Ag	<0.5	<0.5						
La	50	114	40.5		124		17.7	107
Ce	98	185	84				42	
Nd			48				20.9	
Sm			8.4				4.2	
Eu			2.6				1.17	
Tb							0.59	
Dy			7.7				3.8	
Ho							0.78	
Tm								
Yb			2.6				2.00	
Lu							0.28	

Table B3.2: Whole rock major (weight %) and trace (ppm) element geochemisty

Formation	Nimish Formation: volcanic rocks (continued)							
Location	DL-AL	DL-AL	DL-AL	DL-AL	Marble L.	Birch L.	Birch L.	Birch L.
Year	1986	1986	1986	1987	1985	1985	1985	1985
Sample	F6-5	B7-4A	B7-5	R1-4	28-12	21-3A	21-3B	21-3G
Lithology	IMVC	SIVC	IMVC	PLBS	PPIV	BSLT	PPBS	BSLT
Geochem #	554	602	604	1106	240	182	183	188
SiO2	64.2	66.71	70.47	54.9	46.5	46.4	47.8	46.2
Al2O3	15.1	15.39	13.81	17.1	12.5	15.7	20.1	15.2
Fe2O3(t)	6.85	4.57	2.07	8.19	11.1	14.0	9.17	15.3
Fe2O3		0.80	0.50					
FeO		3.40	1.42					
MgO	0.93	0.79	0.42	2.15	11.2	4.06	2.83	4.56
CaO	0.35	0.26	0.30	2.84	9.51	7.09	7.28	6.73
Na2O	0.20	2.65	0.94	5.01	2.22	2.87	3.28	2.51
K2O	10.6	7.73	10.02	3.78	0.93	2.04	2.23	2.08
TiO2	0.62	0.88	0.60	2.58	1.11	3.47	1.94	3.39
MnO	0.03	0.03	0.01	0.07	0.18	0.28	0.13	0.25
P2O5	0.08	0.24	0.16	0.49	0.12	0.55	0.34	0.52
LOI	1.47	0.89	0.51	1.93	3.54	1.93	4.47	2.08
Total	100.6	99.95	99.40	99.3	99.2	98.6	99.8	99.2
Rb	280	108	140	101	20	61	80	80
Sr	5	41	36	552	410	501	600	450
Y	70	28	37	25	30	29	40	30
Zr	440	238	409	148	50	234	180	200
Nb	80	42	44	54	30	47	60	60
Ba	680	1100	1460	1300	870	1118	630	2000
Hf								
Ta			4.42	2.57				
Cr	20			22	1300	52	20	44
Co	8			46	76	93	51	82
Ni	2			29	260	69	34	67
Cu	10.0			36.0	130	170	86.0	190
Zn	62.0	131	37	94.0	85.0	140	110	160
Pb	4			1	1	1	4	1
U			1.10	0.67	2.5	2.5	2.5	2.5
Th			7.66	3.31	1	4	4	3
Au	<1	<1	<1	<1	<1	<1	<1	1
Ag				<0.5	<0.5	<0.5	<0.5	<0.5
La			55.9	36.9	12	47	50	53
Ce			125.2	86.2	26	103	89	101
Nd			57.3	44.2				
Sm			10.3	8.7				
Eu			2.4	2.54				
Tb			1.43	1.20				
Dy			7.4	6.1				
Ho			1.69	1.20				
Tm								
Yb			4.8	2.7				
Lu			0.83	0.43				

Table B3.2: Whole rock major (weight %) and trace (ppm) element geochemisty

Formation	Nimish Formation: volcanic rocks (continued)							
Location	Birch L.	Birch L.	Birch L.	Birch L.	Birch L.	Birch L.	Birch L.	Birch L.
Year	1985	1985	1985	1985	1985	1985	1985	1985
Sample	21-3H	21-3J	B2-1	B2-2	B2-3	B2-4A	B2-4B	B2-5
Lithology	PPBS	BSLT	PLBS	BSLT	BSLT	BSLT	AMBS	BSLT
Geochem #	189	190	194	195	196	197	198	199
SiO2	49.1	45.3	44.5	45.6	42.6	47.7	47.9	47.4
Al2O3	20.6	13.8	15.0	15.5	14.2	15.5	12.8	13.5
Fe2O3(t)	9.10	14.7	12.9	12.1	13.9	13.4	12.8	12.1
Fe2O3								
FeO								
MgO	3.10	6.14	7.94	7.07	8.89	4.98	9.91	10.2
CaO	6.94	10.3	9.65	9.67	11.2	5.11	6.03	6.50
Na2O	3.42	2.16	1.89	1.93	1.39	4.13	2.90	2.69
K2O	2.08	0.55	1.11	1.18	0.59	1.99	0.65	0.57
TiO2	2.21	2.00	1.90	1.90	1.82	2.02	0.94	0.91
MnO	0.13	0.22	0.19	0.16	0.20	0.26	0.23	0.22
P2O5	0.36	0.25	0.29	0.28	0.28	0.75	0.23	0.15
LOI	2.85	3.31	3.39	2.93	4.08	2.62	4.93	4.62
Total	100.1	98.8	98.9	98.5	99.3	98.8	99.5	99.1
Rb	80	10	40	25	20	40	10	20
Sr	810	230	420	446	330	300	130	180
Y	30	10	20	23	10	50	20	10
Zr	130	100	150	149	140	150	50	40
Nb	40	40	50	36	50	20	20	10
Ba	990	210	640	577	420	2130	560	310
Hf		3		4				
Ta		2		2				
Cr	26	14	150	150	140	22	720	1200
Co	56	69	68	68	78	74	65	65
Ni	38	63	170	170	180	50	210	240
Cu	99.0	170	91.0	95.0	80.0	21.0	66.0	92.0
Zn	78.0	120	91.0	89.0	110	210	110	100
Pb	1	1	1	1	1	1	1	1
U	2.5	2.5	2.5	2.5	2.5	2.5	2.5	2.5
Th	3	3	3	3.0	3	2	0.5	0.5
Au	<1	<1	<1	<1	<1	<1	<1	2
Ag	<0.5	<0.5	<0.5	<0.5	<0.5	0.5	<0.5	<0.5
La	38	27	34	34	31	49	17	13
Ce	67	52	65	61	58	110	36	25
Nd								
Sm								
Eu								
Tb								
Dy								
Ho								
Tm								
Yb								
Lu								

Table B3.2: Whole rock major (weight %) and trace (ppm) element geochemisty

Formation	Nimish Formation: volcanic rocks (continued)							
Location	Birch L.	Birch L.	DL-AL	DL-AL	DL-AL	DL-AL	DL-AL	DL-AL
Year	1985	1985	1985	1985	1985	1985	1985	1985
Sample	B2-7	B2-8	D1-1A	D1-2	D4-4	23-10	23-13B	23-14A
Lithology	AMIV	BSLT	AMBS	AMBS	IMVC	SIVC	BSLT	RYLT
Geochem #	202	203	1	8	47	89	93	94
SiO2	49.8	52.6						
Al2O3	12.3	13.0						
Fe2O3(t)	10.9	12.0						
Fe2O3								
FeO								
MgO	9.14	5.64						
CaO	8.48	6.86						
Na2O	2.79	2.97						
K2O	0.47	1.85						
TiO2	0.60	1.23						
MnO	0.17	0.19						
P2O5	0.10	0.38						
LOI	4.16	2.16						
Total	99.2	99.1						
Rb	40	50						
Sr	250	400						
Y	5	30						
Zr	10	70						
Nb	30	20						
Ba	280	1150						
Hf								
Ta								
Cr	1500	250	1600	44	6	4	1	1700
Co	65	57	69	76	19	7	7	76
Ni	270	100	530	70	5	4	4	470
Cu	15.0	42.0	210	110	35	8.0	24.0	98.0
Zn	130	130	89	140	120	240.0	170	120
Pb	1	8	1	2	6	10	6	2
U	2.5	2.5	2.5	2.5	2.5	2.5	6	2.5
Th	0.5	1	0.5	3.0	9	16	26	0.5
Au	1	<1	5.0	<1	2	11	<1	12
Ag	<0.5	<0.5	<0.5	<0.5	<0.5	<0.5	<0.5	<0.5
La	8	28						
Ce	20	55						
Nd								
Sm								
Eu								
Tb								
Dy								
Ho								
Tm								
Yb								
Lu								

Table B3.2: Whole rock major (weight %) and trace (ppm) element geochemisty

Formation	Nimish Fm: volcanic rocks			Nimish Formation: intrusive rocks			
Location	DL-AL	DL-AL	DL-AL	DL-AL	DL-AL	DL-AL	DL-AL
Year	1985	1987	1987	1985	1985	1985	1985
Sample	24-1	W6-4	W9-4	D1-3	24-4B	24-14A	25-2
Lithology	BSLT	BSLT	BSLT	DIBS	GBBR	GBBR	GBBR
Geochem #	98	970	1003	9	102	112	116
SiO2				47.20	46.2	51.3	48.0
Al2O3				15.90	9.87	16.7	16.3
Fe2O3(t)				12.80	10.2	10.6	11.8
Fe2O3							
FeO							
MgO				6.86	16.5	2.01	6.12
CaO				7.26	9.32	4.71	8.76
Na2O				2.33	1.11	5.25	2.70
K2O				1.40	0.37	3.83	1.35
TiO2				1.59	0.69	1.65	1.12
MnO				0.20	0.18	0.33	0.20
P2O5				0.28	0.10	0.53	0.25
LOI				2.85	4.54	1.77	2.85
Total				98.80	99.5	99.2	99.6
Rb		78	48	40	8	142	40
Sr		208	323	510	138	262	660
Y		21	30	20	10	112	10
Zr		202	153	80	49	1211	80
Nb		9	35	30	5	316	20
Ba		492	1567	380	492	2079	690
Hf		7	5				
Ta		0.5	0.5				
Cr	200			18	2400	1	58
Co	65			60	64	36	66
Ni	160			73	470	8	84
Cu	67.0			28	86.0	8.0	44.0
Zn	130			150	91	250	97.0
Pb	6			1	6	16	2
U	2.5			2.5	2.5	2.5	2.5
Th	0.5	13.8	3.6		0.5	5	1
Au	3			0.5	2	0.5	1
Ag	<0.5			0.25	0.25	0.25	0.25
La		36	41	22	8	44	26
Ce				46	27	51	48
Nd							
Sm							
Eu							
Tb							
Dy							
Ho							
Tm							
Yb							
Lu							

Table B3.2: Whole rock major (weight %) and trace (ppm) element geochemistry

Formation	Nimish Formation: intrusive rocks (continued)							
Location	DL-AL	DL-AL	DL-AL	DL-AL	DL-AL	DL-AL	DL-AL	DL-AL
Year	1985	1985	1985	1986	1986	1986	1986	1986
Sample	25.5	4-9.	21-1C	W4-4	W4-5	W4-16	W4-11	W6-1
Lithology	GBBR	GBBR	GBBR	GBBR	GBBR	GBBR	GBBR	GBBR
Geochem #	120	162	177	324	325	338	331	348
SiO2	48.1	45.8	40.8	47.63	62.60	46.5	45.8	46.5
Al2O3	15.2	16.4	12.9	14.48	13.49	16.5	16.7	21.5
Fe2O3(t)	10.3	15.7	13.0	12.46	9.36	10.8	10.7	8.76
Fe2O3		3.7		1.73	5.58			
FeO		10.8		9.66	3.41			
MgO	5.66	4.34	4.97	6.55	0.25	7.62	8.58	2.32
CaO	6.66	7.24	9.59	6.25	2.29	9.19	9.23	4.78
Na2O	0.71	4.2	2.19	3.34	4.43	2.42	2.45	3.68
K2O	2.59	0.86	0.69	2.49	5.33	1.91	1.42	3.59
TiO2	1.10	2.62	5.53	3.40	0.62	1.21	1.12	2.09
MnO	0.14	0.20	0.23	0.20	0.24	0.16	0.17	0.19
P2O5	0.24	0.38	0.54	0.26	0.06	0.13	0.12	0.35
LOI	8.70	4.08	8.47	3.40	1.63	3.47	3.62	4.31
Total	99.5	100.6	99.0	99.71	100.09	100.1	100.1	98.4
Rb	83	16	24	43	96	52	33	200
Sr	251	622	304	330	70	438	351	630
Y	15	21	22	18	50	14	8	30
Zr	81	191	242	176	288	65	68	150
Nb	8	54	42	28	51	14	15	50
Ba	496	444	341	887	266	829	302	1630
Hf								
Ta				2.84		1.01		
Cr	170		150	326		230	160	50
Co	61		98			55	55	51
Ni	130		120	86	12	89	130	41
Cu	60.0		110			73.0	58.0	73.0
Zn	110.0		130	114	182	81.0	69.0	63.0
Pb	2		1			1	1	1
U	2.5		2.5	0.4		0.22		
Th	0.5		3	2.3		1.29		
Au	0.5		0.25	0.5		0.5	2	0.5
Ag	<5		<5					
La	19	36	34	25.5		12.6	10	
Ce	44		85	65		31		
Nd				33.9		14.4		
Sm				7.7		3.5		
Eu				2.24		1.03		
Tb				0.94		0.54		
Dy				4.4		3.1		
Ho				0.94		0.60		
Tm				0.25				
Yb				1.65		1.36		
Lu				0.27		0.20		

Table B3.2: Whole rock major (weight %) and trace (ppm) element geochemistry

Formation	Nimish Formation: intrusive rocks (continued)							
Location	DL-AL	DL-AL	DL-AL	DL-AL	DL-AL	DL-AL	DL-AL	DL-AL
Year	1986	1986	1986	1986	1986	1986	1986	1986
Sample	W9-7	W12-6	W12-9	W13-4	W15-2	W19-3A	W19-4	W19-5
Lithology	GBBR	GBBR	GBBR	GBBR	GBBR	GBBR	GBBR	GBBR
Geochem #	380	413	416	421	436	474	476	477
SiO2	49.3	57.8	57.3	43.9	48.5	43.0	48.0	47.3
Al2O3	13.1	15.1	15.1	12.8	15.5	13.9	15.0	15.5
Fe2O3(t)	12.1	9.51	9.27	16.6	12.0	14.9	13.5	12.8
Fe2O3								
FeO								
MgO	5.97	0.98	1.03	6.27	6.88	7.48	5.14	6.68
CaO	6.56	2.46	3.41	7.86	8.10	6.25	8.31	8.37
Na2O	1.91	4.42	4.18	3.11	3.12	2.11	3.15	3.05
K2O	4.56	4.82	5.09	0.46	0.80	1.80	1.51	1.11
TiO2	2.09	1.28	1.29	2.95	1.41	2.51	2.11	1.55
MnO	0.28	0.19	0.19	0.29	0.18	0.45	0.21	0.18
P2O5	0.39	0.41	0.42	0.22	0.16	0.30	0.43	0.26
LOI	2.70	2.08	1.77	3.77	3.00	6.00	2.16	2.77
Total	99.2	99.4	99.4	98.3	99.8	98.9	99.7	99.7
Rb	64	56	120	21	50	54	30	50
Sr	369	150	220	164	450	229	585	570
Y	26	21	40	25	20	24	23	10
Zr	134	471	570	134	60	175	130	80
Nb	15	44	60	31	30	40	17	20
Ba	1420	1700	1880	344	300	1150	888	580
Hf								
Ta	0.89	1.68						
Cr	120	30	30	40	40	40	70	70
Co	52	17	20	73	58	61	59	59
Ni	41	2	6	43	62	49	49	86
Cu	44.0	6.0	9.0	170	39.0	140	38.0	40.0
Zn	90.0	120	160	120	91.0	120	120	110
Pb	1	10	2	1	2	1	8	1
U	0.23	0.50						
Th	1.31	3.86						
Au	1	0.5	0.5	0.5	0.5	1	0.5	2
Ag								
La	26.1	48.7		25		40	29	
Ce	67	110						
Nd	33.4	47.8						
Sm	7.2	8.7						
Eu	1.95	2.15						
Tb	1.03	1.01						
Dy	5.2	5.0						
Ho	1.15	1.12						
Tm								
Yb	2.58	2.92						
Lu	0.39	0.46						

Table B3.2: Whole rock major (weight %) and trace (ppm) element geochemistry

Formation	Nimish Formation: intrusive rocks (continued)							
Location	DL-AL	DL-AL	DL-AL	DL-AL	DL-AL	DL-AL	DL-AL	DL-AL
Year	1986	1986	1986	1986	1986	1986	1986	1986
Sample	W20-5	W21-7	W23-1	W23-2	W23-5A	W30-1	R3-6	R3-12
Lithology	GBBR	GBBR	GBBR	PXNT	GBBR	GBBR	GBBR	GBBR
Geochem #	484	492	498	499	502	504	528	535
SiO2	48.1	43.3	48.2	48.0	48.2	47.7	45.8	42.4
Al2O3	13.9	15.1	14.9	12.4	19.2	15.6	16.1	14.2
Fe2O3(t)	11.3	14.9	12.5	15.4	10.2	12.3	13.7	13.5
Fe2O3								
FeO								
MgO	8.80	4.09	6.19	4.73	2.81	6.69	7.09	8.82
CaO	9.09	8.26	9.34	9.91	7.14	6.47	6.67	9.54
Na2O	2.69	2.83	2.28	2.15	4.04	1.63	2.97	1.97
K2O	1.13	2.69	1.29	1.43	1.87	2.57	1.59	1.24
TiO2	1.31	2.86	1.27	1.95	1.71	1.22	1.85	2.07
MnO	0.20	0.23	0.20	0.28	0.15	0.25	0.21	0.20
P2O5	0.16	0.28	0.27	0.39	0.35	0.26	0.19	0.28
LOI	3.23	3.54	2.70	3.08	2.77	4.23	3.39	3.93
Total	100.1	98.3	99.3	99.9	98.7	99.1	99.7	98.4
Rb	60	90	60	45	60	57	43	50
Sr	390	620	490	517	790	308	516	526
Y	5	21	10	24	10	18	19	24
Zr	70	156	70	108	80	82	139	169
Nb	20	43	20	14	30	9	29	39
Ba	500	839	580	684	930	823	636	899
Hf								
Ta	0.59							
Cr	160	30	90	70	20	100	30	230
Co	48	62	54	57	45	64	63	69
Ni	90	22	76	23	14	97	50	180
Cu	92.0	84.0	52.0	74.0	23.0	68.0	33.0	110
Zn	79.0	130	120	150	88.0	120	94.0	100
Pb	1	1	1	1	1	4	1	1
U	0.15						.	
Th	0.87							
Au	0.5	0.5	1	0.5	1	4	0.5	0.5
Ag								
La	12.3	31		29		21	20	29
Ce	30							
Nd	16.2							
Sm	3.8							
Eu	1.16							
Tb	0.63							
Dy	3.6							
Ho	0.63							
Tm								
Yb	1.51							
Lu	0.26							

Table B3.2: Whole rock major (weight %) and trace (ppm) element geochemistry

Formation	Nimish Formation: intrusive rocks (continued)							
Location	DL-AL	DL-AL	DL-AL	DL-AL	DL-AL	DL-AL	DL-AL	DL-AL
Year	1986	1986	1986	1986	1986	1986	1986	1986
Sample	F2-3	F7-1	F8-3B	F8-4	F8-9	F8-11	B8-4	B8-9
Lithology	DIBS	GBBR	GBBR	GBBR	GBBR	GBBR	GBBR	GBBR
Geochem #	538	555	559	560	565	567	619	624
SiO2	56.5	43.0	39.4	45.1	47.8	47.7	47.2	47.4
Al2O3	13.0	16.3	16.1	18.0	15.5	16.4	15.6	15.5
Fe2O3(t)	9.39	6.63	22.7	13.6	12.2	12.0	13.1	13.5
Fe2O3								
FeO								
MgO	0.66	4.54	5.18	5.02	6.30	6.20	6.55	5.77
CaO	15.4	23.9	3.68	5.83	8.07	8.79	7.79	7.42
Na2O	0.20	0.19	2.32	3.93	3.59	2.99	2.86	2.60
K2O	0.10	0.19	3.30	1.45	0.81	1.40	1.70	2.32
TiO2	1.92	0.66	2.16	2.12	1.58	1.20	1.61	1.73
MnO	0.10	0.12	0.21	0.19	0.19	0.18	0.19	0.20
P2O5	0.62	0.08	0.32	0.31	0.27	0.24	0.24	0.34
LOI	1.85	4.08	4.70	3.47	3.00	2.62	2.62	2.62
Total	99.8	99.7	100.3	99.2	99.5	100.0	99.6	99.6
Rb	20	5	390	60	40	34	60	70
Sr	1240	5	350	680	540	768	460	760
Y	5	5	10	20	5	17	20	20
Zr	220	70	150	160	80	67	90	70
Nb	40	60	40	60	20	8	30	20
Ba	20	180	730	940	560	1220	510	1130
Hf								
Ta						0.50		
Cr	30	130	30	20	70	90	50	50
Co	20	30	66	67	56	56	60	61
Ni	8	60	54	53	83	83	77	51
Cu	5.0	37.0	71.0	89.0	39.0	48.0	39.0	52.0
Zn	19.0	59.0	470	91.0	120	91.0	100	110
Pb	8	1	6	1	10	6	6	1
U						0.18		
Th						0.93		
Au	1	0.5	0.5	1	1	7	1	0.5
Ag								
La						19.4		
Ce						43.1		
Nd						22.6		
Sm						4.4		
Eu						1.44		
Tb						0.64		
Dy						3.5		
Ho						0.83		
Tm								
Yb						2.4		
Lu						0.29		

Table B3.2: Whole rock major (weight %) and trace (ppm) element geochemistry

Formation	Nimish Formation: intrusive rocks (continued)							
Location	DL-AL	DL-AL	DL-AL	DL-AL	DL-AL	DL-AL	DL-AL	DL-AL
Year	1986	1986	1986	1986	1986	1986	1986	1986
Sample	B9-10A	B13-8	B16-5A	B19-1A	B19-1B	B19-5	CHL-1	B20-2
Lithology	PPGB	GBBR	SYNT	GBBR	GBBR	GBBR	GBBR	GBBR
Geochem #	641	681	708	737	738	743	750	753
SiO2	50.0	47.4	71.2	48.6	45.6	49.4	49.5	46.9
Al2O3	15.3	15.7	13.6	13.5	13.8	15.3	14.0	11.9
Fe2O3(t)	12.8	13.5	3.47	17.3	18.5	12.8	12.0	18.2
Fe2O3				3.9	2.9	2.1	2.4	3.2
FeO				12.1	14.0	9.6	8.6	13.5
MgO	2.79	6.41	0.15	2.01	5.42	6.72	8.15	4.59
CaO	5.86	7.85	0.59	7.97	8.38	8.90	7.42	8.45
Na2O	3.61	2.64	6.80	5.23	3.61	2.36	4.64	4.31
K2O	3.08	1.86	2.93	0.70	0.54	1.61	0.36	0.19
TiO2	2.14	1.62	0.45	2.37	2.74	1.22	1.47	3.07
MnO	0.18	0.20	0.03	0.36	0.25	0.21	0.24	0.29
P2O5	0.62	0.31	0.05	0.80	0.37	0.31	0.18	0.42
LOI	2.31	2.85	0.54	3.49	3.98	3.30	4.10	4.21
Total	98.9	100.5	100.2	101.0	101.8	101.2	101.3	101.1
Rb	90	43	60					
Sr	470	479	260					
Y	20	18	80					
Zr	250	91	750					
Nb	40	13	130					
Ba	1090	863	1870	150	400	750	1200	220
Hf								
Ta			7.11					
Cr	30	50	40	19	28	82	290	15
Co	47	61	10	24	50	40	41	52
Ni	14	62	4	11	79	95	120	26
Cu	11.0	44.0	14.0	27	220	38	110.0	69
Zn	130	100	33.0	10	120	86	79	140
Pb	2	1	8	160	8	1	1	3
U			0.71					
Th			18.3					
Au	0.5	0.5	0.5					
Ag								
La		21	130.0	61	26	16	9	23
Ce			278.9					
Nd			104.9					
Sm			18.4					
Eu			1.79					
Tb			2.55					
Dy			13.7					
Ho			3.00					
Tm								
Yb			8.20	5.2	2.4	1.5	1.0	2.3
Lu			1.28					

Table B3.2: Whole rock major (weight %) and trace (ppm) element geochemistry

Formation	Nimish Formation: intrusive rocks (continued)							
Location	DL-AL	DL-AL	DL-AL	DL-AL	DL-AL	DL-AL	DL-AL	DL-AL
Year	1986	1986	1986	1986	1986	1986	1986	1987
Sample	B20-3	B20-4	B20-14	B21-8A	B26-12	B27-7	B27-2D	W10-1
Lithology	GBBR	GBBR	GBBR	GBBR	DIRT	GBBR	GBBR	PXNT
Geochem #	754	755	766	774	795	808	802	1004
SiO2	47.6	44.9	44.8	45.0	46.9	45.8	42.5	49.4
Al2O3	13.5	13.5	13.3	14.3	14.2	15.3	12.8	14.2
Fe2O3(t)	12.9	16.5	17.8	12.3	11.5	10.2	18.0	14.8
Fe2O3	2.2		3.1					4.46
FeO	9.6		13.2					9.3
MgO	6.55	5.44	5.64	8.62	7.16	7.24	5.46	3.39
CaO	11.9	8.67	10.1	5.64	11.9	12.9	9.49	5.65
Na2O	2.94	2.82	3.05	1.47	2.85	1.96	1.96	3.48
K2O	0.89	1.49	1.18	2.37	0.40	1.06	1.82	2.93
TiO2	1.76	2.73	3.23	2.19	1.50	1.24	3.44	2.66
MnO	0.22	0.25	0.28	0.35	0.19	0.16	0.30	0.26
P2O5	0.23	0.29	0.37	0.21	0.15	0.14	0.25	0.64
LOI	3.63	2.77	3.44	7.08	2.31	3.62	2.54	2.39
Total	101.2	99.5	101.9	99.7	99.2	99.8	98.8	99.1
Rb		34		37	13	40	51	52
Sr		290		131	298	410	367	288
Y		26		17	11	10	25	34
Zr		167		123	55	30	143	185
Nb		42		28	13	30	34	28
Ba	930	909	300	956	389	300	1040	1760
Hf								
Ta								2.24
Cr	23	70	24	210	40	360	40	1
Co	39	73	47	60	55	48	82	34
Ni	77	65	78	76	83	89	72	10
Cu	80	160	220	82.0	100	72.0	240	25
Zn	87	130	120	97.0	84.0	74.0	150	170
Pb	5	1	4	1	1	1	1	1
U								0.48
Th								3.17
Au		2		3	0.5	2	1	0.5
Ag								<5
La	15	29	20	21	12		26	43.7
Ce								103
Nd								48.7
Sm								10.1
Eu								3.07
Tb								1.35
Dy								7.1
Ho								1.32
Tm								0.44
Yb	1.4		2.2					3.39
Lu								0.59

Table B3.2: Whole rock major (weight %) and trace (ppm) element geochemistry

Formation	Nimish Formation: intrusive rocks (continued)							
Location	DL-AL	DL-AL	DL-AL	DL-AL	DL-AL	DL-AL	DL-AL	DL-AL
Year	1987	1987	1987	1987	1987	1987	1987	1987
Sample	W10-4	W10-8	W10-14B	W11-3A	W11-6	B5-1A	B7-3A	B9-1
Lithology	ULTR	GBBR	ULTR	PRDT	GBBR	GBBR	GBBR	GBBR
Geochem #	1007	1011	1018	1021	1025	1130	1154	1167
SiO2	40.8	47.4	41.3	44.0	44.2	45.3	46.5	43.1
Al2O3	7.89	13.8	9.07	8.08	7.28	14.2	15.6	13.7
Fe2O3(t)	11.8	15.5	13.6	11.8	11.4	15.5	11.2	13.4
Fe2O3	2.58	4.39	2.38	2.02	2.06			
FeO	8.3	10.0	10.1	8.8	8.4			
MgO	23.1	3.71	20.4	18.7	19.1	4.90	7.04	13.0
CaO	7.37	8.96	6.85	11.4	12.3	10.1	10.6	8.12
Na2O	0.12	3.17	0.14	0.19	0.17	2.87	2.66	1.95
K2O	0.05	1.49	1.82	0.01	0.01	1.05	0.70	0.13
TiO2	0.75	2.87	0.92	0.87	0.80	2.46	1.47	1.38
MnO	0.18	0.28	0.19	0.21	0.18	0.25	0.16	0.20
P2O5	0.10	0.60	0.11	0.08	0.07	0.32	0.14	0.15
LOI	7.31	2.00	5.39	4.54	4.23	2.39	3.23	4.70
Total	99.28	98.89	99.08	99.32	99.26	99.5	100.4	100.0
Rb	15	32	100	9	6	28	22	5
Sr	30	486	19	21	18	407	335	237
Y	9	30	7	7	8	17	22	15
Zr	53	153	46	39	36	161	50	50
Nb	7	26	8	4	3	67	16	21
Ba	16	936	23	30	18	427	260	179
Hf								
Ta	0.45	2.09	0.63	0.37	0.38			
Cr	5000	1	2500	2800	3300	32	280	930
Co	81	42	83	68	71	45	39	78
Ni	1000	9	740	630	650	62	79	380
Cu	79	19.0	60	98.0	100	170	97.0	64.0
Zn	71	170	95	85.0	74.0	150	86.0	110
Pb	1	1	1	1	1	6	1	1
U	0.17	0.45	0.18	0.11	0.15			
Th	0.85	2.8	0.82	0.41	0.45			
Au	0.5	0.5	0.5			0.5	0.5	0.5
Ag	<5	<5	<5			<5	<5	<5
La	9.5	37.4	8.5	5.3	4.8			
Ce	21	88	21	12.4	11.9			
Nd	10.6	43.8	10.9	8.0	7.1			
Sm	2.3	9.2	2.6	2.2	2.0			
Eu	0.72	2.64	0.72	0.73	0.62			
Tb	0.29	1.23	0.39	0.35	0.3			
Dy	1.8	6.3	2.3	2.2	1.8			
Ho	0.35	1.40	0.42	0.47	0.40			
Tm	0.11	0.40	0.14	0.15	0.14			
Yb	0.87	3.02	0.91	1.29	0.91			
Lu	0.14	0.53	0.17	0.17	0.15			

Table B3.2: Whole rock major (weight %) and trace (ppm) element geochemistry

Formation	Nimish Formation: intrusive rocks (continued)							
Location	DL-AL	DL-AL	Marble L.	Marble L.	Birch L.	Birch L.	Birch L.	Birch L.
Year	1985	1985	1985	1985	1985	1985	1985	1985
Sample	23-1	24-11	19-2A	28-11	19-9A	19-9D	19-9E	19-2B
Lithology	DYKE	GBBR	GBBR	GBBR	PXNT	GBBR	GBBR	GBBR
Geochem #	73	109	205	239	217	220	221	206
SiO2			49.8	48.2	40.5	42.0	42.2	50.5
Al2O3			13.7	12.0	6.93	7.92	7.00	14.0
Fe2O3(t)			13.7	10.5	15.4	13.3	14.9	13.1
Fe2O3								
FeO								
MgO			3.71	8.81	19.9	17.4	17.7	2.85
CaO			5.01	13.5	6.95	10.1	8.96	5.54
Na2O			2.96	2.66	0.48	0.44	0.45	3.42
K2O			2.10	0.12	0.26	0.23	0.23	2.99
TiO2			3.06	1.16	2.51	2.58	2.46	2.80
MnO			0.20	0.18	0.22	0.18	0.17	0.30
P2O5			1.34	0.12	0.29	0.33	0.28	1.07
LOI			3.08	2.54	5.08	3.93	4.16	2.16
Total			98.9	99.9	99.0	98.9	98.9	99.0
Rb			36	10	10	30	10	90
Sr			255	190	200	220	200	670
Y			38	10	20	10	20	40
Zr			348	40	150	160	140	370
Nb			55	20	40	40	40	80
Ba			1290	60	220	170	180	1440
Hf								
Ta								
Cr	14	140	280	380	3100	3300	2800	1
Co	10	69	57	57	100	100	110	43
Ni	15	110	120	110	930	880	900	4
Cu	12.0	79.0	26.0	280	110	190	210	0.25
Zn	21.0	150	13.0	89.0	99.0	78.0	81.0	170
Pb	24	2	1	1	1	1	1	8
U	2.5	2.5	2.5	2.5	2.5	2.5	2.5	2.5
Th	7	2	5	1	1	2	1	4
Au	10	0.5	0.5	0.5	0.5	0.5	0.5	0.5
Ag	<5	<5	<5	<5	<5	<5	<5	<5
La			78	13	26	26	23	83
Ce			174	25	59	58	53	165
Nd								
Sm								
Eu								
Tb								
Dy								
Ho								
Tm								
Yb								
Lu								

Table B3.2: Whole rock major (weight %) and trace (ppm) element geochemistry

Formation	Nimish Fm: intrusive rx.		Miscellaneous
Location	Birch L.	Birch L.	DL-AL
Year	1985	1985	1985
Sample	26-1	19-9C	D3-5E
Lithology	PXNT	GBBR	QTVN
Geochem #	222	219	35
SiO2	49.9		
Al2O3	15.4		
Fe2O3(t)	12.2		
Fe2O3			
FeO			
MgO	4.55		
CaO	7.70		
Na2O	2.65		
K2O	3.01		
TiO2	1.72		
MnO	0.18		
P2O5	0.37		
LOI	2.08		
Total	100.0		
Rb	47	12	
Sr	513	196	
Y	24	14	
Zr	150	144	
Nb	14	31	
Ba	1310	159	
Hf			
Ta	1.08		
Cr	12		4
Co	61		1
Ni	42		1
Cu	41.0		5.5
Zn	120		8.5
Pb	2		1
U	0.20		2.5
Th	1.17		0.5
Au	0.5		4
Ag	<5		<5
La	26.9	24	
Ce	66		
Nd	32.4		
Sm	7.0		
Eu	2.06		
Tb	0.93		
Dy	4.5		
Ho	0.99		
Tm			
Yb	2.43		
Lu	0.37		

Appendix C: Electron Microprobe Analyses

C1: Analytical Procedure

The chemical compositions of selected clinopyroxene mineral grains comprising Nimish Formation intrusive rocks were determined on both Material Analysis Company (MAC) and Cameca-CAMEBAX electron microprobes at the Geological Survey of Canada, Ottawa, Ontario. Carbon coated polished thin sections of six ultramafic rocks and four gabbros were prepared and the results of 42 analyses obtained from 21 individual grains are presented in Appendix C2.

The MAC electron microprobe produced quantitative energy dispersive spectrometer (EDS) analyses operating with a 20 kV accelerating voltage and 10 nanoampere sample current. Microprobe calibration standards for this instrument were well characterized silicate and oxide materials in use at the GSC microprobe laboratory. Data reduction was by means of the software program EDDI (Pringle, 1989). In general, the precision and accuracy in the analyses is quoted at ±2% of the concentration for major and significant minor oxides greater than 2%. For those concentrations at or near the detection limit, the precision and accuracy is significantly poorer (G. Pringle, personal communication).

The Cameca-CAMEBAX microprobe is fitted with a wavelength dispersive spectrometer (WDS) and produces quantitative data which is reduced by the PAP correction program of Pouchou and Pichoir (1986). Quoted accuracy and precision in the analyses for this instrument is similar to that of the MAC electron microprobe.

The purpose of this study was to document the chemical compositions of the sole significant surviving primary phase in the altered Nimish assemblages. This was done in order to see whether the information obtained from the clinopyroxene chemistry complements the interpretations reached through whole rock and trace-element studies.

C2: Compilation of Clinopyroxene Microprobe Data

Analytical data are reported in Table C2.1. The analyses of grains from selected ultramafic samples are first presented followed by those analyses from gabbros. They are grouped according to sample, grain identity, and classified as interior or rim relative to grain boundaries. Each analysis includes the concentration of major elements, the structural formulae calculated on the basis of six oxygen, calculated end member compositions (wollastonite, enstatite, and ferrosilite), magnesium number (Mg#), and Q-J components.

Table C2.1: Electron Microprobe Analyses - Clinopyroxene

Formation	Nimish Formation: ultramafic rocks							
Location	DL-AL	DL-AL	DL-AL	DL-AL	DL-AL	DL-AL	DL-AL	DL-AL
Year	1987	1987	1987	1987	1987	1987	1987	1987
Sample	W10-4	W10-4	W10-4	W10-4	W10-14B	W10-14B	W10-14B	W10-14B
Lithology	PRDT	PRDT	PRDT	PRDT	PRDT	PRDT	PRDT	PRDT
Geochem #	1007	1007	1007	1007	1018	1018	1018	1018
Instrument	Cameca	Cameca	Cameca	Cameca	MAC	MAC	MAC	MAC
Grain Ident. #	C1	C1	C4	C4	C1	C1	C2	C2
Position	Interior	Rim	Interior	Rim	Interior	Rim	Interior	Rim
SiO_2	51.07	51.34	52.79	51.75	50.07	49.84	50.21	48.79
Al_2O_3	4.59	4.32	2.70	3.75	3.47	3.58	2.68	3.22
Fe_2O_3	0.30	0.39	0.24	0.51	3.66	3.88	3.41	3.60
TiO_2	0.68	0.62	0.57	0.81	0.78	1.08	0.80	2.13
Cr_2O_3	1.38	1.24	0.55	0.57	1.14	1.04	0.76	0.23
MgO	15.67	15.75	16.71	16.21	16.28	15.75	16.13	15.13
FeO	4.39	3.98	4.68	4.70	1.90	2.70	2.71	3.96
MnO	0.13	0.12	0.17	0.13	0.20	0.05	0.02	0.04
CaO	21.80	22.07	21.64	21.67	22.90	22.94	22.75	22.43
Na_2O	0.26	0.31	0.26	0.24	0.00	0.00	0.00	0.03
K_2O	0.03	0.02	0.02	0.00	0.06	0.09	0.03	0.12
Total	100.30	100.16	100.33	100.34	100.46	100.95	99.50	99.68
Si	1.868	1.878	1.925	1.890	1.837	1.827	1.862	1.820
Al	0.198	0.186	0.116	0.161	0.150	0.155	0.117	0.142
Fe^{+3}	0.008	0.011	0.007	0.014	0.101	0.107	0.095	0.101
Mg	0.855	0.859	0.908	0.883	0.890	0.861	0.892	0.841
Fe^{+2}	0.134	0.122	0.143	0.144	0.058	0.083	0.084	0.124
Ca	0.854	0.865	0.845	0.848	0.900	0.901	0.904	0.896
Na	0.018	0.022	0.018	0.017	0.000	0.000	0.000	0.002
K	0.001	0.001	0.001	0.000	0.003	0.004	0.001	0.006
Ti	0.019	0.017	0.016	0.022	0.022	0.030	0.022	0.060
Mn	0.004	0.004	0.005	0.004	0.006	0.002	0.001	0.001
Cr	0.040	0.036	0.016	0.016	0.033	0.030	0.022	0.007
Total (6 Oxygen)	3.999	4.001	4.000	3.999	4.001	3.999	4.000	4.000
Wo	46.36	46.87	44.58	45.24	48.69	48.85	48.09	48.16
En	46.36	46.54	47.89	47.09	48.16	46.66	47.44	45.20
Fs	7.28	6.59	7.53	7.67	3.15	4.49	4.47	6.64
Total	100.00	100.00	100.00	100.00	100.00	100.00	100.00	100.00
Mg#	86.43	87.60	86.41	86.00	93.86	91.23	91.39	87.20
J	0.036	0.044	0.036	0.034	0.000	0.000	0.000	0.004
Q	1.843	1.846	1.896	1.875	1.848	1.845	1.880	1.861
Q+J	1.879	1.890	1.932	1.909	1.848	1.845	1.880	1.865
J/(Q+J)	0.019	0.023	0.019	0.018	0.000	0.000	0.000	0.002

Table C2.1: Electron Microprobe Analyses - Clinopyroxene

Formation	Nimish Formation: ultramafic rocks							
Location	DL-AL	DL-AL	DL-AL	DL-AL	DL-AL	DL-AL	DL-AL	DL-AL
Year	1987	1987	1987	1987	1987	1987	1987	1987
Sample	W11-6	W11-6	W11-6	W11-6	W11-3A	W11-3A	W11-3A	W11-3A
Lithology	PXNT	PXNT	PXNT	PXNT	PXNT	PXNT	PXNT	PXNT
Geochem #	1025	1025	1025	1025	1021	1021	1021	1021
Instrument	MAC	MAC	MAC	MAC	MAC	MAC	MAC	MAC
Grain Ident. #	C1	C1	C2	C2	C1	C1	C2	C2
Position	Interior	Rim	Interior	Rim	Interior	Rim	Interior	Rim
SiO_2	50.15	50.08	50.42	49.58	50.17	51.08	51.74	50.08
Al_2O_3	2.89	2.54	2.91	3.66	3.26	2.28	2.70	3.37
Fe_2O_3	4.06	3.19	3.99	3.63	3.32	2.57	2.83	3.75
TiO_2	0.45	1.25	0.55	0.70	0.45	0.70	0.20	0.75
Cr_2O_3	1.29	0.24	1.36	1.12	1.37	0.44	1.19	0.59
MgO	16.78	15.60	16.69	15.85	16.48	16.43	19.12	15.91
FeO	1.20	4.80	1.56	2.52	1.95	3.95	1.98	3.17
MnO	0.09	0.12	0.13	0.29	0.18	0.14	0.18	0.22
CaO	22.53	21.91	22.69	22.24	22.33	21.97	20.02	22.39
Na_2O	0.00	0.00	0.00	0.00	0.00	0.00	0.00	0.00
K_2O	0.08	0.07	0.11	0.10	0.06	0.07	0.05	0.07
Total	99.52	99.80	100.41	99.69	99.57	99.63	100.01	100.30
Si	1.852	1.863	1.849	1.836	1.853	1.890	1.882	1.846
Al	0.126	0.111	0.126	0.160	0.142	0.099	0.116	0.146
Fe^{+3}	0.113	0.089	0.110	0.101	0.092	0.072	0.077	0.104
Mg	0.924	0.865	0.912	0.875	0.907	0.906	1.037	0.874
Fe^{+2}	0.037	0.149	0.048	0.078	0.060	0.122	0.060	0.098
Ca	0.891	0.873	0.892	0.883	0.884	0.871	0.780	0.884
Na	0.000	0.000	0.000	0.000	0.000	0.000	0.000	0.000
K	0.004	0.003	0.005	0.005	0.003	0.003	0.002	0.003
Ti	0.012	0.035	0.015	0.019	0.012	0.019	0.005	0.021
Mn	0.003	0.004	0.004	0.009	0.006	0.004	0.006	0.007
Cr	0.038	0.007	0.039	0.033	0.040	0.013	0.034	0.017
Total (6 Oxygen)	4.000	3.999	4.000	3.999	3.999	3.999	3.999	4.000
Wo	48.13	46.26	48.14	48.08	47.73	45.85	41.56	47.64
En	49.87	45.83	49.27	47.67	49.02	47.71	55.23	47.10
Fs	2.00	7.91	2.59	4.25	3.25	6.44	3.21	5.26
Total	100.00	100.00	100.00	100.00	100.00	100.00	100.00	100.00
Mg#	96.14	85.28	95.02	91.81	93.78	88.12	94.51	89.95
J	.0.000	0.000	0.000	0.000	0.000	0.000	0.000	0.000
Q	1.852	1.887	1.852	1.836	1.851	1.899	1.877	1.856
Q+J	1.852	1.887	1.852	1.836	1.851	1.899	1.877	1.856
J/(Q+J)	0.000	0.000	0.000	0.000	0.000	0.000	0.000	0.000

Table C2.1: Electron Microprobe Analyses - Clinopyroxene

Formation	Nimish Formation: ultramafic rocks							
Location	DL-AL	DL-AL	DL-AL	DL-AL	DL-AL	DL-AL	DL-AL	DL-AL
Year	1987	1987	1987	1987	1987	1987	1987	1987
Sample	W14-5	W14-5	W14-5	W14-5	W10-11	W10-11	W10-11	W10-11
Lithology	ULTR	ULTR	ULTR	ULTR	ULTR	ULTR	ULTR	ULTR
Geochem #	1064	1064	1064	1064	1014	1014	1014	1014
Instrument	MAC	MAC	MAC	MAC	MAC	MAC	MAC	MAC
Grain Ident. #	C1	C1	C2	C2	C1	C1	C2	C2
Position	Interior	Rim	Interior	Rim	Interior	Rim	Interior	Rim
SiO_2	52.25	51.44	48.86	51.75	51.37	51.80	52.24	49.80
Al_2O_3	2.39	2.72	4.52	2.96	2.61	2.16	2.52	3.20
Fe_2O_3	0.76	2.27	2.65	1.20	2.81	2.49	3.29	2.87
TiO_2	0.27	0.58	0.94	0.46	0.17	0.19	0.22	0.91
Cr_2O_3	1.47	0.44	0.82	0.88	1.34	1.37	1.03	0.87
MgO	19.32	16.04	14.53	16.37	19.33	19.64	19.56	15.73
FeO	3.46	4.38	5.66	3.89	1.72	1.88	1.53	3.52
MnO	0.15	0.00	0.17	0.07	0.17	0.21	0.14	0.13
CaO	19.22	22.54	21.50	22.79	19.56	19.37	20.01	22.30
Na_2O	0.00	0.00	0.00	0.00	0.00	0.00	0.00	0.00
K_2O	0.05	0.08	0.01	0.00	0.05	0.07	0.12	0.02
Total	99.34	100.49	99.66	100.37	99.13	99.18	100.66	99.35
Si	1.909	1.889	1.825	1.894	1.882	1.895	1.885	1.852
Al	0.103	0.118	0.199	0.128	0.113	0.093	0.107	0.140
Fe^{+3}	0.021	0.063	0.074	0.033	0.077	0.069	0.089	0.080
Mg	1.053	0.878	0.809	0.893	1.056	1.071	1.052	0.872
Fe^{+2}	0.106	0.134	0.177	0.119	0.053	0.058	0.046	0.109
Ca	0.753	0.887	0.860	0.894	0.768	0.759	0.774	0.889
Na	0.000	0.000	0.000	0.000	0.000	0.000	0.000	0.000
K	0.002	0.004	0.000	0.000	0.002	0.003	0.006	0.001
Ti	0.007	0.016	0.026	0.013	0.005	0.005	0.006	0.025
Mn	0.005	0.000	0.005	0.002	0.005	0.007	0.004	0.004
Cr	0.042	0.013	0.024	0.025	0.039	0.040	0.029	0.026
Total (6 Oxygen)	4.001	4.002	3.999	4.001	4.000	4.000	3.998	3.998
Wo	39.38	46.69	46.60	46.89	40.92	40.21	41.33	47.51
En	55.08	46.23	43.82	46.86	56.27	56.74	56.21	46.63
Fs	5.54	7.08	9.58	6.25	2.81	3.05	2.46	5.86
Total	100.00	100.00	100.00	100.00	100.00	100.00	100.00	100.00
Mg#	90.87	86.72	82.07	88.24	95.25	94.90	95.80	88.85
J	0.000	0.000	0.000	0.000	0.000	0.000	0.000	0.000
Q	1.912	1.899	1.846	1.906	1.877	1.888	1.872	1.870
Q+J	1.912	1.899	1.846	1.906	1.877	1.888	1.872	1.870
J/(Q+J)	0.000	0.000	0.000	0.000	0.000	0.000	0.000	0.000

Table C2.1: Electron Microprobe Analyses - Clinopyroxene

Formation	Nimish Formation: gabbro							
Location	DL-AL	DL-AL	DL-AL	DL-AL	DL-AL	DL-AL	DL-AL	DL-AL
Year	1986	1986	1986	1986	1986	1986	1987	1987
Sample	B19-3A	B19-3A	B19-3A	B19-3A	B19-3A	B19-3A	W10-6	W10-6
Lithology	GBBR	GBBR	GBBR	GBBR	GBBR	GBBR	GBBR	GBBR
Geochem #	740	740	740	740	740	740	1009	1009
Instrument	MAC	MAC	MAC	MAC	MAC	MAC	MAC	MAC
Grain Ident. #	C1	C1	C2	C2	C3	C3	C2	C2
Position	Interior	Rim	Interior	Rim	Interior	Rim	Interior	Rim
SiO_2	49.48	49.52	49.13	48.95	49.27	49.93	49.90	49.52
Al_2O_3	3.38	3.04	2.86	2.80	3.17	2.52	5.22	4.51
Fe_2O_3	4.26	4.25	5.69	4.51	4.12	2.00	3.60	4.19
TiO_2	1.13	1.28	1.01	1.22	1.04	1.32	1.04	0.83
Cr_2O_3	0.14	0.05	0.12	0.09	0.18	0.06	0.29	0.24
MgO	14.57	13.93	15.67	13.83	16.21	13.25	16.61	16.38
FeO	5.21	6.00	3.50	6.29	3.88	9.15	3.15	2.24
MnO	0.07	0.25	0.14	0.10	0.17	0.15	0.08	0.09
CaO	22.45	22.62	21.33	22.11	20.86	21.84	21.60	21.91
Na_2O	0.00	0.00	0.09	0.00	0.00	0.00	0.00	0.00
K_2O	0.11	0.15	0.10	0.10	0.10	0.02	0.01	0.09
Total	100.80	101.09	99.64	100.00	99.00	100.24	101.50	100.00
Si	1.834	1.839	1.833	1.840	1.841	1.877	1.808	1.821
Al	0.148	0.133	0.126	0.124	0.14	0.112	0.223	0.195
Fe^{+3}	0.119	0.119	0.160	0.128	0.116	0.057	0.098	0.116
Mg	0.805	0.771	0.872	0.775	0.903	0.743	0.897	0.898
Fe^{+2}	0.162	0.186	0.109	0.198	0.121	0.288	0.095	0.069
Ca	0.892	0.900	0.853	0.891	0.835	0.880	0.838	0.863
Na	0.000	0.000	0.007	0.000	0.000	0.000	0.000	0.000
K	0.005	0.007	0.005	0.005	0.005	0.001	0.000	0.004
Ti	0.031	0.036	0.028	0.034	0.029	0.037	0.028	0.023
Mn	0.002	0.008	0.004	0.003	0.005	0.005	0.002	0.003
Cr	0.004	0.001	0.004	0.003	0.005	0.002	0.008	0.007
Total (6 Oxygen)	4.002	4.000	4.001	4.001	4.000	4.002	3.997	3.999
Wo	47.98	48.45	46.50	47.79	44.92	46.06	45.79	47.17
En	43.33	41.52	47.54	41.60	48.56	38.88	49.00	49.07
Fs	8.69	10.03	5.96	10.61	6.52	15.06	5.21	3.76
Total	100.00	100.00	100.00	100.00	100.00	100.00	100.00	100.00
Mg#	83.29	80.54	88.86	79.67	88.16	72.08	90.38	92.88
J	0.000	0.000	0.014	0.000	0.000	0.000	0.000	0.000
Q	1.859	1.857	1.834	1.864	1.859	1.911	1.830	1.830
Q+J	1.859	1.857	1.848	1.864	1.859	1.911	1.830	1.830
J/(Q+J)	0.000	0.000	0.008	0.000	0.000	0.000	0.000	0.000

Table C2.1: Electron Microprobe Analyses - Clinopyroxene

Formation	**Nimish Formation: gabbro**							
Location	DL-AL	DL-AL	DL-AL	DL-AL	DL-AL	DL-AL	DL-AL	DL-AL
Year	1987	1987	1987	1987	1987	1987	1987	1987
Sample	W10-8	W10-8	W10-8	W10-8	W10-8	W10-8	W10-13A	W10-13A
Lithology	GBBR	GBBR	GBBR	GBBR	GBBR	GBBR	GBBR	GBBR
Geochem #	1011	1011	1011	1011	1011	1011	1016	1016
Instrument	MAC	MAC	MAC	MAC	MAC	MAC	MAC	MAC
Grain Ident. #	C1	C1	C2	C2	C4	C4	C1	C1
Position	Interior	Rim	Interior	Rim	Interior	Rim	Interior	Rim
SiO_2	50.38	50.53	50.50	50.38	50.99	50.44	49.52	49.08
Al_2O_3	1.85	1.28	2.44	2.37	1.64	3.25	2.92	2.85
Fe_2O_3	1.68	1.56	2.02	1.59	0.63	1.05	2.86	3.58
TiO_2	1.17	0.79	1.35	1.42	1.09	1.70	1.61	1.56
Cr_2O_3	0.07	0.02	0.14	0.14	0.12	0.05	0.12	0.05
MgO	13.73	11.35	13.69	13.73	13.83	13.19	14.24	14.30
FeO	9.39	12.65	8.82	9.41	10.05	10.26	6.34	5.84
MnO	0.24	0.42	0.27	0.17	0.20	0.15	0.23	0.21
CaO	21.14	21.34	21.63	21.28	21.03	20.79	22.33	22.14
Na_2O	0.00	0.00	0.00	0.00	0.00	0.00	0.00	0.00
K_2O	0.06	0.12	0.13	0.06	0.06	0.04	0.08	0.00
Total	99.71	100.06	100.99	100.55	99.64	99.93	100.25	99.61
Si	1.901	1.930	1.881	1.885	1.923	1.865	1.849	1.843
Al	0.082	0.058	0.107	0.105	0.073	0.144	0.128	0.126
Fe^{+3}	0.048	0.045	0.057	0.045	0.018	0.030	0.080	0.101
Mg	0.772	0.646	0.760	0.766	0.777	0.741	0.793	0.801
Fe^{+2}	0.296	0.404	0.275	0.294	0.317	0.324	0.198	0.183
Ca	0.855	0.873	0.863	0.853	0.850	0.840	0.893	0.891
Na	0.000	0.000	0.000	0.000	0.000	0.000	0.000	0.000
K	0.003	0.006	0.006	0.003	0.003	0.002	0.004	0.000
Ti	0.033	0.023	0.038	0.040	0.031	0.048	0.045	0.044
Mn	0.008	0.014	0.009	0.005	0.006	0.005	0.007	0.007
Cr	0.002	0.001	0.004	0.004	0.004	0.001	0.004	0.001
Total (6 Oxygen)	4.000	4.000	4.000	4.000	4.002	4.000	4.001	3.997
Wo	44.44	45.40	45.48	44.58	43.71	44.09	47.42	47.52
En	40.16	33.60	40.05	40.03	39.99	38.92	42.07	42.70
Fs	15.40	21.00	14.47	15.39	16.30	16.99	10.51	9.78
Total	100.00	100.00	100.00	100.00	100.00	100.00	100.00	100.00
Mg#	72.27	61.53	73.45	72.223	72.82	71.04	80.02	81.36
J	0.000	0.000	0.000	0.000	0.000	0.000	0.000	0.000
Q	1.923	1.923	1.898	1.913	1.944	1.905	1.884	1.875
Q+J	1.923	1.923	1.898	1.913	1.944	1.905	1.884	1.875
J/(Q+J)	0.000	0.000	0.000	0.000	0.000	0.000	0.000	0.000

Table C2.1: Electron Microprobe Analyses - Clinopyroxene

Formation	**Nimish Formation: gabbro**	
Location	DL-AL	DL-AL
Year	1987	1987
Sample	W10-13A	W10-13A
Lithology	GBBR	GBBR
Geochem #	1016	1016
Instrument	MAC	MAC
Grain Ident. #	C2	C2
Position	Interior	Rim
SiO_2	50.97	51.14
Al_2O_3	2.50	2.45
Fe_2O_3	3.88	3.34
TiO_2	0.95	0.76
Cr_2O_3	0.10	0.20
MgO	16.09	16.21
FeO	3.91	3.21
MnO	0.20	0.15
CaO	22.43	22.80
Na_2O	0.00	0.00
K_2O	0.08	0.10
Total	101.11	100.36
Si	1.867	1.880
Al	0.108	0.106
Fe^{+3}	0.107	10.092
Mg	0.879	0.888
Fe^{+2}	0.120	0.099
Ca	0.880	0.898
Na	0.000	0.000
K	0.004	0.005
Ti	0.026	0.021
Mn	0.006	0.005
Cr	0.003	0.006
Total (6 Oxygen)	4.000	4.000
Wo	46.85	47.64
En	46.77	47.13
Fs	6.38	5.23
Total	100.00	100.00
Mg#	88.00	90.00
J	0.000	0.000
Q	1.879	1.885
Q+J	1.879	1.885
J/(Q+J)	0.000	0.000

Appendix D: Normal-type Mid-Ocean Ridge Basalt (N-MORB) normalizing values used in extended trace element diagrams

D1: N-MORB Values

Normalizing values to Normal-type Mid-Ocean Ridge Basalt (N-MORB) were obtained from two sources and are listed as follows:

Element	N-MORB value	Source
Th	0.2 ppm	Pearce (1982)
Ta	0.18 ppm	Pearce (1982)
Nb	3.5 ppm	Pearce (1982)
La	2.50 ppm	Sun and McDonough (1989)
Ce	10.0 ppm	Pearce (1982)
Nd	7.30 ppm	Sun and McDonough (1989)
Zr	74 ppm	Sun and McDonough (1989)
Sm	2.63 ppm	Sun and McDonough (1989)
Ti	7600 ppm	Sun and McDonough (1989)
Y	30 ppm	Pearce (1982)
Yb	3.4 ppm	Pearce (1982)
Lu	0.455 ppm	Sun and McDonough (1989)

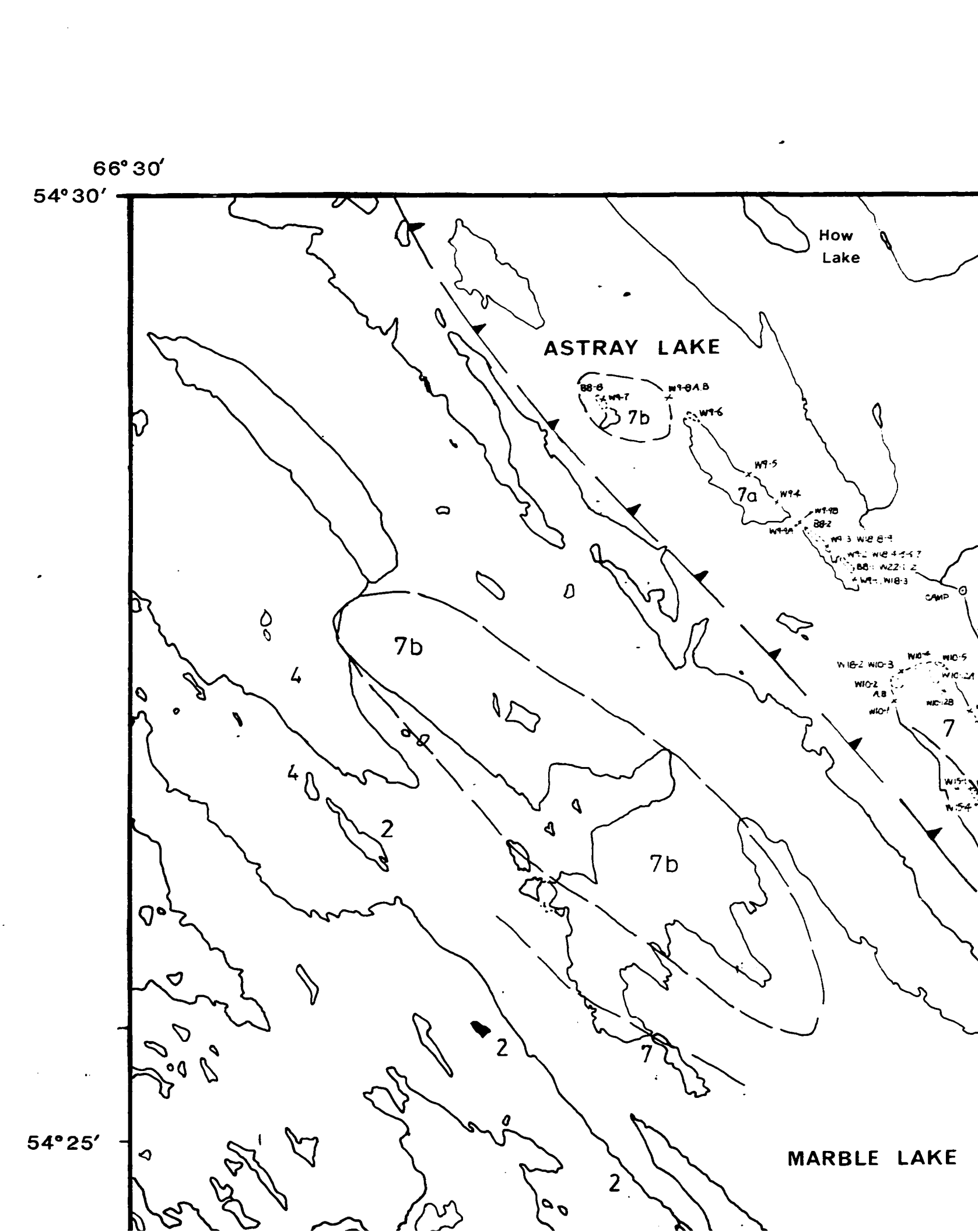
66° 30′
54° 30′
How Lake
ASTRAY LAKE
7b
7a
CAMP
7
4
2
1
54° 25′
MARBLE LAKE

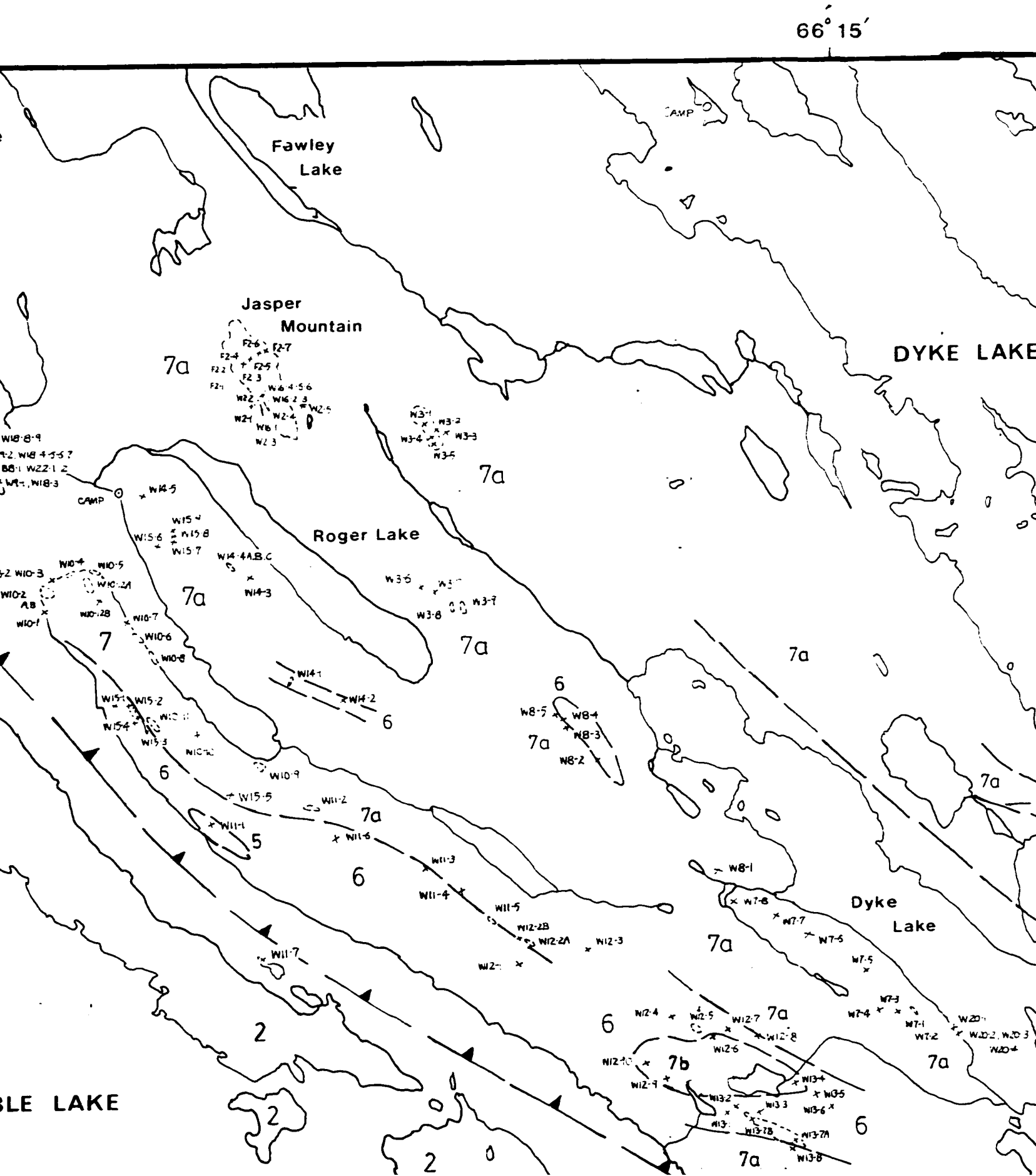
66° 15′
CAMP
Fawley
Lake
Jasper
Mountain
DYKE LAKE
Roger Lake
Dyke
Lake
7a
7b
7
6
5
2
F2-6
F2-7
F2-4
F2-5
F2-2
F2-3
F2-1
W6-4-5-6
W2-2
W6-2-3
W2-5
W2-1
W2-4
W6-1
W2-3
W3-1
W3-2
W3-4
W3-3
W3-5
W18-8-9
W18-4-5-6-7
W22-1-2
W18-3
W14-5
W15-4
W15-6
W15-8
W15-7
W14-4A,B,C
W14-3
W10-4
W10-5
W10-3
W10-2A
W10-2
A,B
W10-2B
W10-1
W10-7
W10-6
W10-8
W14-1
W14-2
W15-1
W15-2
W15-4
W10-11
W15-3
W10-10
W10-9
W15-5
W11-2
W11-1
W11-6
W11-3
W11-4
W11-5
W11-7
W12-2B
W12-2A
W12-3
W12-1
W3-6
W3-8
W3-7
W8-5
W8-4
W8-3
W8-2
W8-1
W7-6
W7-7
W7-5
W7-3
W7-4
W7-1
W7-2
W20-1
W20-2, W20-3
W20-4
W12-4
W12-5
W12-7
W12-8
W12-6
W12-10
W12-9
W13-4
W13-5
W13-2
W13-3
W13-6
W13-1
W13-7B
W13-7A
W13-8
BLE LAKE

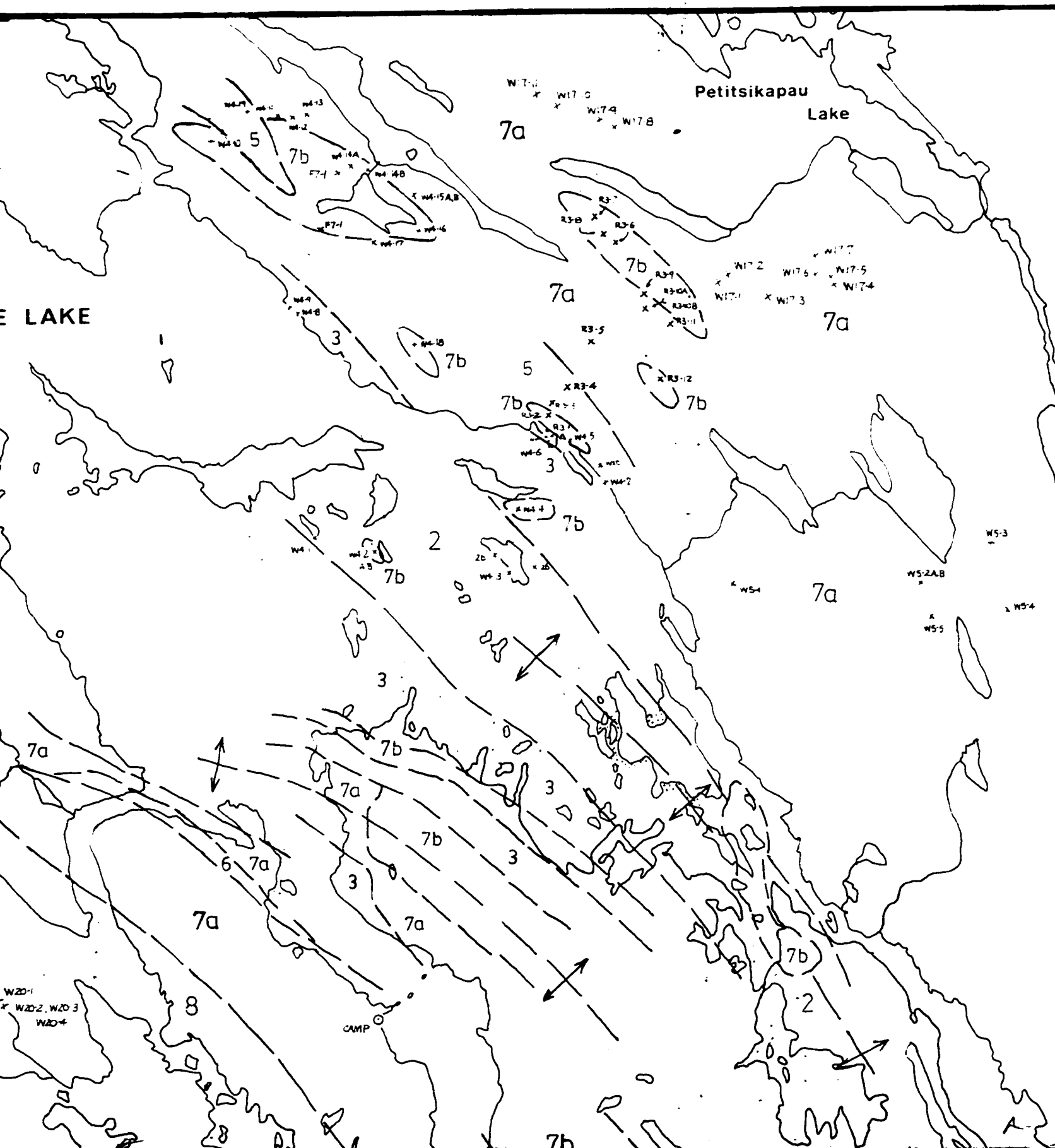
Petitsikapau
Lake
E LAKE
7a
7b
5
3
2
6
8
CAMP

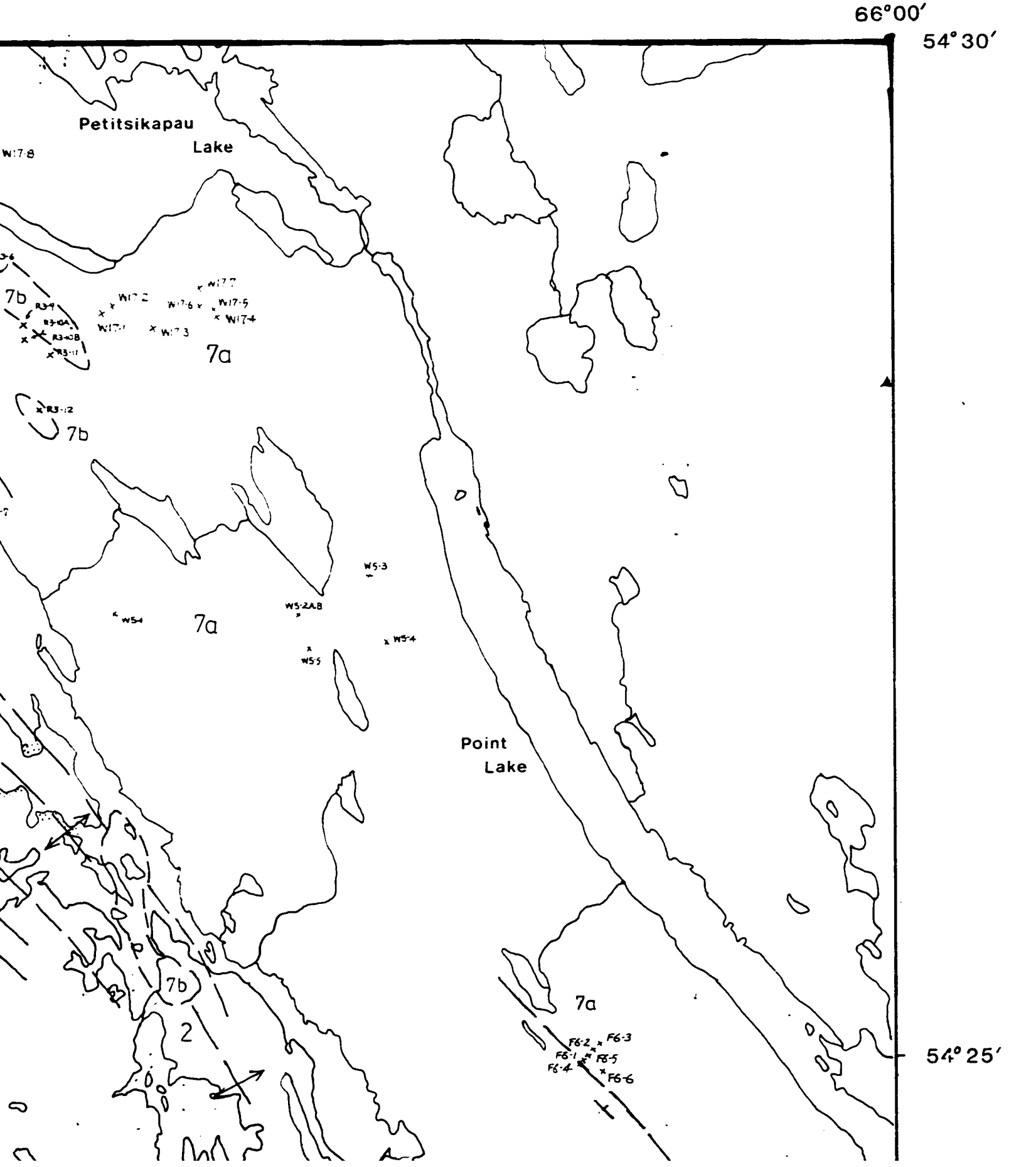
66°00′
54°30′
Petitsikapau
Lake
W17-8
7b
R3-9
R3-10A
R3-10B
R3-11
W17-2
W17-1
W17-6
W17-7
W17-5
W17-4
W17-3
7a
R3-12
7b
W5-3
W5-2A,B
W5-4
W5-5
W5-1
7a
Point
Lake
7b
2
7a
F6-2
F6-3
F6-1
F6-5
F6-4
F6-6
54°25′

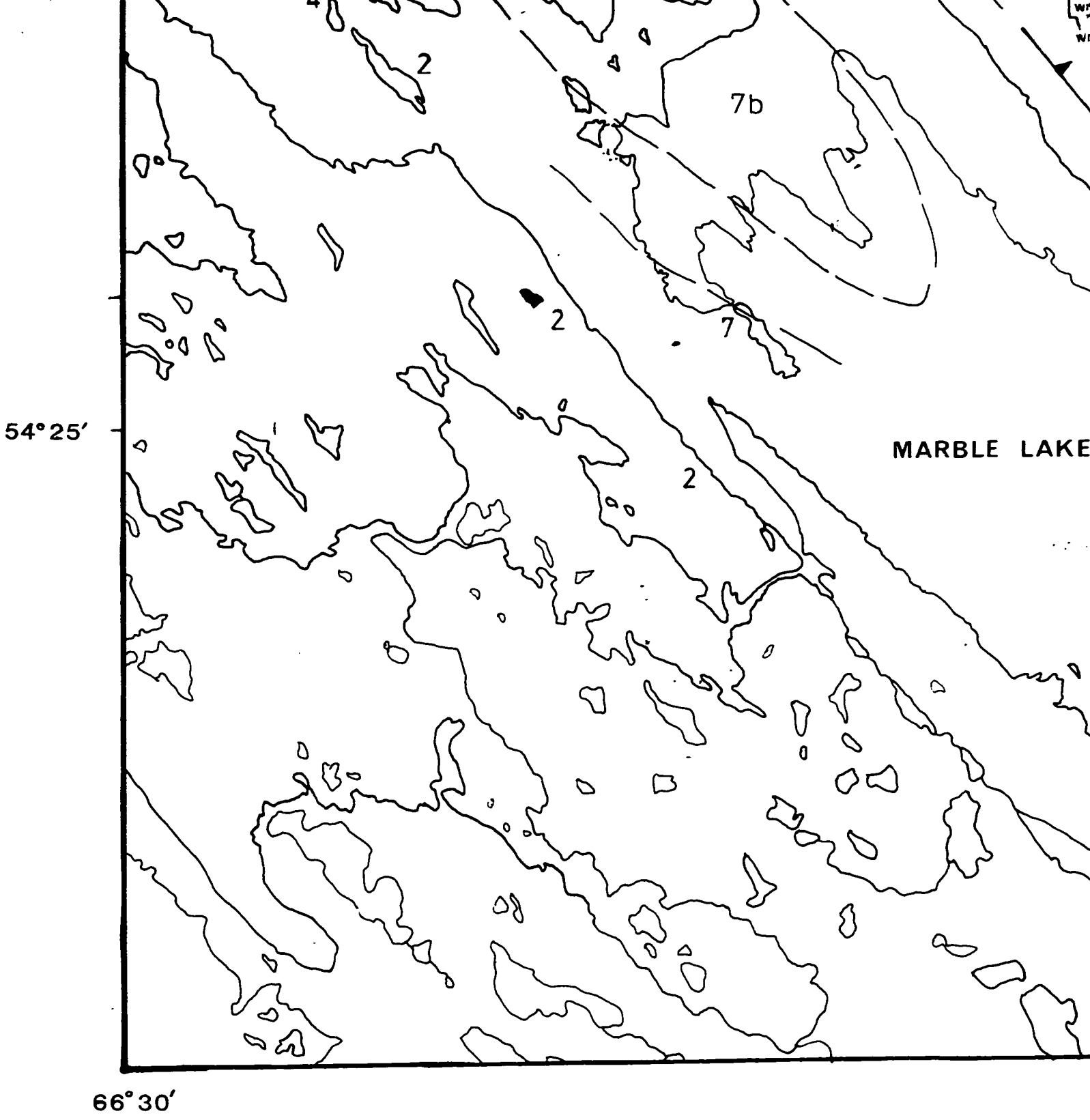

Map A

(to accompany Watanabe, 1996)

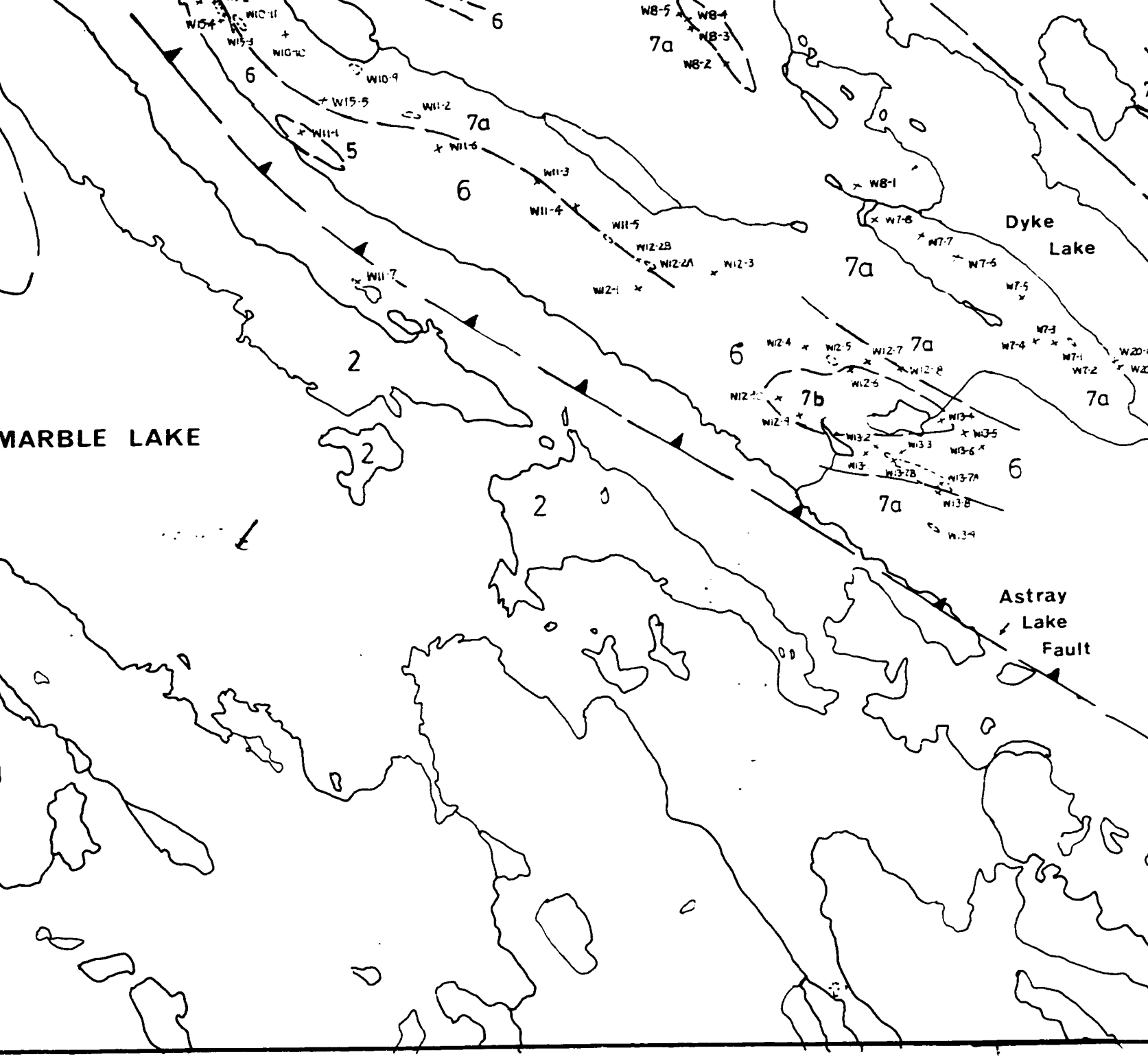

Geology of the Dyke Lake – Astra

SCALE 1:50,000

1 0 1

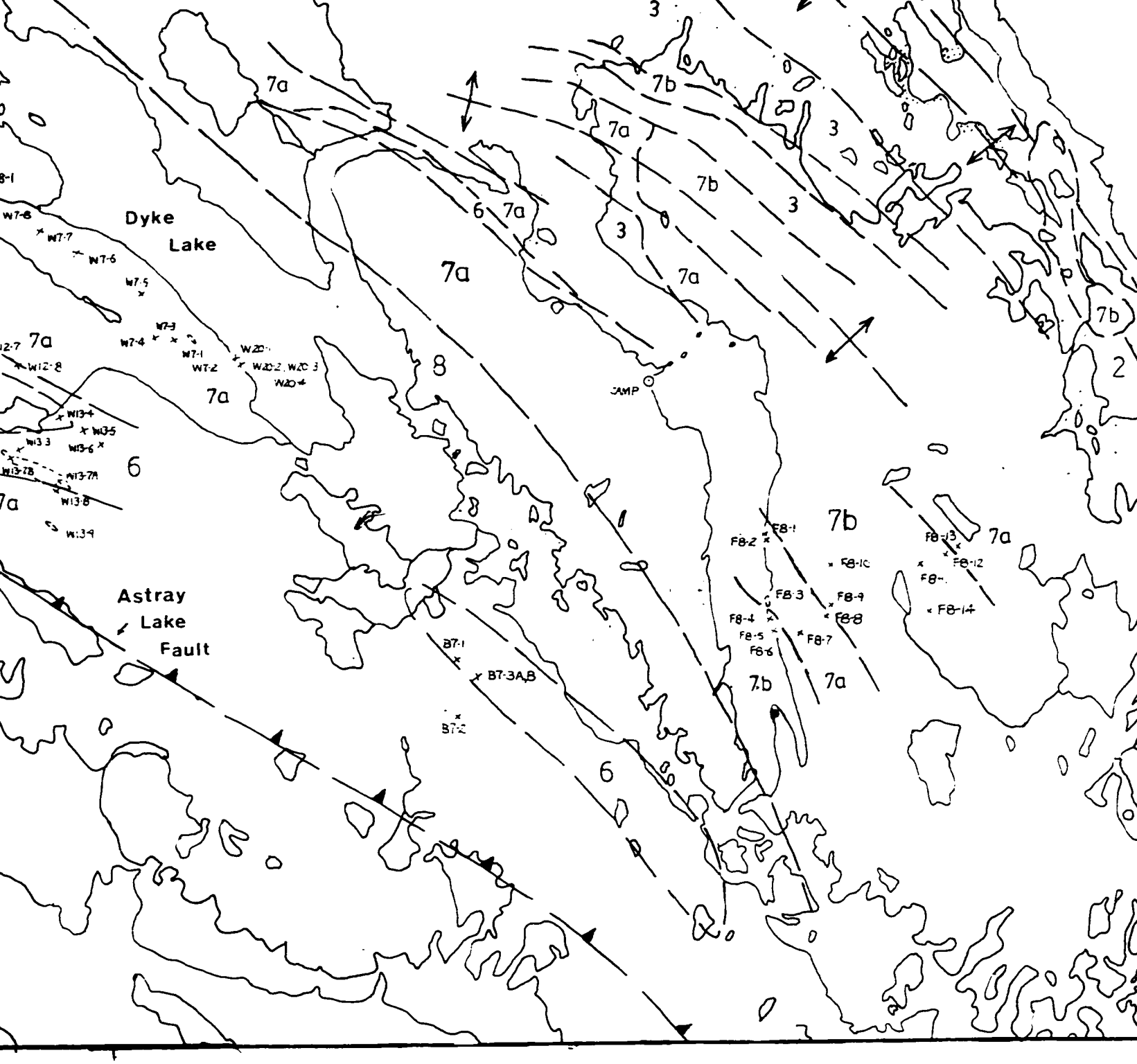

66° 15′

Dyke Lake – Astray Lake region.

SCALE 1:50,000

1 2 3 Miles

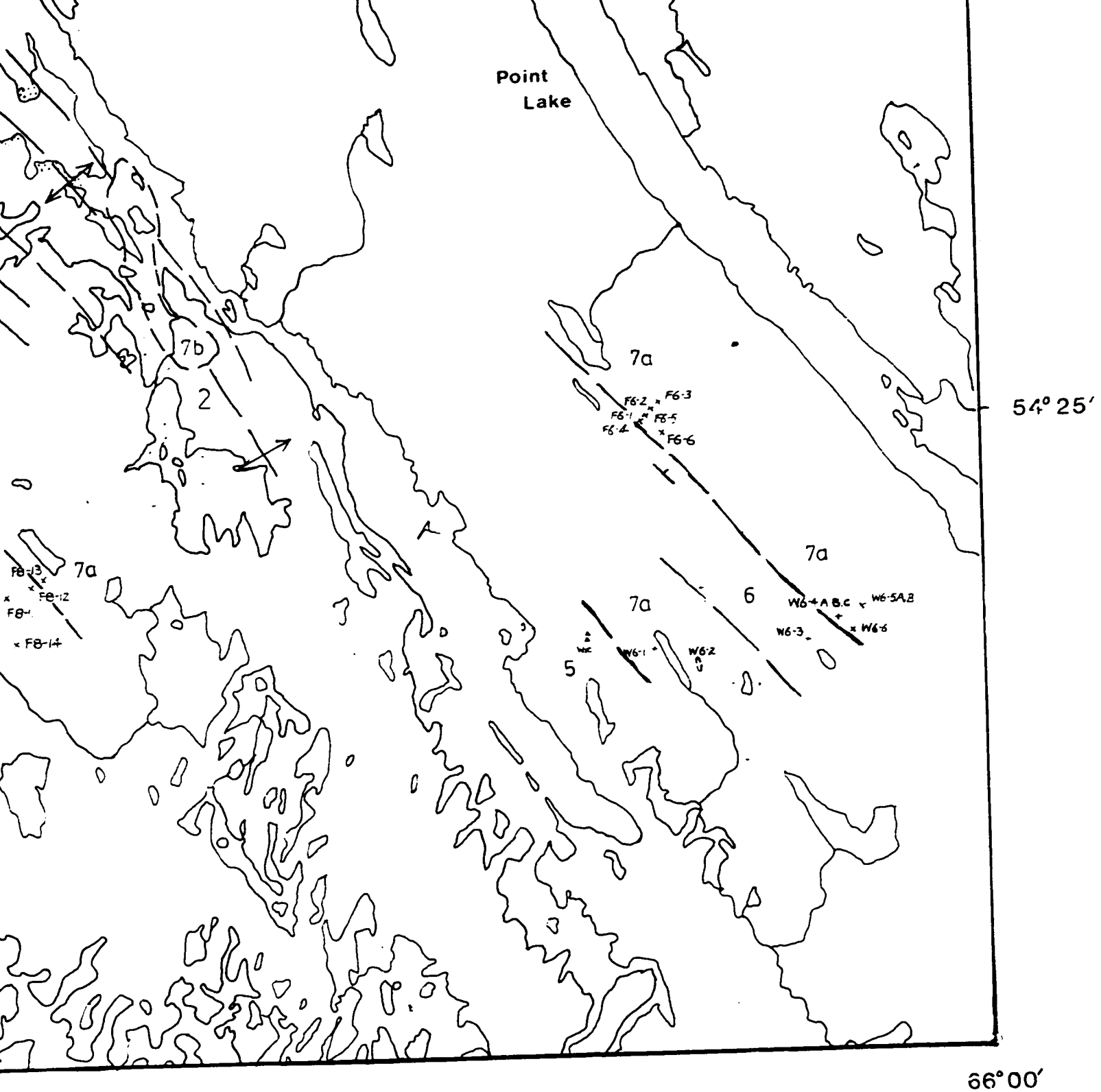
Point
Lake
7b
2
7a
F6-2
F6-3
F6-1
F6-5
F6-4
F6-6
54° 25′
7a
F8-13
F8-12
F8-14
7a
7a
6
W6-4 A B.C
W6-5A.B
W6-3
W6-6
5
W6-1
W6-2
66° 00′


TN
33°38′W

MAP B (2)

N

33°38'W

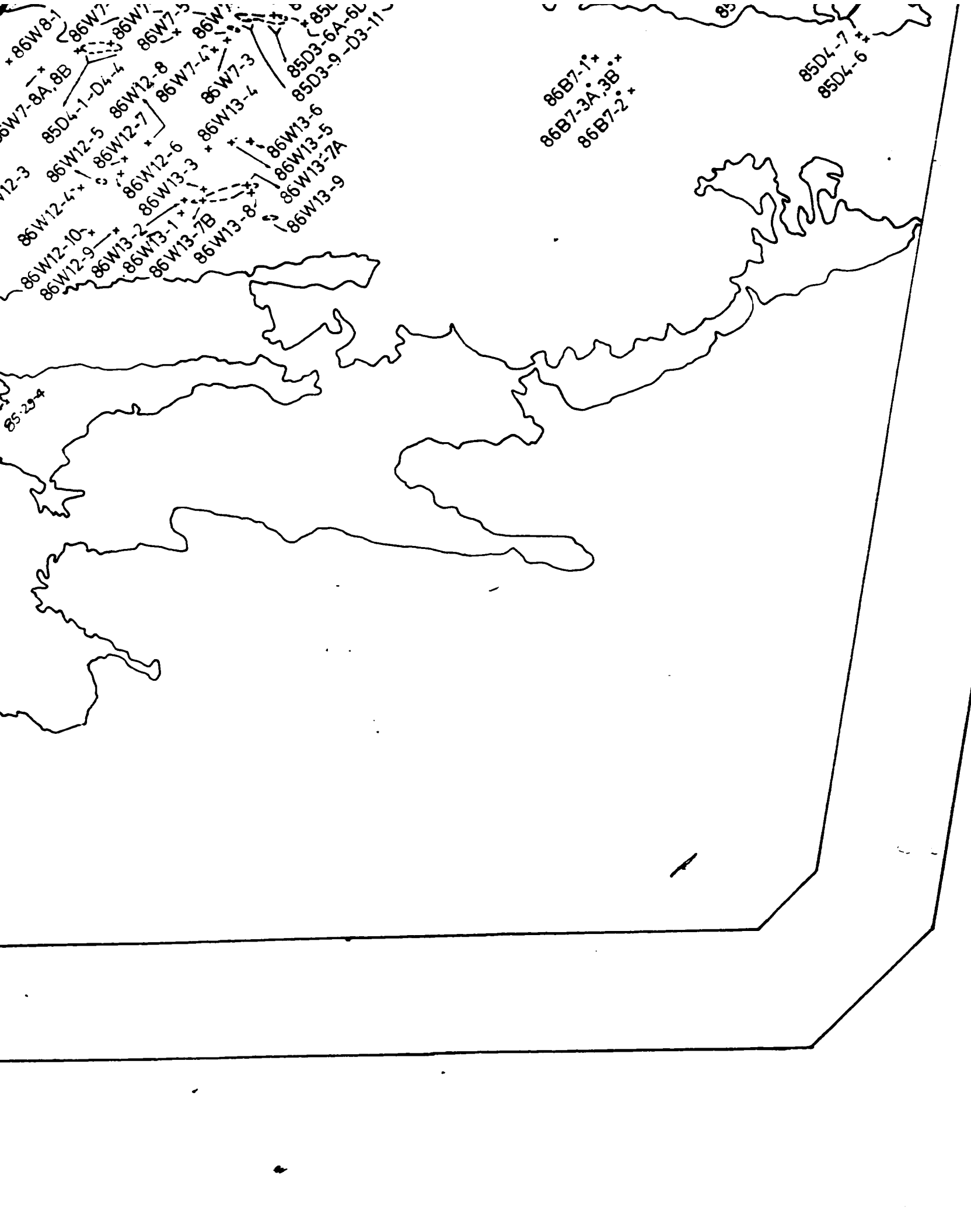
86W8-1
86W7-8A,8B
85D4-1-D4-4
86W12-8
86W12-5
86W12-7
86W12-4
86W12-6
86W12-10
86W12-9
86W13-2
86W13-1
86W13-7B
86W13-8
86W13-3
86W7-4
86W7-3
86W13-4
85D3-6A-6
85D3-9-D3-11
86W13-6
86W13-5
86W13-7A
86W13-9
86B7-1
86B7-3A,3B
86B7-2
85D4-7
85D4-6
85294

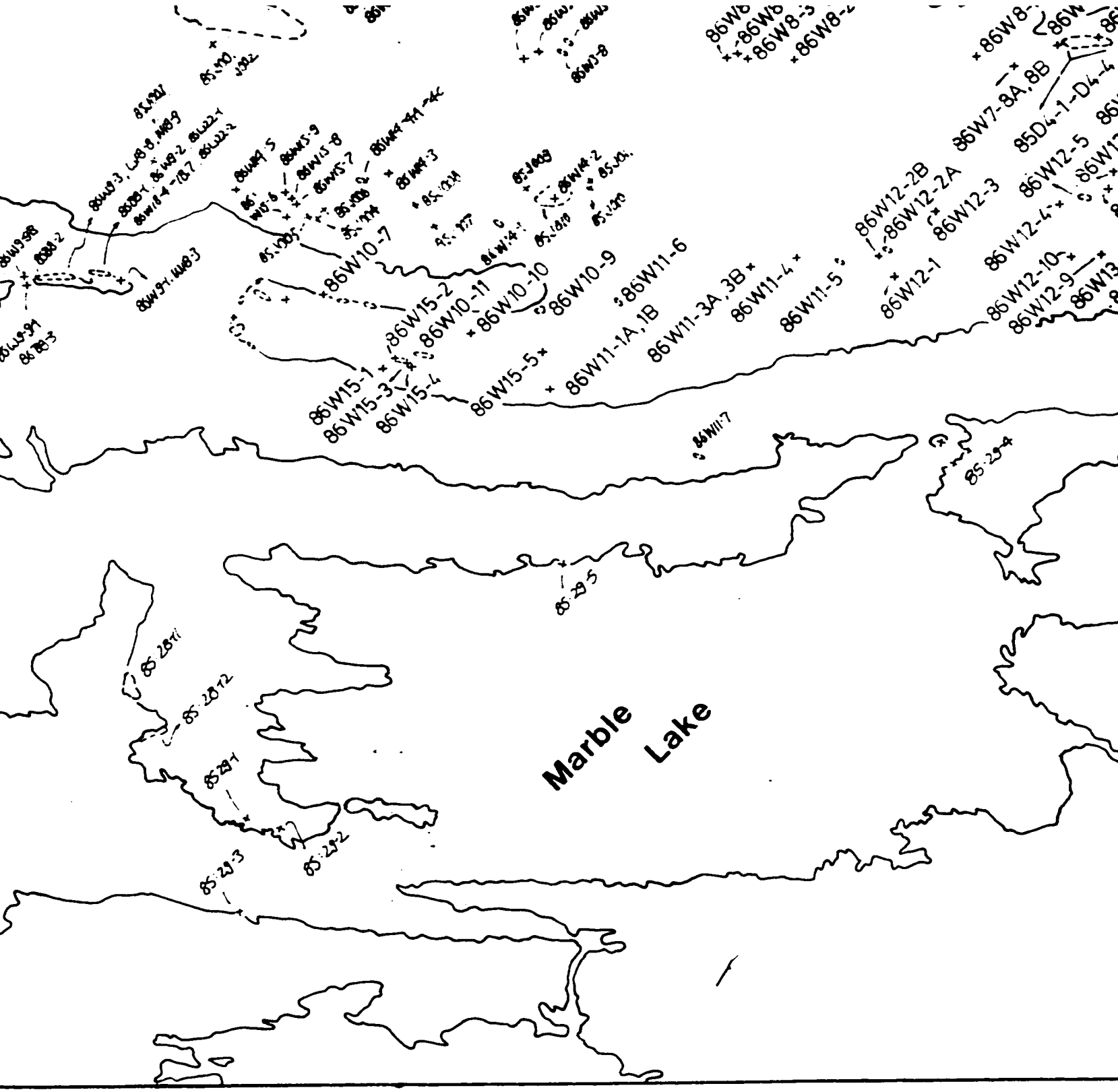
86W10-7
86W15-2
86W10-11
86W10-10
86W10-9
86W11-6
86W11-1A, 1B
86W11-3A, 3B
86W11-4
86W11-5
86W12-2B
86W12-2A
86W12-3
86W12-1
86W12-5
86W12-4
86W12-10
86W12-9
86W15-1
86W15-3
86W15-4
86W15-5
86W7-3A, 8B
85D4-1-D4-4
Marble
Lake

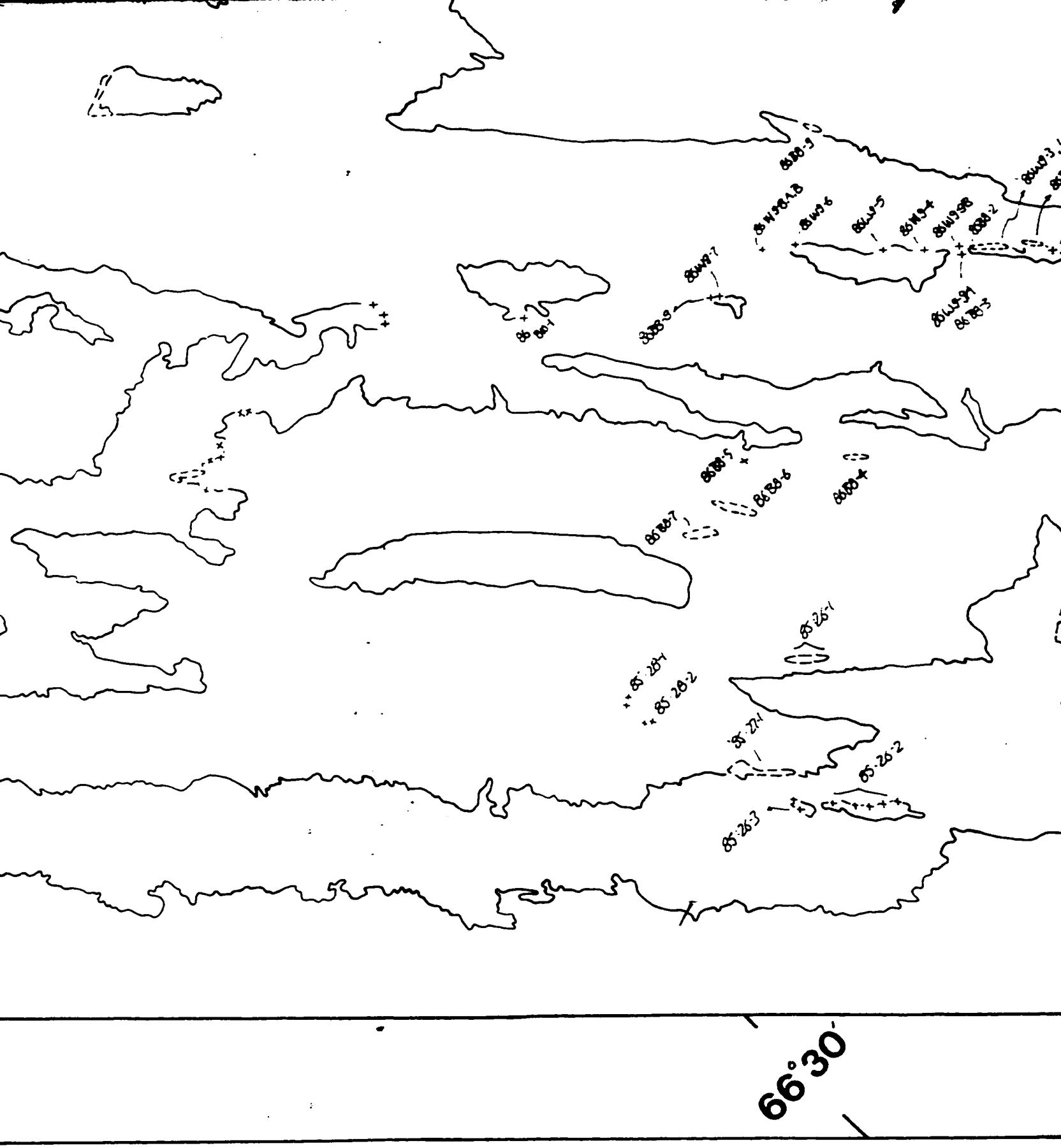
66°30'

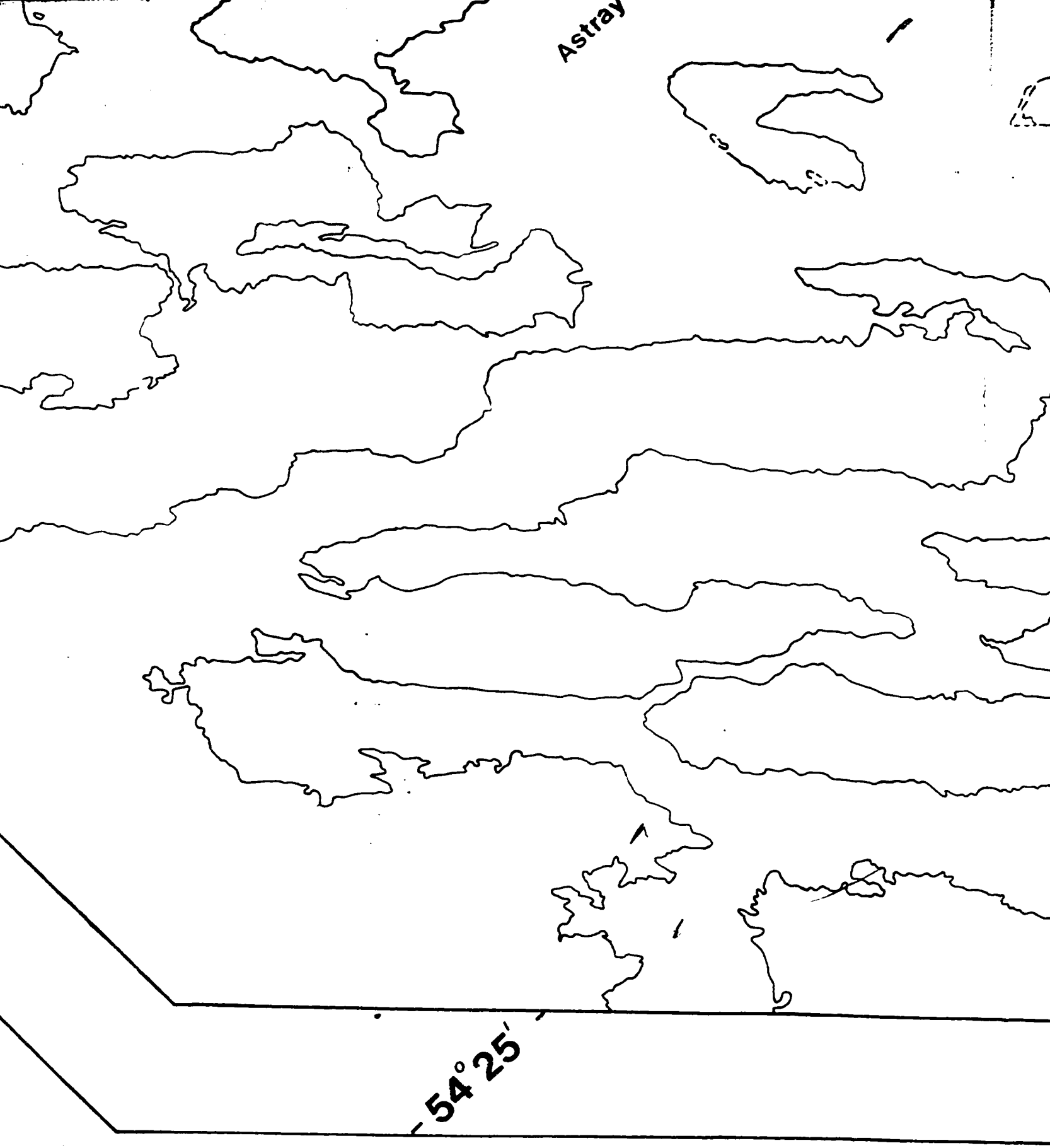
Astray
54° 25'

87WG-2
87WG-1

MAP B (to accompany Watanabe, 1996)

Scale: 1:50,000

2 miles

1 0 1 2

...ake – Astray Lake region, western Labrador

...cations for 1985–1987 field work

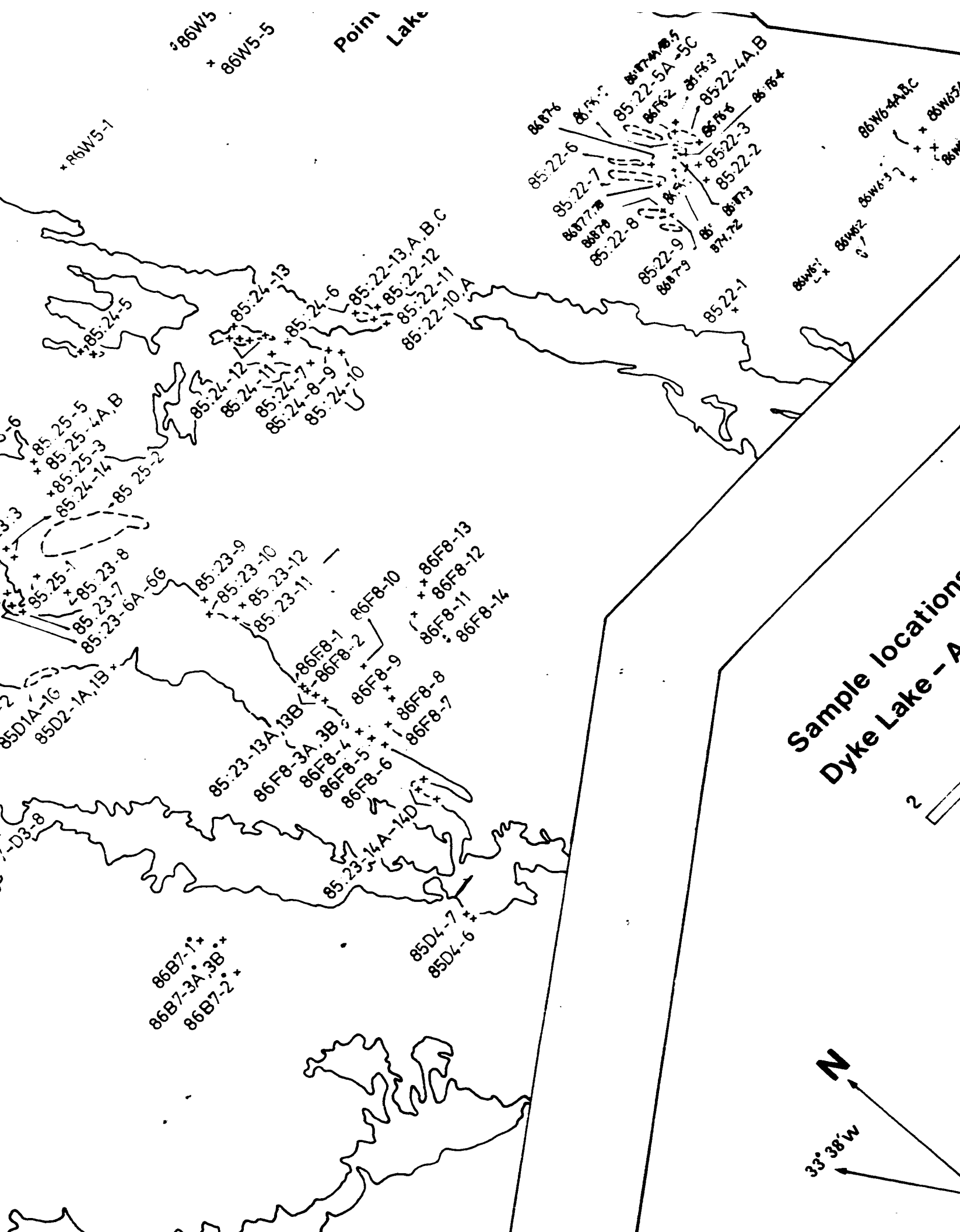
86W5
86W5-5
86W5-1
85:22-6
85:22-7
85:22-8
85:22-9
85:22-5A-5C
85:22-4A,B
85:22-3
85:22-2
85:22-1
85:22-13A,B,C
85:22-12
85:22-11
85:22-10,A
85:24-13
85:24-6
85:24-5
85:24-12
85:24-11
85:24-7
85:24-8-9
85:24-10
85:25-5
85:25-4A,B
85:25-3
85:24-14
85:25-2
85:25-1
85:23-8
85:23-7
85:23-6A-6G
85:23-9
85:23-10
85:23-12
85:23-11
86F8-1
86F8-2
86F8-10
86F8-9
86F8-13
86F8-12
86F8-11
86F8-14
85:23-13A,13B
86F8-3A,3B
86F8-4
86F8-5
86F8-6
86F8-8
86F8-7
85:23-14A-14D
85D1A-1G
85D2-1A,1B
85D4-7
85D4-6
86B7-1
86B7-3A,3B
86B7-2
86W6-4A,B,C
86W6-3
86W6-2
Sample locations
Dyke Lake - A
N
33° 38' W


86W4-19
86W4-11
86W4-12
86W4-13
86W4-10
86F7-1
86W4-14A
86W4-14B
86W4-15A,B
86W4-17
86W4-16
86W4-18
86R3-6
86R3-9
86R10A,B
86R3-5
86R3-12
86R3-4
86R3-3
86R3-2
86R3-1
86W4-6
86W4-5
86W4-7
86W5-1
86W4-9
86W4-8
86W4-4
86W4-3
86W19-5
86W19-7
86W19-6
86W4-1
86W4-2A,B
85.25-8
85.25-7
85.25-6
85.25-5
85.25-4A,B
85.25-3
85.24-3
85.24-4
85.24-2
85.24-1
85.23-4
85.23-3
85.23-2
85.24-16
85.25-1
85.23-8
85.23-7
85.23-1
85D2-6
85D2-7-D2-10
85D3-1
85D1-8-D1-10
85.24-15
85D1-7
85D1-6
85D1-5
85D3-2
85D3-4
85D1-2-D1-4
85.23-5
85D2-3-D2-5
85D2-2
85D1A-1G
85D2-1A,1B
85D3-3
86W8-5
86W8-4
86W8-3
86W8-22
86W8-1
86W7-7
86W7-6
86W7-5
86W7-8A,8B
85D4-1-D4-4
86W7-1-W7-2
86W20-1
86W20-2-W20-4
86W7-4
86W7-3
86W13-4
85D3-5A-5E
85D3-6A-6D
85D3-7-D3-8
85D3-9-D3-11
86W12-8
86W12-5
86W12-7
86W12-2B
86W12-2A
86W12-3
86W12-1
86W12-4
86W12-6
86W13-3
86W13-6
86W13-5
86W13-7A
86W13-9
86W12-10
86W12-9
86W13-2
86W13-1
86W13-7B
86W13-8
86W11-6
86W11-3A,3B
86W11-4
86W11-5
86W11-1A,1B
86W10-9
86W10-10


86W21-2-W21-6
86W21-7
86W21-8
86W21-1
86W21-9A,B
Dyke Lake
86W19-3A,B
86W19-1
86W19-2
86W15-2
86W10-7


87W3-6
87W2-9
87W3-5
87W3-4
87W3-16-22
87W3-14
87W3-15
87W5-7
87W5-6
87W5-5
87W5-4
87W5-3A,B
87W2-10
87W2-11
87W3-3
87W3-2
87W2-5
87W2-2
87W2-3
87W1-7
87W5-2
87W5-1
87W2-1
87W2-7
87W1-1,2-4,2-6;
87W1-8-W1-11
86B27-4, 86B20-5
Astray Lake


87W4-2
87W4-1
87W4-4
87W4-3
86B19-8
86B19-9


87W4-2
87W4-1
87W6-1
87W6-2

1985–1987 field work
Region, western Labrador
2 miles
85-22-1
85-22-2
85-22-3
85-22-4A,B
85-22-5A-5C
85-22-9
86W6-4A,B,C
86W6-5A,B
86W6-3
86W6-2
86W6-1


86W17-7
86W17-6
86W17-5
86W17-4
86W17-2
86W17-1
86W17-3
86R3-8
86R3-9
86R1CA,B
86R3-11
86R3-5
86R3-12
86W5-3
86W5-2A,B
86W5-4
86W5-5
Point
Lake
86R3-4
86R3-3
86R3-2
86R3-1
86W4-5
86W4-7
86W4-6
86W5-1
86W4-4
86W4-3
86W4-2A,B
85-22-5A-5C
85-22-6
85-22-7
85-22-8
85-22-9
85-22-13,A,B,C
85-22-12
85-22-11
85-22-10,A
85-24-13
85-24-6
85-24-5
85-24-12
85-24-11
85-24-7
85-24-8-9
85-24-10
85-25-8
85-25-7
85-25-6
85-25-5
85-25-4A,B
85-25-3
85-25-2
85-24-14
85-24-4
85-24-3
85-23-4
85-23-3


Petitsikapau Lake
86W19-3A,B
86W19-4
86W19-5
86W19-7
86W19-6
86W19-1
86W19-2
86W4-19
86W4-11
86W4-12
86W4-13
86W4-10
86W4-14A
86W4-14B
86F7-1
86W4-15A,B
86R3-7
86R3-8
86R3-6
86R3-9
86R10A,B
86W4-17
86W4-16
86W4-18
86R3-4
86R3-3
86R3-2
86W4-9
86W4-8
86W4-1

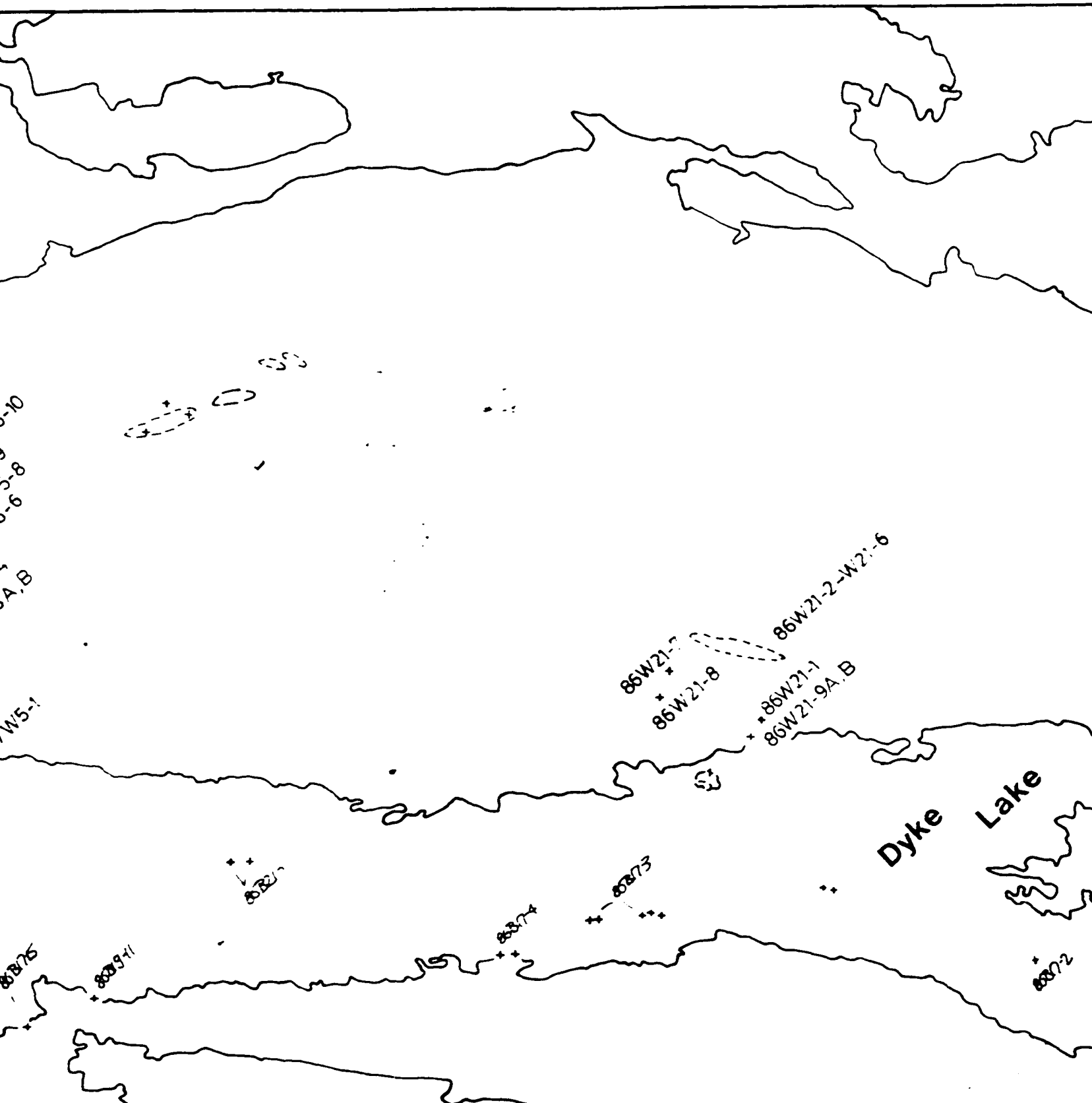
86W21-2-W21-6
86W21-8
86W21-1
86W21-9A,B
Dyke
Lake

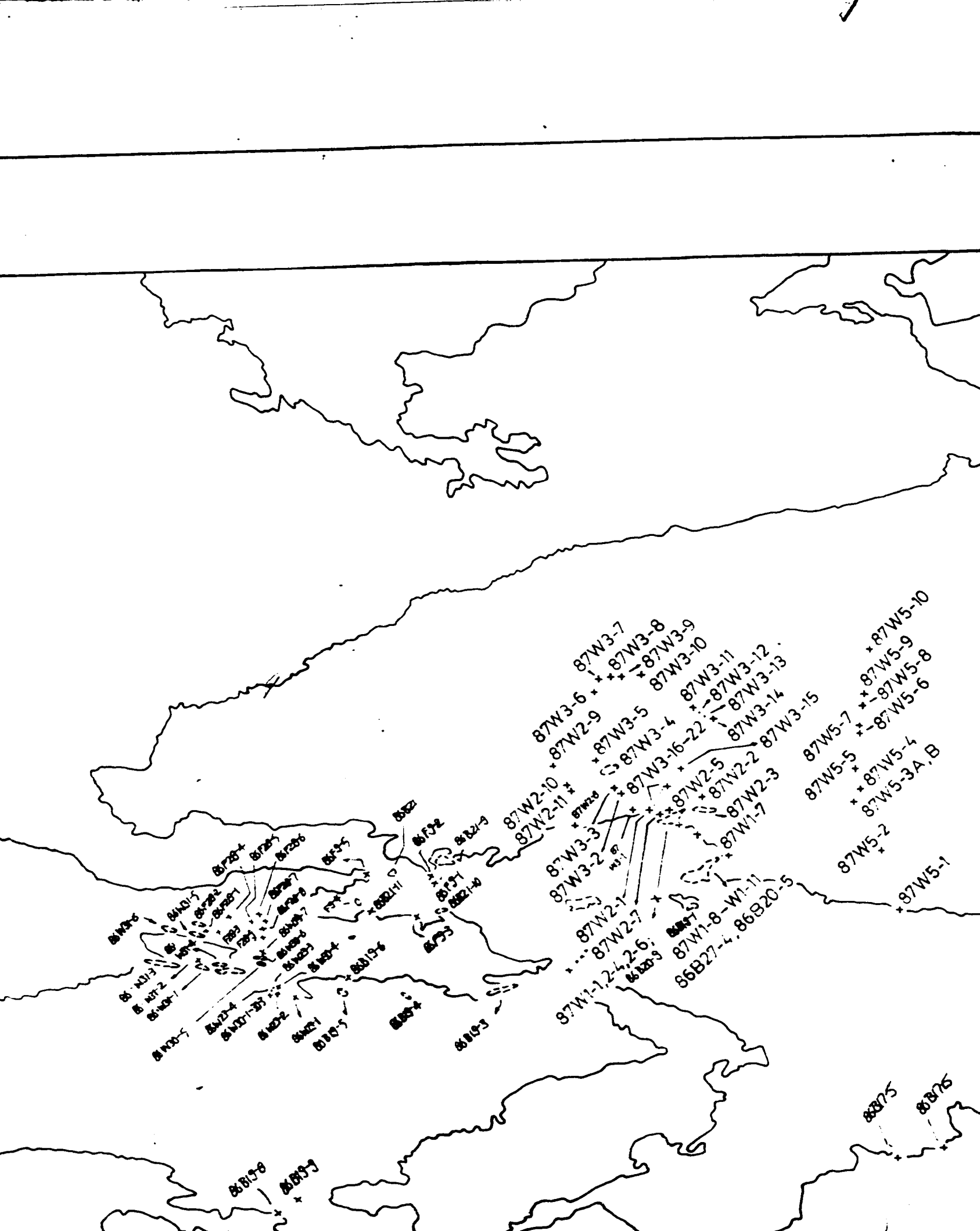
87W3-7
87W3-8
87W3-9
87W3-6
87W2-9
87W3-10
87W3-5
87W3-11
87W3-12
87W3-4
87W3-13
87W3-16-22
87W3-14
87W3-15
87W2-10
87W2-11
87W3-3
87W2-5
87W2-2
87W2-3
87W3-2
87W1-7
87W2-1
87W2-7
87W1-1,2-4,2-6;
87W1-8-W1-11
86B27-4, 86B20-5
87W5-10
87W5-9
87W5-7
87W5-8
87W5-5
87W5-6
87W5-4
87W5-3A, B
87W5-2
87W5-1

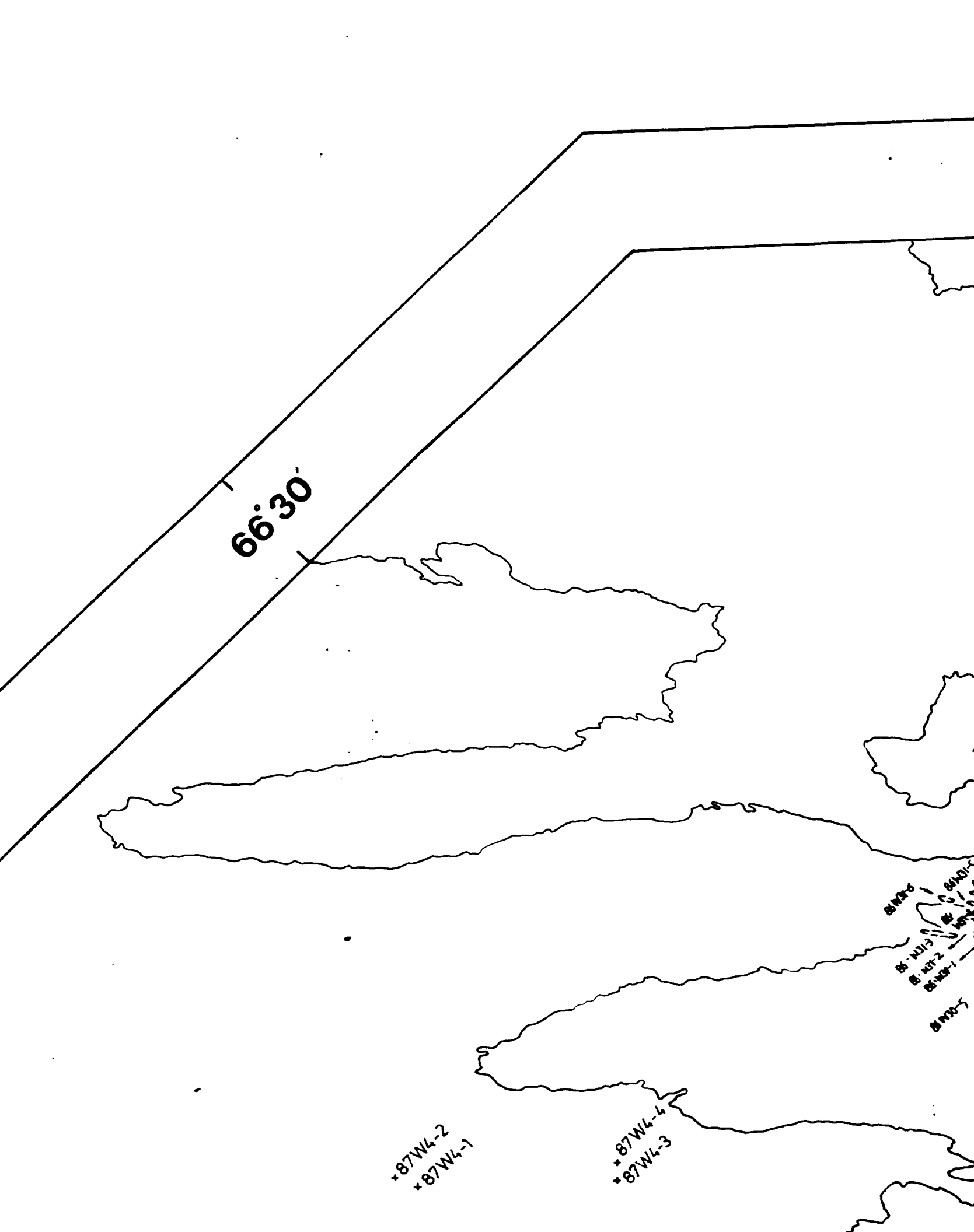
66°30'
87W4-2
87W4-1
87W4-4
87W4-3

66.30

IMAGE EVALUATION
TEST TARGET (QA-3)

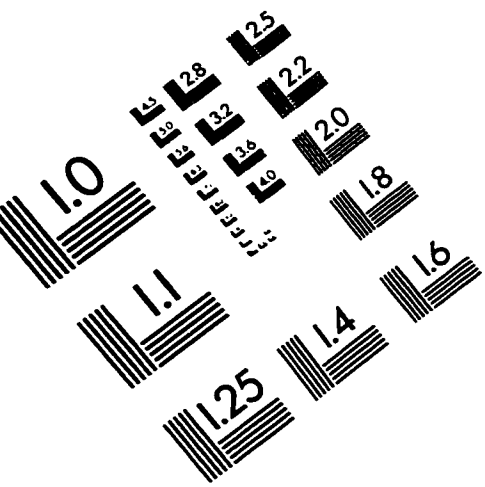

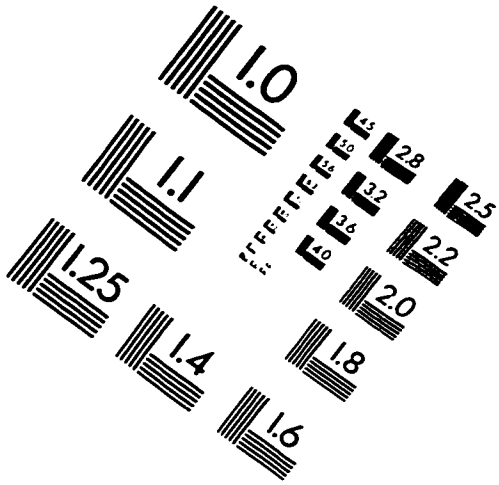

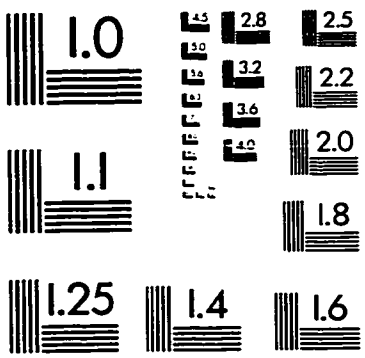

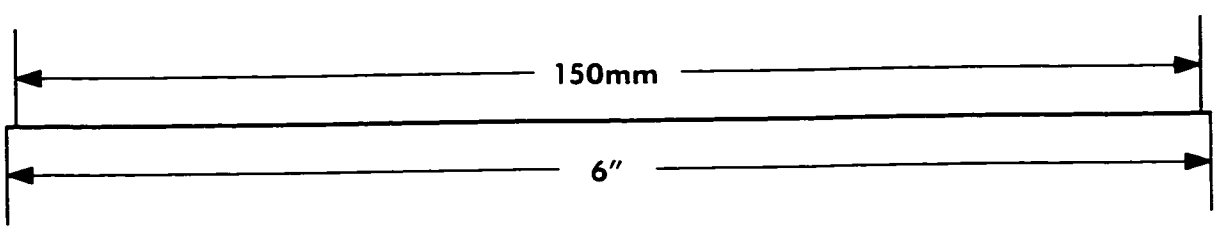

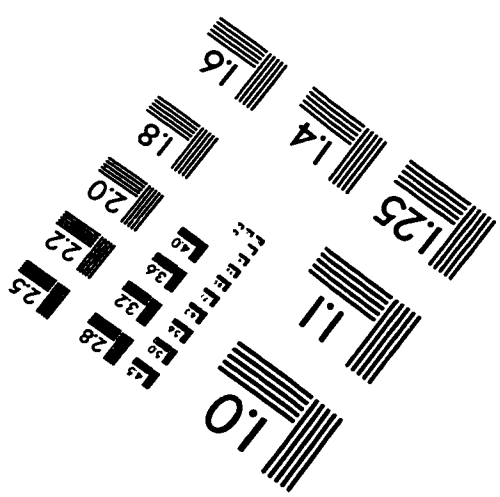

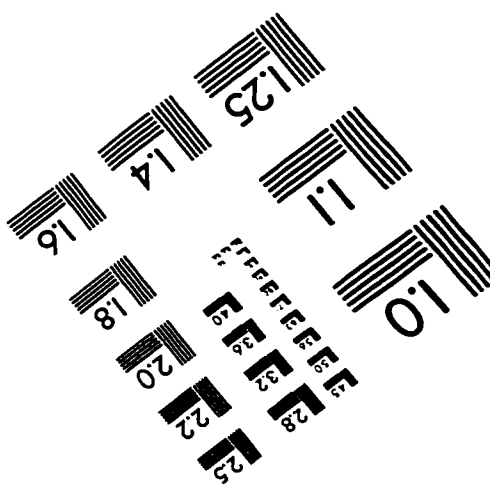

APPLIED IMAGE, Inc
1653 East Main Street
Rochester, NY 14609 USA
Phone: 716/482-0300
Fax: 716/288-5989